

**ANALYTICAL DESIGN AND DEVELOPMENT OF  
RESONANT CONVERTER BASED FAST CAPACITOR  
CHARGING POWER SUPPLY (>40 kJ/s)**

By

**PASULA NARESH**

(ENGG01201104013)

(Bhabha Atomic Research Centre, Mumbai)

*A thesis submitted to the Board of Studies in  
Engineering Sciences*

*In partial fulfillment of requirements*

*For the Degree of*

**DOCTOR OF PHILOSOPHY**

**OF**

**HOMI BHABHA NATIONAL INSTITUTE**



**August, 2016**

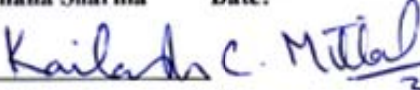
# Homi Bhabha National Institute

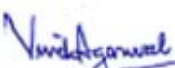
## Recommendations of the Viva Voce Board

As members of the Viva Voce Board, we certify that we have read the dissertation prepared by Pasula Naresh, entitled "Analytical design and development of resonant converter based fast capacitor charging power supply (>40kJ/s)" and recommend that it may be accepted as fulfilling the dissertation requirement for the Degree of Doctor of Philosophy.

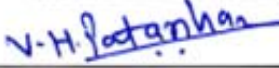
  
Chairman: Prof. A.P. Tiwari Date: 31/8/16

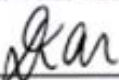
  
Guide/ Convener: Prof. Archana Sharma Date: 31-8-16

  
Co-Guide: Prof. K.C. Mittal Date: 31/8/2016

  
External Examiner: Prof. Vivek Agarwal Date: 31.8.16

  
Member 1: Prof. A.K. Bhattacharjee Date: 31/8/2016

  
Member 2: Prof. V.H. Patankar Date: 31.08.2016

  
Member 2: Prof. D.C. Kar Date: 31.08.2016

Final approval and acceptance of this dissertation is contingent upon the candidate's submission of the final copies of the dissertation to HBNI.

I hereby certify that I have read this dissertation prepared under my direction and recommend that it may be accepted as fulfilling the dissertation requirement.

Date: 31.08.2016

Place: Mumbai

  
Guide: Dr. Archana Sharma 31-8-16

## **STATEMENT BY AUTHOR**

This dissertation has been submitted in partial fulfillment of requirements for an advanced degree at Homi Bhabha National Institute (HBNI) and is deposited in the Library to be made available to borrowers under rules of the HBNI.

Brief quotations from this dissertation are allowable without special permission, provided that accurate acknowledgement of source is made. Requests for permission for extended quotation from or reproduction of this manuscript in whole or in part may be granted by the Competent Authority of HBNI when in his or her judgment the proposed use of the material is in the interests of scholarship. In all other instances, however, permission must be obtained from the author.

Pasula Naresh

## **DECLARATION**

I, hereby declare that the investigation presented in the thesis has been carried out by me. The work is original and has not been submitted earlier as a whole or in part for a degree / diploma at this or any other Institution / University.

Pasula Naresh

# LIST OF PUBLICATIONS

## I. International journals

1. **P. Naresh**, C. Hitesh, A. Patel, T. Kolge, Archana Sharma and K.C. Mittal “Analysis and development of fourth order LCLC resonant based capacitor charging power supply for pulsed power applications”, Rev. Sci. Instruments, 84, 084706 (2013), Published by AIP Publishing LLC.
2. **P. Naresh**, Ankur Patel, Archana Sharma and K.C. Mittal, “Conducted Noise Analysis and protection of 45 kJ/s,  $\pm 50$  kV Capacitor Charging Power Supply when Interfaced with Repetitive Marx Based Pulsed Power System”, Rev. Sci. Instruments, 86, 094701 (2015), Published by the AIP Publishing LLC.
3. C.S.Reddy, A.S.Patel, **P.Naresh**, Archana Sharma and K C Mittal “ Experimental investigations of Argon Spark gap Recovery times by developing a High Voltage Double Pulsed Generator” Rev. Sci. Instruments, 85, 064703(2014), Published by the AIP Publishing LLC.
4. Romesh Chandra, A Roy, R Menon, K Senthil, A.S Patel, Igor Ventizenko, A. Mashchennko, Ranjeet Kumar, Tanmay Kolge, **Naresh. P.**, V.K. Sharma, Ritu Agarwal, Archana Sharma and K.C. Mittal “Explosive Emission Properties of Cathode Material in Relativistic Electron Beam Generation” in IEEE Transactions on Plasma Science, Vol. 42, No. 11, November 2014, pp.3491-3497.
5. **Naresh P** and Archana Sharma, “Analysis and development of 4kV, 9 kHz Repetitive Capacitor Charging Power Supply for Solid State Switch Based Pulsedr Application”, in IEEE Transactions on Plasma Science (**Major review submitted**).

## II. International Conferences papers

1. **Naresh. P.**, Ankur Patel, Tanmay kolge, Ranjeet kumar, Archana Sharma, K.C. Mittal and D.P. Chakravarthy “Voltage Feedback Control for Fast - High Voltage Capacitor Charging

- Power Supply”, Published in 12th International Conference on Electromagnetic Interference and compatibility 2012, INCEMIC – 2012, Bangalore, pp. 64-67.
- 2) **Pasula Naresh**, Ankur Patel, Tanmay Kolge, Hitesh Choudhary, Archana Sharma, Kailash C. Mittal “Novel High Frequency Converter cum Inverter Based Capacitor Charging Power Supply (CCPS)”, 2014 IEEE International power modulator and high voltage conference, 1-5 June,2014, pp. 603-606.
  - 3) **Pasula Naresh**, Ankur Patel, Tanmay Kolge, Hitesh Choudhary, Archana Sharma, Kailash C. Mittal, “Comparitive Analysis of 2nd and 4th Order Resonant Based Capacitor Charging Power Supplies”, 2014 IEEE International power modulator and high voltage conference,1-5 June,2014, pp. 607-610.
  - 4) C S Reddy, **Pasula Naresh**, Ramanujam Sarathi, Archana Sharma<sup>1</sup>, Kailash C. Mittal<sup>1</sup> “Spark Gap Discharge Properties Measured by Optical Emission Spectroscopy”, 2014 IEEE International power modulator and high voltage conference, 1-5 June,2014, pp. 458-461.
  - 5) C.S. Reddy, **Pasula Naresh**, Ankur Patel, Archana Sharma, Kailash C. Mittal “Voltage Recovery Characteristics of Spark Gap Using a Repetitive Pulsedd Power System”, 2014 IEEE International power modulator and high voltage conference, 1-5 June,2014, pp. 512-515.
  - 6) Archana Sharma, **Pasula Naresh**, Romesh Chandra, K. Senthil, Sabyasachi Mitra, Sandeep Kumar Singh “Characterization of Flash X-Rays Source and Radiography Results of Newly Developed Kali-30GE Relativistic Electron Beam System”, 2014 IEEE International power modulator and high voltage conference, 1-5 June,2014, pp. 370-373.
  - 7) Archana Sharma, **Pasula Naresh**, Ranjeet Kumar, Romesh Chandra, Jayanta Mondal, Kailash C. Mittal “Sub-Nanosecond Pulsed Generator and Electron Beam Source for

nTOF Applications”, 2014 IEEE International power modulator and high voltage conference, 1-5 June,2014, pp. 73-75.

### **III. National conference**

1. **Naresh.P.**, Ankur Patel, Tanmay kolge, Ranjeet kumar, Archana Sharma, K.C. Mittal and D.P. Chakravarthy “Design and Development of Fast - High Voltage Capacitor Charging Power Supply”, Published in VEDA – 2012, Pilani.

Pasula Naresh

Dedicated to.....

My Beloved Family and

My Teachers

My Friends

## ACKNOWLEDGEMENT

First and foremost I would like to express my deep and sincere gratitude to my supervisor Prof. Archana Sharma and Prof. K.C. Mittal for their invaluable guidance, constant encouragement, unstinted inspiration, keen interest and good wishes. I would like to thank Dr. L.M. Gantayet and Prof. R.K. Rajawat their ability to explain things simply and clearly are something I have admired right from my first day in lab, and continue to remain in awe even today. I greatly appreciate his contributions, comments and insights during the course of writing this thesis. Their patience and support has helped me get through some challenging moments. For this, and much more, I remain indebted.

I must thank to my doctoral committee chairman Prof. A.P. Tiwari for his continuous support and valuable suggestions during my research work and for monitoring my progress every year. I would like to express my sincere thanks to my doctoral committee members, Prof. A.K. Bhattacharjee, Prof. S.V.G. Ravindranath, Prof. V.H. Patankar and Prof. D.C. Kar for their critical comments and suggestions during annual review presentations.

My thesis is incomplete if I won't tell my heartfelt and sincere thanks to my adviser (technical) Mr. Ankur Patel. I never forget my close friends Tanmay Kolge, Hitesh Choudhary along with Ankur Patel for their innumerable help during the experiments and data analysis and their suggestions even in my personal life. Without these three friends I could not be much happy during the course of time.

I wish to show my sincere gratitude to Mr. K. Senthil, Mr. V.K. Sharma, Mr. S.S. Mitra, Dr. A.Roy, Mr. Sandeep, Mr. Rehim Rajan, Mr. Ramchandra Chavan, Mr. Love Mishra, Mr. Saroj, Mr. Kulkarni, Mr. Satendra Dagore, Mrs. Rakhee Menon, Mrs. Ritu Agarwal and Mrs. Mangal Pillai.

I would like to express my special thanks to C.S. Reddy, S.V. Tewari, Romesh Chadra, Ranjeet Chaurasiya, Danish Mirza Beig, Garath, Manjunath H.K, Patil, Vaity, Rahul, Shekar

Bane and Mrs. Pushpa Naidu. I would like to express my sincere thanks Ahmed, Dilip, Abdulla, Khaisar, Kamal, GM and Suma, Yusuf and Jasna, Vivek and Anju, Satish and Anusha for their unwavering support during my difficult time and homely feeling at Mumbai. I always cherish the time spent with all of you during these years. I also extend thanks to my batch mates Rajasekhar, Amit, Abhay and Ashwin.

I cannot begin my journey without my loving wife and daughter. They did journey along with me in happiest moments and in worst conditions. They have been my pillars of support and strength for as long as I can remember. I am convinced, I could not have made it this far without their love and encouragement. My gratitude's to my parents, my brothers, sisters and their children, my aunt's and uncle's and brother in law and his family.

Finally, I would like to thank the Department of Atomic Energy for funding my Doctoral research work.

Date:

Pasula Naresh

## SYNOPSIS

High voltage capacitor charging power supplies (CCPS) are used in various industrial and pulsed power applications. Designing a reliable and efficient charging power supply for pulsed power systems is always a complex job because of associated dynamic load such as electron gun, laser, magnetron etc. During generation and discharge of high intensity pulses the associated charging power supply of pulsed power system undergoes a surge reversal of high amplitude in voltage and high frequency (MHz) noise. To protect the CCPS against this impulse noise, fast protection is needed.

Conventionally series resonant converter based CCPS is used for pulsed power applications. They are good for static load conditions. But in case of non-linear loading, these CCPS lacks in providing suitable dynamic protection against surge reversal and high frequency noise during discharging period. Other resonant converters such as parallel LC and third order resonant converter have been utilized previously in the development of high voltage CCPS. These power supplies are also suffering with serious issues like lack of DC blocking and poor part load efficiency. An investigation is needed to find out the root cause behind the failure of charging power supply when interfaced with pulsed power system. So, this motivated to choose research topic on design and development of efficient and reliable resonant converter based fast ( $>40\text{kJ/s}$ ) CCPS with improved protection for pulsed power applications.

To start with, initial investigations are made to find the means to reduce the high peak currents through solid state switches, availing of DC blocking and to improve the load efficiency. Thereafter the research continued towards effective dynamic protection for fast CCPS against high amplitude and short interval surge reversal. To achieve the desired goal, an innovative design of the resonant converter is proposed based on a fourth order LCLC components and is used in the development of fast ( $>40\text{ kJ/s}$ ) and repetitive CCPS. As the intended CCPS is for pulsed power systems viz. Marx generator, a detailed literature survey

on the importance of pulsed power and their applications was carried out [1-2]. Pulsed power system is a combination of energy storage elements (capacitor/inductors) and high power switches (controlled / uncontrolled) connected in different topologies to get required pulsed peak and shape at the output [3]. Second order (series/parallel) resonant converters are popular for constant current, constant voltage and soft switching applications [4-5]. The technical difficulties arise from simultaneous requirements of power rating, repetition rate, energy conversion efficiency, lifetime, cost and protection [6]. The objective of using resonant network in the capacitor charging power supply is to provide load independent constant current, short circuit protection and soft switching. Second order series LC [7-8], parallel LC [9-10] and series-parallel [11] resonant converters have already been utilized to design a charging source for single and repetitive operation for pulsed power applications.

Conventional linear high voltage power supplies are designed to operate at constant or near constant load conditions. For increased average power, repetitive pulsed power systems are used where requirement of output voltage, charging rate, size and weight of the power supply also gets enhanced. Therefore, linear power supplies are not preferred to charge capacitors at high repetition rate. Alternative way is to use switch mode power supplies (SMPS) based on DC-DC converters, wherein the operating frequency is in kHz range. Due to high operating frequency ( $>20\text{kHz}$ ) the size of the energy storage elements gets reduced and output voltage regulation improves compared to conventional HVDC power supply. The soft switching in DC-DC converters have been integrated by incorporating auxiliary circuits, before hard switching. Losses in the inverter stage of power supply got reduced with soft switching (zero current/zero voltage), which in turn improved the efficiency of the converter. Control features have been added to improve the load regulation and line regulation.

Some of the challenges involved in the development of a fast CCPS are

1. It should operate from light load to very high load

2. It should provide load independent constant current
3. It should provide soft switching
4. It should sustain dynamic noise and other EMI related problems

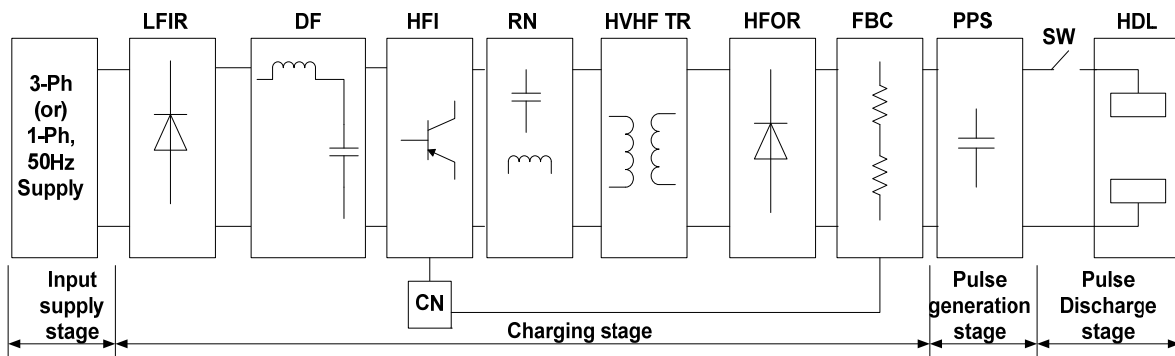


Figure.1. Block Diagram of Capacitor Charging Power Supply with Load

Typical CCPS topology includes low frequency input rectifier (LFIR), DC filter (DF), high frequency inverter (HFI), resonant network (RN), high voltage high frequency transformer (HVHF TR), high frequency output rectifier (HFOR), feedback circuit (FBC), pulsed power system (PPS), switch (SW), highly dynamic load (HDL) and control network (CN), as shown in Figure.1. After the mains input, charging stage of CCPS begins which is divided into two parts viz, low and high frequency stage. In low frequency stage all components are operated at fundamental frequency (50Hz) and in high frequency stage all components are operated at switching frequency ( $>20\text{kHz}$ ). Resonant network (RN) is an important stage in the design of CCPS.

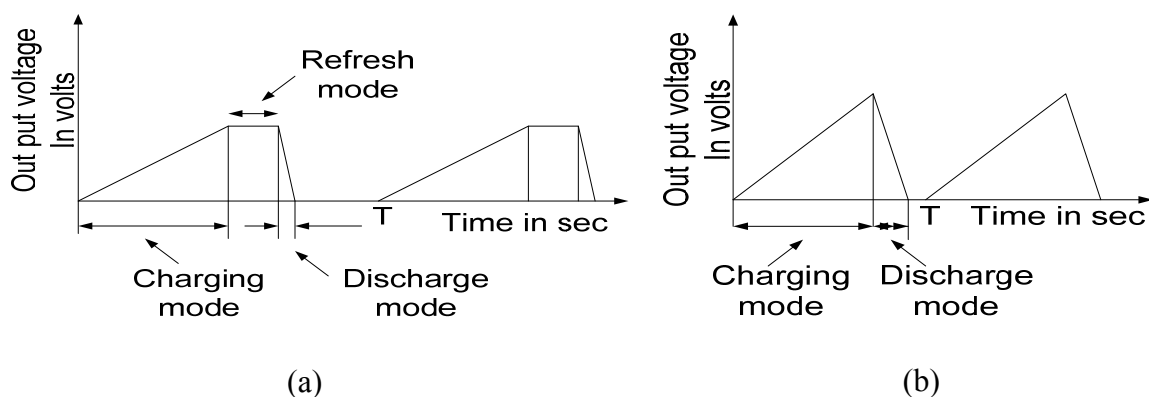


Fig.2 Voltage across capacitors (a) with and (b) without refresh mode in CCPS

Resonant converters are used in CCPS and in DC-DC converters to derive advantages like load independent constant current and soft switching. In pulsed discharge stage the whole energy of pulsed power system delivers to the highly dynamic load (HDL). Charging and discharging stages are the two important stages of CCPS in operation. The voltage profile across energy storage capacitor connected at the output terminals of CCPS is shown in Figure.2.

Capacitors used in pulsed power systems as primary energy storage elements, are charged and isolated from CCPS during discharge mode. In refresh mode it keeps connected with low charging current to compensate the leakage and maintains the voltage level as needed. The rate at which the capacitor charges - discharges energy to the load is called the repetition rate ( $1/T$ ). It may be a few 0.01Hz for large capacitor banks to a few kHz for certain lasers with small stored energy. As repetition rate increases refresh mode time is reduced keeping  $dv/dt$  same. After the energy storage capacitor discharges, it must recharge to a specified voltage with the capacitor charging power supply (CCPS).

Protection is needed for charging power supply both in charging as well as in pulsed discharge stage. Because surge reversal of high amplitude in voltage (in kV) and high frequency noise (in MHz range) is generated mainly due to breakdown of uncontrolled switches (such as spark gaps) during charging (energy storage capacitor of pulsed power system) and due to high energy dissipation to the dynamic load for very short duration of time. The generated noise frequency is in MHz range and it varies from 1MHz to ten multiples of MHz. This noise is a combination of both conducted and radiated noise. Effects of conducted and radiated noise in high voltage DC power supply were discussed previously in [12-13].

Various EMI mitigation techniques were also discussed earlier in [14-16]. This dynamic noise leads to frequent failure of IGBT switches in the inverter stage of power supply. Second

order (series LC and parallel LC) and third order (LCL-T and LCC) resonant converters have been utilized in DC-DC converters for constant current (CC) and constant voltage (CV) application based on load requirement [17-19]. Literature reveals that, when these converters used in the development of high voltage CCPS are suffer with serious drawbacks such as high peak currents, lack of DC blocking, poor part load efficiency and lack of dynamic protection when interfaced with pulsed power system and operated with dynamic load. To overcome the aforementioned shortcomings, proposed a fourth order LCLC resonant converter to design and develop fast CCPS for pulsed power applications.

Mathematical modelling has been done on resonant converter operated CCPS to optimise the lumped parameters. Conditions for load independent constant current and zero current switching in 2<sup>nd</sup> order series LC, parallel LC, 3<sup>rd</sup> order LCL-T and 4<sup>th</sup> order LCLC resonant converter have been derived mathematically.

A comparative study has been done on 2<sup>nd</sup>, 3<sup>rd</sup> and 4<sup>th</sup> order resonant converter based CCPS. The derived conclusion is that the series LC resonant converter provides load independent constant current and zero current switching when  $f_r \geq 2f_s$ , whereas parallel LC, LCL-T and LCLC resonant converters provides load independent constant current and soft switching when switching frequency is equal to resonant frequency ( $f_s=f_r$ ) [20-21].

Thereafter the execution details of proposed 4<sup>th</sup> order resonant converter based CCPS is discussed with the help of simulation and through experimental results. To validate the simulation, a prototype CCPS rated as 200V, 20J/s has been developed. The developed prototype has been tested with a capacitive load of 100  $\mu$ F. A half bridge inverter has been utilized to get square wave voltage with switching frequency of 25 kHz. Load independent constant current and zero current switching has been achieved experimentally on adjusting switching frequency( $f_s$ ) equal to resonant frequency ( $f_r$ ). A generalized control scheme has been proposed in the thesis to provide control signals for switches in the high frequency

inverter stage of CCPS. Based on set parameters (such as charging voltage, charging time and load capacitor value) microcontroller generates the timing signal to free running pulsed width modulator (PWM) controller. In addition microcontroller processes the interrupts and generates the timing signal. The PWM controller provides ON/OFF signals for switches in the inverter stage. This scheme has worked effectively in the developed CCPS.

In CCPS design, one more stage is added to step up the output voltage using ferrite core based HV high frequency (HF) transformer. Leakage inductance of HF transformer is used as second resonant inductor of 4<sup>th</sup> LCLC resonant converter. High voltage high frequency transformer parameters, repetition rate and charging rate are critical design issues in CCPS. Thus a high repetition rate CCPS of ratings: 4 kV, 3.7kJ/s, 9 kHz has been developed and tested with load capacitor of 47nF. The load has been charged to target voltage in 111 $\mu$ s as estimated.

To continue the design of CCPS for higher voltage and repetitive charging, a bipolar high voltage ( $\pm 50$  kV) fast charging (45kJ/s) CCPS has been designed and developed to operate at 10Hz. Protection and controlling are the two important features of a fast capacitor charging power supply. It is already been discussed in the previous section that the dynamic noise leads frequent failure of controlled switches in the inverter stage of charging power supply.

A detailed analysis has been done on noise generation and its mitigation. In most of the cases the impact of conducted noise is more, which leads to failure of charging power supply as compared to radiated noise when operated with highly dynamic load.

The conducted noise is further divided into two

1. Differential mode noise
2. Common mode noise

Differential mode noise propagated to the inverter stage from load via output diode rectifier, HVHF transformer and resonant network. Common mode noise coupled at various power conversion stages of charging power supply through common ground. In the present research work, an attempt has been made to overcome conducted noise effects, which mainly causes frequent failure of IGBT switch in the inverter stage of CCPS. Design parameters have been taken from 45kJ/s and  $\pm 50\text{kV}$  CCPS to carry out mathematical analysis noise generation and its mitigation.

Failure of controlled switches (IGBTs) in the inverter stage of CCPS due to conducted noise is prevented by effective shielding and with proposed LCLC resonant network. Shielding between primary and secondary windings of HVHF transformer will enable us to keep coupling capacitor ( $C_C$ ) value as low as possible ( $\leq 10\text{pF}$ ). The proposed 4<sup>th</sup> order LCLC resonant topology acts as low pass filter for differential mode noise.

Shielding and LCLC low pass filter scale down the noise voltage magnitude at a rate of -10dB and -75dB gain respectively. This high power fast CCPS has been interfaced with 1kJ repetitive Marx based system and tested successfully at 5Hz. The results matched well with mathematical model and simulation data. The developed fast ( $>40\text{kJ/s}$ ) CCPS has been interfaced with 1kJ repetitive Marx based system and tested successfully at 5Hz. The results matched well with mathematical model and simulation data.

In recent days pulsed power systems are using controlled spark gaps, so called triggertrons. In this case spark gap electrodes are charged to a specified voltage with charging source and then supplied a controlled low voltage to break down spark gap. So, a controlling mechanism is required to charge the load capacitor to a specified voltage level. The break down voltage varies from gas to gas as well as with pressures. A photodiode and LED based control scheme has been demonstrated and tested experimentally.

The overall motive of this research work is to design a reliable, efficient and compatible resonant converter based fast CCPS for pulsed power application. Complications with the usage of higher order resonant converter in the power stage have been overcome effectively. The present research work enables the researchers work in higher order resonant converters to make charging power supplies more reliable and efficient. The major contribution of this research work is in the design of fast CCPS for pulsed power applications are

1. A 4<sup>th</sup> order resonant converter based CCPS has been designed and simulated for high pulsed power and dynamic load applications. The proposed converter provides load independent constant current and soft switching when operated at switching frequency equal to resonant frequency.
2. To validate the simulation and mathematical model, a prototype CCPS rated at 200 V, 20 J/s has been developed and load independent constant current is demonstrated with soft switching operation.
3. A high repetition rate CCPS of 4kV, 3.7kJ/s and 9 kHz is designed. High voltage high frequency transformer's leakage inductance is used as one of the resonant inductor.
4. Developed a high charging rate (45 kJ/s) and repetitive (10 Hz) CCPS for 1kJ Marx based system based on 4<sup>th</sup> order LCLC resonant converter and successfully interfaced.
5. The failure of controlled switches (IGBTs) in the inverter stage of CCPS due to conducted noise are prevented by effective shielding and proposed LCLC resonant network.
6. With the proposed topology the cost and size of CCPS has reduced due to minimal number of controlled switches, low peak currents and minimum conduction losses in the inverter stage.
7. A photo diode-LED based voltage control circuit has been developed and tested successfully. This control circuit provides more isolation as compared to other electronic components like isolation amplifier and opto-couplers.

The academic contribution of the thesis is in bringing out a better understanding of high voltage fast CCPS design aspects and noise mitigation with proposed 4<sup>th</sup> order LCLC resonant converter and shielding. The data on application of 4<sup>th</sup> order LCLC resonant converter as constant current source in the design and development of CCPS for pulsed power application, as well as the protection of fast (>40 kJ/s) CCPS against conducted noise with repetitive pulsed power system operating with highly dynamic load has been published.

## REFERENCES

1. Hidenori Akiyama, Takashi Sakugawa, Takao Namihira, "Industrial Applications of Pulsedd Power Technology", IEEE Transactions on Dielectrics and Electrical Insulation Vol. 14, No. 5, October 2007, pp. 1051-1064.
2. E. L. Neau, "Environmental and Industrial Applications of Pulsedd Power Systems", IEEE Transactions on Plasma science, Vol. 22, No. 1, February 1994, pp. 2-10.
3. J.L. Liu, Y. Yin, T.W. Zhan, J.H Feng and H.H Zhong, "Application of A Self-Breakdown Hydrogen Spark Gap Switch on High Power Pulsed Modulator", 16th International Pulsedd power conference, Albuquerque, NM, USA, 17-22<sup>nd</sup> June, 2007, , pp. 455-458.
4. G. Hua, E. Yang, Y. Jiang and F. C. Lee, "Novel Zero-Current-Transition PWM Converters", IEEE Trans. Power Electron, Vol. 9, No. 6, November 1994, pp. 601-606.
5. J. G. Cho, J. A. Sabate, G. Hua and F. C. Lee, "Zero-Voltage and Zero-Current Switching Full Bridge PWM Converter for High Power Applications", IEEE Trans. Power Electron., Vol. 11, No. 4, July 1996, pp. 622-627.
6. Rui Xie, Jiande Wu, Wuhua Li and Xiangning He, "A High Voltage Pulsedd Power Supply with Magnetic Switch for ESP", IEEE Power electronics and applications conference, Aalborg, 2-5<sup>th</sup> Sep,2007, pp. 1-7.

7. M. Schutten, R. L. Steigerwald and M. Kheraluwala, "Characteristics of Load Resonant Converter Operated in High-Power Factor Mode", IEEE Trans. Power Electron. Vol. 7, No. 2, April 1992, pp. 304-314.
8. M. Borage, "Parallel resonant converter as a current source," J. Indian Inst. Sci, 83, 2003, pp. 117–125.
9. M. Gulko and S. Ben-Yaakov, "Current-Sourcing Push-Pull Parallel Resonance Inverter (CS-PPRI): Theory and Application As Discharge Lamp Driver", IEEE Trans. Ind. Electron, Vol. 41, No. 3, June 1994, pp. 285-291.
10. M. Foster, H. Sewell, C. Bingham, D. Stone and D. Howe, "Methodologies for the Design of LCC Voltage-Output Resonant Converters", IEE Proc. Electr. Power. Appl, Vol. 153, No. 4, Sep 2006, pp. 559- 567.
11. H. Pollock and J. O. Flower, "Series-parallel load-resonant converter for controlled-current arc welding power supply," IEE Proc. Electr. Power Appl. 143(3), 1996, pp. 211–218.
12. B. Mammano and B. Carsten, "Understanding and optimizing electromagnetic compatibility in switch mode power supplies," Texas instruments technical notes <http://read.pudn.com/downloads119/ebook/505726/TI%E6%A8%A1%E6%8B%9F%E7%94%B5%E8%B7%AF%E8%AE%B2%E4%B9%89.pdf>.
13. Mohammad Rouhollah, Yazdani, Hosein Farzanehfard and Jawad Faiz, "Classification and Comparison of EMI Mitigation Techniques in Switching Power Converters A Review", Journal of Power Electronics, Vol. 11, No. 5, Sep 2011, pp. 767-777.
14. H. Akagi, H. Hasegawa, and T. Doumoto, "Design, Performance of A Passive EMI Filter for Use with Voltage Source PWM Inverter Having Sinusoidal Output Voltage, Zero Common-Mode Voltage", IEEE Trans. Power Electron., Vol. 19, No. 4, Jul. 2004, pp. 1069-1076.

15. H. Chung, S. Y. R. Hui, and K. K. Tse, "Reduction of Power Converter EMI Emission Using Soft-Switching Techniques", IEEE Trans. Electromagn. Compat., Vol. 40, No. 3, Aug. 1998, pp. 282-287.
16. S. Ogasawara, H. Ayano, and H. Akagi, "An Active Circuit for Cancellation of Common Mode Voltage Generated by A PWM Inverter", IEEE Trans. Power Electron. Vol. 13, No. 5, Sep. 1998, pp. 835-841.
17. A. K. S. Bhat, "Analysis and design of a fixed-frequency LCL-type series resonant converter with capacitive output filter", IEE Proc. Circuits Devices Syst. 144(2), 1997, pp. 97-103.
18. A. Patel, K. V. Nagesh, T. Kolge, and D. P. Chakravathy Mittal "Design and development of repetitive capacitor charging power supply based on series-parallel resonant converter topology", Rev. Sci. Instruments, 83, 045111 (2011), Published by the AIP Publishing LLC.
19. Cardesin, J. M. Alonso, E. Lopez-Corominas, A. J. Calleja, J. Ribas, M. Rico-Secades, and J. Garcia, "Design optimization of the LCC parallelseries inverter with resonant current mode control for 250-W HPS lamp ballast," IEEE Trans. Power Electron., Vol 20, No 2, Sep 2005, pp. 1197-1204.
20. Y. Ang, C. Bingham, M. Foster, D. Stone and D. Howe, "Design Oriented Analysis of Fourth-Order LCLC Converters with Capacitive Output Filter", IEE Proc. Electr. Power. Appl, Vol. 152, No. 2, March 2005, pp. 310- 322.
21. P. Naresh, C. Hitesh, A. Patel, T. Kolge, Archana Sharma and K.C. Mittal "Analysis and development of fourth order LCLC resonant based capacitor charging power supply for pulsed power applications", Rev. Sci. Instruments, 84, 084706 (2013), Published by the AIP Publishing LLC.

# Contents

	<b>Page No.</b>
<b>List of publications</b>	<b>5</b>
<b>Acknowledgement</b>	<b>9</b>
<b>Synopsis</b>	<b>11</b>
<b>List of abbreviations</b>	<b>28</b>
<b>List of symbols</b>	<b>31</b>
<b>List of figures</b>	<b>36</b>
<b>List of tables</b>	<b>45</b>
<b>Chapter-1</b>	<b>47</b>
<b>Introduction</b>	
1.1 Motivation	<b>47</b>
1.2 Background	<b>48</b>
1.3 Proposal	<b>50</b>
<b>Chapter-2</b>	<b>54</b>
<b>Literature survey</b>	
2.1 Background	<b>54</b>
2.2 DC Power Supplies	<b>56</b>
2.2.1 Regulated DC power supply	<b>56</b>
2.2.2 Switched mode power supply	<b>57</b>

2.2.2.1 Types of switching in SMPS	57
2.3 Resonant converters in DC-DC converters	58
2.4 Review of capacitor charging techniques	61
2.5 Capacitor charging power supply (CCPS)	62
2.5.1 Back ground	62
2.6 CCPS in pulsed power systems	65
2.7 Controlling techniques	67
2.8 Protection	68
<b>Summary</b>	<b>69</b>
<b>Chapter-3</b>	<b>71</b>
<b>Feasibilities of different resonant converter topologies</b>	
3.1 Resonant network topologies	73
3.2 Second (2 <sup>nd</sup> ) order resonant network analysis	74
3.2.1 Series LC resonant network analysis	74
3.2.2 Parallel resonant network analysis	77
3.3 Third (3 <sup>rd</sup> ) order LCL-T resonant network analysis	79
3.4 Fourth (4 <sup>th</sup> ) order LCLC resonant network analysis	82
<b>Summary</b>	<b>88</b>
<b>Chapter-4</b>	<b>89</b>
<b>Simulation and development features</b>	

4.1 Development features	<b>89</b>
4.1.1 Input parameters	<b>89</b>
4.1.2 Operation	<b>90</b>
4.1.3 Results	<b>93</b>
4.2 Development of control circuit	<b>99</b>
4.2.1 Operation	<b>100</b>
<b>Summary</b>	<b>102</b>
<b>Chapter-5</b>	
<b>Validation with various pulsed power systems</b>	<b>103</b>
5.1 Development of CCPS for power modulator applications to study spark gap recovery times	<b>103</b>
5.1.1 Design features	<b>103</b>
5.1.2 Development features	<b>104</b>
5.1.3 Experimental set up	<b>106</b>
5.1.4 Results	<b>107</b>
5.2 Development of CCPS for solid state pulser application	<b>109</b>
5.2.1 Development features	<b>110</b>
5.2.2 Experimental set up	<b>113</b>
5.2.3 Results	<b>114</b>
5.3 Development of CCPS for 1kJ Marx based repetitive pulsed power	<b>116</b>

system	
5.3.1 Development features	117
5.3.2 Experimental setup	119
5.3.3 Energy density	121
5.3.4 Results	121
5.3.5 Soft switching	124
5.4 Comparative analysis of 2 <sup>nd</sup> , 3 <sup>rd</sup> and 4 <sup>th</sup> order resonant converters	126
<b>Summary</b>	<b>128</b>
<b>Chapter-6</b>	<b>130</b>
<b>Protection and control features</b>	
6.1 Protection	130
6.1.1 Primary protection	131
6.1.1.1 Short circuit protection	131
6.1.1.2 Over voltage protection	131
6.1.1.3 Arc protection	131
6.1.1.4 Thermal protection	131
6.1.1.5 Protection against false triggering	132
6.1.1.6 Short circuit protection of switch in the inverter stage	132
6.1.1.7 dv/dt protection	132
6.1.2 Secondary protection	133
6.1.2.1 Radiated noise	133

6.1.2.2 Conducted noise	134
6.1.3 EMI mitigation techniques	134
6.1.3.1 EMI Filter	135
6.1.3.2 Soft switching	136
6.1.3.3 Compensation	136
6.1.3.4 Snubber and clamp	137
6.1.3.5 PCB layout and placement optimization	137
6.1.4 Conducted noise analysis and protection of 45 kJ/s and $\pm 50$ kV	139
LCLC resonant based CCPS	
6.1.4.1 Analysis of conducted EMI in CCPS	139
6.1.4.2 Effect of common mode noise on IGBT	140
6.1.4.3 Effect of differential mode noise on IGBT	145
6.1.4.4 Simulation results	146
6.1.4.5 Experimental results	149
6.2 Controlling Techniques	152
6.2.1 Operation	154
6.4.2 Observations	156
<b>Summary</b>	<b>156</b>
<b>Chapter-7</b>	<b>158</b>
<b>Conclusion and Future research</b>	

7.1 Conclusion	158
7.2 Future research	161
<b>References</b>	<b>162</b>
<b>Appendix</b>	<b>177</b>

## List of abbreviations

CCPS	-	Capacitor charging power supply
BWO	-	Backward wave oscillator
HVHF TR	-	High voltage high frequency transformer
LIA	-	Linear induction accelerator
IES	-	Inductive energy storage
MOSFET	-	Metal oxide semiconductor field effect transistor
IGBT	-	Insulated gate bi-polar transistor
SMPS	-	Switched mode power supply
BJT	-	Bi-polar junction transistor
SCR	-	Silicon controlled rectifier
EMI	-	Electromagnetic interference
EMC	-	Electromagnetic compliance
SSS	-	Solid state switch
ZCS	-	Zero current switch
ZVS	-	Zero voltage switch
SRC	-	Series resonant converter
PRC	-	Parallel resonant converter
DC	-	Direct current
AC	-	Alternate current
CC	-	Constant current
CV	-	Constant voltage
DCFN	-	DC filter network
HFI	-	High frequency inverter

RN	-	Resonant network
FBC	-	Feedback circuit
TR	-	Transformer
PPS	-	Pulsed power system
HDL	-	Highly dynamic load
CN	-	Controls
CCM	-	Continuous conduction mode
DCM	-	Discontinuous conduction mode
KVL	-	Kirchoff's voltage law
KCL	-	Kirchoff's current law
RMS	-	Rootmean square
AVG	-	Average
ADC	-	Analog to digital converter
DAC	-	Digital to analog converter
PWM	-	Pulsed width modulator
IC	-	Integrated circuit
CT	-	Current transformer
LISN	-	Line impedance stabilization network
DM	-	Differential mode
CM	-	Common mode
LED	-	Light emitting diode
PD	-	Photo diode
PT	-	Pulsed transformer
SG	-	Spark gap
HFOR	-	High frequency output rectifier

- LS - Load section
- BNC - Bayonet Neill-Concelman
- DSP - Digital signal processor
- PCB - Printed circuit board
- CAD - Computer aided design
- HMI - Human machine interface

## List of symbols

$f_s$	-	Switching frequency
$f_o$ and $f_r$	-	Resonant frequency
$L$	-	Inductor
$C$	-	Capacitor
$di/dt$	-	Rate of change of current
$dv/dt$	-	Rate of change of voltage
$Z_{Tot}$	-	Total impedance
$Z_L$	-	Load impedance
$L_r$	-	Resonant inductor
$C_r$	-	Resonant capacitor
$\omega_o$	-	Angular resonant frequency
$\omega_s$	-	Angular switching frequency
$V_{in}$	-	Input voltage
$I_L$	-	Load current
$\omega_n$	-	Normalized Angular frequency
$n$	-	Turns ratio
$V_s$	-	Source voltage
$V_{DC}$	-	Input DC voltage
$R_L$	-	Load resistance
$\omega_1$	-	First angular resonant frequency
$\omega_2$	-	Second angular resonant frequency
$\omega_3$	-	Third angular resonant frequency
$\omega_4$	-	Fourth angular resonant frequency

$X_1$	-	Reactance of first branch
$X_2$	-	Reactance of second branch
$X_3$	-	Reactance of third branch
$L_{r1}$	-	First resonant inductor
$L_{r2}$	-	Second resonant inductor
$C_{r1}$	-	First resonant capacitor
$C_{r2}$	-	Second resonant capacitor
$x$	-	Ratio of $L_{r2}$ to $L_{r1}$
$y$	-	Ratio of $C_{r2}$ to $C_{r1}$
$H$	-	Current gain
$M$	-	Voltage gain
$V_o$	-	Output voltage
$I_{Lr1}$	-	Current through $L_{r1}$
$I_{Lr1,N}$	-	Normalized current through $L_{r1}$
$I_{Lr1,rms}$	-	RMS current through $L_{r1}$
$I_{Lr2}$	-	Current through $L_{r2}$
$I_{Lr2,N}$	-	Normalized current through $L_{r2}$
$I_{Lr2,rms}$	-	RMS current through $L_{r2}$
$I_{Cr1}$	-	Current through $C_{r1}$
$I_{Cr1,N}$	-	Normalized current through $C_{r1}$
$I_{Cr1,rms}$	-	RMS current through $C_{r1}$
$I_{Cr2}$	-	Current through $C_{r2}$
$I_{Cr2,N}$	-	Normalized current through $C_{r2}$
$I_{Cr2,rms}$	-	RMS current through $C_{r2}$
$V_{Lr1}$	-	Voltage across $L_{r1}$

$V_{Lr1,N}$	-	Normalized Voltage across $L_{r1}$
$V_{Lr1,rms}$	-	RMS Voltage across $L_{r1}$
$V_{Lr2}$	-	Voltage across $L_{r2}$
$V_{Lr2,N}$	-	Normalized Voltage across $L_{r2}$
$V_{Lr2,rms}$	-	RMS Voltage across $L_{r2}$
$V_{Cr1}$	-	Voltage across $C_{r1}$
$V_{Cr1,N}$	-	Normalized Voltage across $C_{r1}$
$V_{Cr1,rms}$	-	RMS Voltage across $C_{r1}$
$V_{Cr2}$	-	Voltage across $C_{r2}$
$V_{Cr2,N}$	-	Normalized Voltage across $C_{r2}$
$V_{Cr2,rms}$	-	RMS Voltage across $C_{r2}$
$I_o$	-	Output current
$I_{in}$	-	Input current
$V_o$	-	Output voltage
$V_{in}$	-	Input voltage
$V_{rms}$	-	RMS voltage
$C_{DC1}, C_{DC2}$ and $C_{DC}$	-	DC link capacitors
$M_1$	-	MOSFET one
$M_2$	-	MOSFET two
$D_1$	-	Anti parallel diode of $M_1$
$D_2$	-	Anti parallel diode of $M_2$
$T_{ch}$	-	Charging time
$C_L$	-	Load capacitor
$T_{Total}$	-	Total time

$T_{\text{Charge}}$	-	Charging time
$T_{\text{Discharge}}$	-	Discharging time
$T_{\text{Refresh}}$	-	Refresh time
$V_{\text{sec}}$	-	Secondary voltage of HVHF TR
$V_{\text{pri}}$	-	Primary voltage of HVHF TR
$C_{\text{CE}}$	-	Collector to emitter capacitor
$C_L^1$	-	Load capacitor reflected to primary of HVHF TR
$C_2$	-	Secondary winding capacitance of HVHF TR
$C_2^1$	-	Secondary winding capacitance of HVHF TR reflected to primary
$L_2^1$	-	Secondary leakage inductance of HVHF TR reflected to primary
$L_1$	-	Leakage inductance of HVHF TR when secondary shorted
$C_1$	-	Winding capacitance of primary of HVHF TR
$C_C$	-	Coupling capacitance between primary and secondary of HVHF TR
$L_m$	-	Magnetizing inductance
$V_1$	-	Reversal voltage
$V_2$	-	Voltage across collector emitter capacitor of IGBT
$C_{\text{DC}}$	-	DC Link capacitor
$R_{\text{total}}$	-	Total resistance
$R_{f1}$	-	Feedback resistor 1
$R_{f2}$	-	Feedback resistor 2
$C_{f1}$	-	Feedback capacitor
$V_{\text{ref}}$	-	Reference voltage
$D_{i1}-D_{i6}$	-	Low frequency input rectifier diodes
$D_{o1}-D_{o8}$	-	High frequency output rectifier diodes
$S_1-S_4$ and $D_1-D_4$		IGBT switches and their respective anti parallel diodes

- GND - Ground
- $C_{L1}$  and  $C_{L2}$  - Load capacitors
- PG<sub>1</sub>-PG<sub>4</sub> - Pulsed generators
- R<sub>1</sub>-R<sub>2</sub> - Divider resistors

## List of figures

<b>Figure name</b>	<b>Page No.</b>
<b>Figure.2.1</b>	<b>55</b>
Schematic diagram of pulsed power facility	
<b>Figure.2.2</b>	<b>59</b>
Basic schematic diagram of DC-DC converter	
<b>Figure.2.3</b>	<b>60</b>
Topological structures of single, two, three and four branch resonant converter topologies	
<b>Figure.2.4</b>	<b>61</b>
Characteristics of different charging schemes	
<b>Figure.2.5</b>	<b>63</b>
Charging pattern of CCPS ( $1/T$ is the repetition rate)	
<b>Figure.2.6</b>	<b>64</b>
Charging pattern of CCPS without refresh time	
<b>Figure.2.7</b>	<b>65</b>
Detailed schematic diagram of pulsed power facility	
<b>Figure.3.1</b>	<b>72</b>
Block diagram of CCPS with pulsed power system	
<b>Figure.3.2</b>	<b>73</b>
Topological structures of 2 <sup>nd</sup> , 3 <sup>rd</sup> and 4 <sup>th</sup> order resonant	

<b>Figure.3.3</b>	<b>74</b>
Series LC resonant converter for mathematical analysis	
<b>Figure.3.4</b>	
Load current vs normalized frequency characteristics of series LC resonant converter	<b>76</b>
<b>Figure.3.5</b>	
Parallel LC resonant converter for mathematical analysis	<b>77</b>
<b>Figure.3.6</b>	
LCL-T resonant converter for mathematical analysis	<b>80</b>
<b>Figure.3.7</b>	
LCLC resonant converter for mathematical analysis	<b>82</b>
<b>Figure.3.8</b>	
Current gain (H) vs normalized frequency ( $\omega_n$ )	<b>85</b>
<b>Figure.4.1</b>	
Circuit diagram of half bridge inverter based CCPS with LCLC resonant topology	<b>91</b>
<b>Figure.4.2</b>	
Equivalent circuits in each of cycle of switching period	
(a) +ve half cycle and	
(b) -ve half cycle	<b>92</b>

<b>Figure.4.3</b>	
Experimental setup of proposed CCPS with LCLC resonant topology	<b>93</b>
<b>Figure.4.4</b>	
Voltage profile across load capacitor (100 $\mu$ F)	
(a) Simulation	
(b) experimental	<b>94</b>
<b>Figure.4.5</b>	
Current through load capacitor (100 $\mu$ F)	<b>95</b>
<b>Figure.4.6</b>	
Current through resonant inductor ( $L_{r1}$ )	
(a) Simulation	
(b) Experimental	<b>95</b>
<b>Figure.4.7</b>	
Inverter output voltage vs current through $L_{r1}$ to verify ZCS	
(a) Simulation	
(b) Experimental	<b>96</b>
<b>Figure.4.8</b>	
Current direction in each mode of ZVS	<b>97</b>
<b>Figure.4.9</b>	<b>98</b>

PWM signals for switches in the inverter stage vs current through  $L_{r1}$  to verify ZVS

**Figure.4.10** **100**  
Block diagram of control circuit

**Figure.5.1** **104**  
Block diagram of proposed CCPS with power modulator

**Figure.5.2** **105**  
Basic schematic circuit diagram of 4<sup>th</sup> order LCLC resonant based CCPS with feedback

**Figure.5.3** **107**  
Experimental setup of 4<sup>th</sup> order LCLC resonant topology with power modulator

**Figure.5.4** **108**  
Voltage profile across load capacitor (100 $\mu$ F)

**Figure.5.5** **108**  
Current through load capacitor (100 $\mu$ F)

**Figure.5.6** **109**  
Current profile observed through  $L_{r1}$

**Figure.5.7** **109**

Basic block diagram of charging source

**Figure.5.8**

111

Typical circuit diagram of LCCL resonant based charging source

**Figure.5.9**

113

Experimental setup with high voltage pulsedr

**Figure.5.10**

114

Simulation results of charging voltage and current through resonant inductor

**Figure.5.11**

114

Experimental results of charging voltage and current through resonant inductor

**Figure.5.12**

115

Simulation results of charging voltage with 9 kHz repetition rate

**Figure.5.13**

116

Experimental results of charging voltage and with 9 kHz repetition rate

**Figure.5.14**

117

Typical circuit diagram of LCCL resonant based charging source

**Figure.5.15**

120

Experimental setup of 45 kJ/s CCPS along with 1kJ/s Marx based system

**Figure.5.16**

120

Experimental setup of 45 kJ/s

(a) Front view

(b) Back view

(c) Left hand side view

(d) Right hand side view

**Figure.5.17**

Charging voltage profile across load capacitor ( $0.9\mu\text{F}$ )

**122**

(a) +ve charging

(b) -ve charging

**Figure.5.18**

Current profile through resonant inductor ( $L_{r1}$ )

**123**

**Figure.5.19**

Voltage profile across  $0.9\mu\text{F}$  capacitor (+ve) with 5Hz repetition rate

**124**

**Figure.5.20**

Current through  $L_{r1}$  vs inverter output voltage to verify ZCS

**124**

**Figure.5.21**

Current through  $L_{r1}$  vs PWM controlling signals for IGBTs in the inverter circuit to verify ZVS

**125**

**Figure.5.22**

**127**

Simulation circuit of CCPS for comparative analysis

<b>Figure.6.1</b>	<b>135</b>
Typical EMI filter network	
<b>Figure.6.2</b>	<b>140</b>
Circuit diagram of power supply with parasitic capacitance without faraday shielding	
<b>Figure.6.3</b>	<b>141</b>
Common mode current ( $I_{CM}$ ) to find the effective voltage across CE terminals of IGBT	
<b>Figure.6.4</b>	<b>142</b>
Circuit diagram of power supply with parasitic capacitance with faraday shielding	
<b>Figure.6.5</b>	<b>142</b>
Topological structure of LCLC network with high frequency transformer parameters	
<b>Figure.6.6</b>	<b>144</b>
Magnitude and phase plot for equation 6.1	
<b>Figure.6.7</b>	<b>145</b>
Topological structure of LCLC network with CE capacitance of IGBT with resonant network	
<b>Figure.6.8</b>	<b>146</b>
Magnitude and phase plot for the equation 6.2	

**Figure.6.9**

Simulation circuit to see the effect of conducted noise

- (a) For common mode noise
- (b) For differential noise **147**

**Figure.6.10**

Conducted noise voltage (Red) and voltage across the capacitor (Blue)

[Between one of the terminal of HVHF transformer to the ground]

- (a) For 10pF  $C_c$  **148**
- (b) For 5nF  $C_c$

**Figure.6.11**

Differential noise voltage (Red) and voltage across CE terminal capacitance of IGBT (Blue) **149**

**Figure.6.12**

Common mode noise

- (a) Voltage between 1<sup>st</sup> terminal of primary of HVHF transformer to ground **150**
- (b) Voltage between 2<sup>nd</sup> terminal of primary of HVHF transformer to the ground

**Figure.6.13**

Differential mode noise

- (a) Voltage across primary terminals of HVHF transformer **151**

(b) Voltage across inverter output

**Figure.6.14**

**152**

Block diagram of pulsed power facility with feedback control circuit

**Figure.6.15**

**153**

Internal circuit of feedback box is shown in Figure.5.10.

**Figure.6.16**

**154**

Experimental setup of feedback (top view)

**Figure.6.17**

Voltage profile across load capacitor (100 $\mu$ F)

**155**

(a) Simulation

(b) Experimental

## List of tables

<b>Table Name</b>	<b>Page No.</b>
<b>Table.3.1</b> Summarized table 1	<b>86</b>
<b>Table.3.2</b> Summarized table 2	<b>87</b>
<b>Table.4.1</b> Rating of 20J/s CCPS	<b>89</b>
<b>Table.4.2</b> Components list of 20J/s CCPS	<b>91</b>
<b>Table.5.1</b> Rating of 500J/s CCPS	<b>103</b>
<b>Table.5.2</b> Components list of 500J/s CCPS	<b>106</b>
<b>Table.5.3</b> Rating of 3.7 kJ/s CCPS	<b>110</b>
<b>Table.5.4</b> Components list of 3.7 kJ/s CCPS	<b>112</b>

<b>Table.5.5</b>	<b>117</b>
Rating of 45 kJ/s CCPS	
<b>Table.5.6</b>	<b>119</b>
Components list of 45 kJ/s CCPS	
<b>Table.5.7</b>	<b>127</b>
Comparison table	

# Chapter-1

## Introduction

---

High voltage capacitor charging power supplies (CCPS) are used in various industrial and pulsed power applications. Designing a reliable and efficient charging power supply for pulsed power systems is always a complex job because of associated dynamic load such as electron gun, laser, magnetron etc. During generation and discharge of high intensity pulses the associated charging power supply of pulsed power system undergoes a surge reversal of high amplitude in voltage and high frequency (MHz) noise.

To protect the CCPS against this impulse noise, fast protection is needed. Conventionally series resonant converter based CCPS is used for pulsed power applications. They are good for static load conditions. But in case of non-linear loading, these CCPS lacks in providing suitable dynamic protection against surge reversal and high frequency noise during discharging period.

Other resonant converters such as parallel LC and third order resonant converter have been utilized previously in the development of high voltage CCPS. These power supplies are also suffering with serious issues like lack of DC blocking and poor part load efficiency. An investigation is needed to find out the root cause behind the failure of charging power supply when interfaced with pulsed power system.

### 1.1 Motivation

A research topic on design and development of efficient and reliable resonant converter based fast ( $>40\text{kJ/s}$ ) CCPS with improved protection for pulsed power applications has been chosen.

## 1.2 Background

Over last two decades pulsed power technology has been using for various non-military, medical and defence applications. Accelerator and pulsed power division, BARC, Mumbai is one of those working on this technology to generate high intensity pulses and electron beams using pulsed power systems for medical and industrial applications. A suitable capacitor charging power supply (CCPS) is required to charge pulsed power systems.

The power supply is termed as capacitor charging power supply instead simple DC power supply. Since, pulsed power system is a combination of switches (controlled and uncontrolled) and energy storage (capacitors and inductors) elements connected in different fashion to obtained required pulsed width and rise time. Designing a reliable and compatible charging power supply with charging rate more than 40kJ/s for pulsed power system is still a barrier and a challenging task. Technical difficulty arises from simultaneous requirements on power rating, energy conversion efficiency, lifetime and cost. Designing a power supply to charge simple capacitor is not a difficult task, but designing a high charging rate and repetitive power supply for particular application is a difficult task. Charging rate, repetition rate, protection, compatibility and cost are the critical design issues. So, only few research laboratories and manufacturing companies are working on these kinds of power supplies. Usage of resonant converters in the development of capacitor charging power supply (CCPS) becomes popular due to their inherent short circuit proof, load independent constant current and soft switching.

Two element (series LC and parallel LC), three elements (LCL, CLC, CLL and LLC) resonant converter based CCPS are used for the design of CCPS. Designers are restricted them self up to three energy storage elements in the resonant converter stage of power supply due to complexity, number of frequencies and overall size of power supply. Series LC

resonant converter based CCPS is more commonly used charging power supply in pulsed power technology. Most of the times 2<sup>nd</sup> and 3<sup>rd</sup> order resonant based CCPS are suffer from protection against dynamic noise generated at load end of pulsed power supply. Highly dynamic loads like Klystron, Magnetron and backward wave oscillator (BWO) when connected to pulsed power system generates highly dynamic noise which leads to frequent failure of controlled switches in the inverter stage of power supply.

Dynamic noise is generated due to mismatched load at the output of the pulsed power (PP) system. When a pulsed power (PP) system sees the mismatched load, part of the energy reflects and it becomes ringing of 10-100MHz frequency. It is difficult to attenuate this high frequency noise while charging the capacitor of PP system. The proposed fourth order resonant converter based capacitor charging power supply (CCPS) provides constant current and for energy reflection the same resonant network will acts like a low pass filter. The design is such a way that it fulfils both the purposes while charging and discharging.

Second and third order resonant converter based CCPS, operating with pulsed power systems are incapable of attenuating these kinds of energy reflections during charging and discharging times of pulsed power system. Controlled switches in the inverter stage are mostly effected due to dynamic noise. In these power supplies dynamic noise leads to frequent failure of IGBT switches in the inverter stage. Because it generated high voltage across CE terminals of IGBT switches without any attenuation.

So, the running cost of the power supply will be increases. The time arises to investigate a compatible, fast and repetitive CCPS for pulsed power application, which can overcome all the difficulties in two element and three element resonant based CCPS. To overcome the limitations of two and three element resonant converter based CCPS it is the time to explore a new kind of resonant converter topology for pulsed power application.

Main requirements of CCPS when designing for pulsed power applications are

1. It should operate for wide range load variation
2. It should provide inherent short circuit protection
3. It should provide load independent constant current
4. It should provide soft switching
5. It should overcome dynamic noise effects.

The first five conditions can be fulfilled by two element and three element resonant converter based CCPS either increasing number of switches or else operating at different conditions, but the 5<sup>th</sup> condition cannot fulfilled by two element and three element resonant converter based CCPS. Because two elements and three elements resonant converter based CCPS are lacking in compatibility and reliability with pulsed power system. In this research proposed a fourth (4<sup>th</sup>) order resonant converter and its application in the design of CCPS for pulsed power application. The proposed 4<sup>th</sup> order resonant converter based CCPS fulfil all the five requirements. Third and fourth conditions are crucial in the design and choosing a resonant topology. Since, the load for a power supply is an energy storage capacitor and it is need to be charged with constant current to overcome in drawing short circuit power from mains. In addition the chosen resonant topology should provide soft switching (i.e. either zero current switching or zero voltage switching) to minimize the losses in the inverter stage of power supply.

### **1.3 Proposal**

To design and develop a reliable and compatible charging power supply for pulsed power applications, wherein charging rate is in the multiples of 10kJ/s, typically more than 40kJ/s. A resonant converter based capacitor charging power supply (CCPS) with an improved protection schemes are proposed for various pulsed power applications.

Various challenges involved in designing of charging source. They are

1. Topology selection
2. Load independent constant current
3. Soft switching
4. High voltage and high frequency transformer design
5. Protection
6. Feedback technique

The above mentioned parameters become so critical in designing power supplies higher charging rates. So, the power supply should withstand various problems from the load side.

The proposed 4<sup>th</sup> order resonant converter provides load independent constant current at switching frequency ( $f_s$ ) equal to resonant frequency ( $f_r$ ). Soft switching (zero current switching) operating conditions are derived mathematically in the further chapters. In addition this converter provides zero voltage switching by adjusting dead time between two controlled switches of same leg of H-type full bridge inverter circuit. Investigated total four 4<sup>th</sup> order resonant converter based CCPS for four different pulsed power applications. One of the four 4<sup>th</sup> order resonant based CCPS prototype developed to see basic operation and to observe the load independent constant current and soft switching. The second resonant topology has been utilized to design CCPS for power modulator application by incorporating high voltage high frequency (HVHF) transformer, wherein the design utilized the leakage inductance of HVHF transformer is one of the resonant elements to make the system compact. The third topology is used to develop a high repetition rate (9 kHz) CCPS for solid state switch based pulser application. Finally a fourth resonant topology has been utilized in the development of fast (45kJ/s), repetitive (10Hz) and bi-polar (+/- 50kV) CCPS for 1kJ Marx based system. Previously developed (or) the power supplies which are available in the market are lacking in providing protection for power supply against dynamic noise. Improvements in the protection schemes will improve the reliability and makes the power

supply compatible with pulsed power system operated with highly dynamic loads. There are two basic protection and they are primary protection and secondary protection. These include short circuit protection, over voltage protection, arc protection (an arc protection we need to detect the arc first. Arc will be detected by putting CT in the ground path. This CT will sense the noise and intimate to the controller. When this arc continues for 5 to 6 times then a alarming signal generated by micro controller), thermal protection, protection against false triggering, short circuit protection of switch in the inverter stage, dv/dt protection, radiated noise and conducted noise. All these protections schemes are in corporate in the power supply to make power supply reliable. More importantly protection against conducted noise has been overcome effectively in the power supply by incorporating shielding between primary and secondary of HVHF transformer and with that of proposed 4<sup>th</sup> order resonant topology. The detailed analysis of this protection scheme, generation of conducted noise, its effect of conducted noise and how it leads to failure of controlled switch in the inverter stage CCPS has been discussed in coming chapters.

Controlling techniques plays an important role in the power supply design, wherein the charging voltage across load capacitor is controlled. A recent advancement occurs in the field of pulsed power technology using controlled spark gaps, so called trigetrons. In this case sprak gap electrodes are charged to a specified voltage through an energy storage capacitor with charging source and then apply a controlled low voltage to break down spark gap. So, a controlled mechanism is needed to charge the load to a specified voltage level. Otherwise spark gap continuously breaks down due to over voltage across load capacitor.

Feedback controlling techniques are adopted in CCPS to charge load capacitor to various voltage levels. A light emitting diode (LED) and photo diode based feedback controlled scheme have been demonstrated to control the voltage across load capacitor. Input to this controlled circuit is obtained from lower arm resistor of voltage divider which is connected

across load capacitor and compares with the reference voltage. The error signal will control the on-off timing of controlled switches in the inverter stage. Once the target voltage reaches then the error becomes zero, under this condition the power delivered to the load is zero. Simulation and experimental results are verified and validated with the mathematical results for each 4<sup>th</sup> order resonant based CCPS for different pulsed power applications. The proposed 4<sup>th</sup> order resonant based CCPS is cost effective, reliable, compatible and compact for a specific rating over all two element and three element resonant based CCPS for pulsed power applications. This research and development guides the designers how they can choose resonant converters, which topology can provide constant current gain, high voltage gain and how one can protect the CCPS from conducted noise generated at load with 4<sup>th</sup> order resonant converter.

The literature on pulsed power systems, application of resonant converters in the design of power supply, resonant converters types and their application in pulsed power technology, merits and limitations, protection schemes and controlling techniques are presented in chapter 2. In chapter 3 discussed feasibilities of various resonant converter topologies for constant current application for the design of power supply for pulsed power applications. In chapter 4 presented the design, simulation and experimental details of selected 4<sup>th</sup> order resonant converter topologies. Chapter 5 covers the development and testing of other 4<sup>th</sup> order resonant converter based CCPS and their validation with pulsed power system. In chapter 6 presented the effective protection schemes to handle EMI related issues, in addition presented a control scheme for voltage control. Conclusions and future scope are presented in chapter 7.

# Chapter-2

## Literature survey

---

A literature survey has been done in the field of pulsed power technology, power supplies, application of resonant converters in DC power supplies, controlling and protection of power supplies for pulsed power application has been investigated and presented in this chapter.

### 2.1 Background

Pulsed power is a kind of technology in which energy accumulates over a long period of time and releases it into a load for very short duration of time, thus generates a very high instantaneous power. Over the last two decades, more and more non-military applications of pulsed power technology have been studied. More than one hundred possible applications can now be listed. In particular gas and water processing, sterilization, nano-particle processing and surface treatment to name a few. More about industrial, defence, environmental and medical applications of pulsed power systems have been discussed in [1-2]. The average power delivered to a load is very high in very short span of time. In such cases the amplitudes of both voltage and currents are very high. Narrow pulses (with high peaks in voltage and currents) generated by pulsed power systems are used in the generation of high power microwave, electron beams and flash x-rays. Marx based systems (single and replate), linear induction accelerator (LIA), inductive energy storage (IES), pulser and power modulator are the few pulsed power systems used in the generation of short pulses. Replate is nothing but repetitive mode of operation. In pulsed power system this mode operation is preferred to

deliver more average power in a single burst. One burst can be of many shots. Aforementioned systems are used in medical, commercial, industrial and non military applications. Pulsed power systems are primarily energy storage systems, in which capacitors, inductors, un controlled and sometimes controlled switches are connected in different fashion to generate postulated pulses with certain rise time and pulsed duration. Pulsed power systems with capacitive energy storage employed various switches named as magnetic, semiconductor and spark gap switches. Magnetic switches are saturable inductors that utilize the nonlinear magnetization of magnetic material, especially the saturation. When the magnetic material used in the switch is unsaturated, the magnetic switch has high impedance which represents the “off state”. When the core becomes saturated, it has much lower (typically a factor  $\mu r$  lower) impedance which is the “on state” Semiconductor switches used in pulsed power systems include thyristors, MOSFET’s (Metal-Oxide-Semiconductor Field-Effect Transistor), and IGBT’s (Insulated Gate Bipolar Transistor).

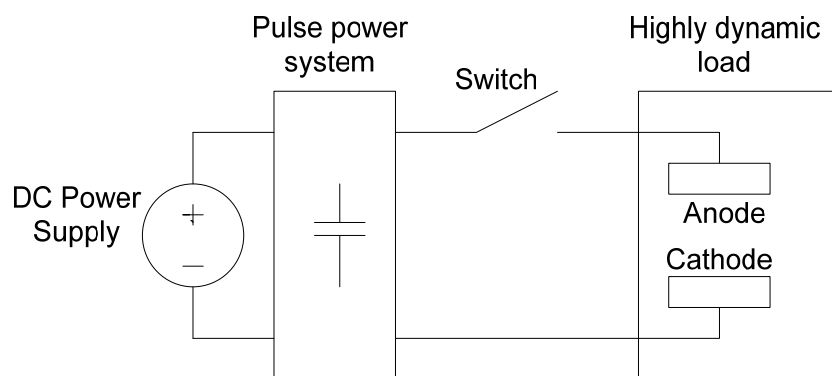


Figure.2.1: Schematic diagram of pulsed power facility

Thyristors can hold a high voltage in excess of several kV and carry a large current (kA). However, the switching time is slow ( $\sim \mu s$ ), and thyristors are often used for microsecond pulsed generation. Spark gap switches are widely used in pulsed power systems. In comparison with other switches, the main advantages of spark gap switches are a high hold-off voltage, large conducting current, high energy efficiency and low cost. More on these

devices encountered in [3-5]. Schematic diagram of pulsed power system along with DC power supply and load is shown in Figure.2.1. In this diagram pulsed power system has been shown with a simple block consisting of energy storage capacitor. Pulsed power systems need to be the command trigger type.

In the command trigger type system, once the charging completes it requires to give trigger to the PP systems. So in CCPS, charging is made with constant current (CC) and once it reaches particular voltage, pulsed power system erects and goes to zero voltage. Again we need to reach to the same level in the definite and fast time, there you need the CCPS. But in conventional, it cannot fast and definite.

The energy stored in the pulsed power system is delivered to a highly dynamic load through a controlled or uncontrolled switch. To charge the capacitor of pulsed power system needs a DC power supply with proper protection. Power supply is a heart for pulsed power system, where it has to handle dynamic noise generated in the system and short circuit conditions.

## **2.2 DC Power Supplies**

### **2.2.1 Regulated DC power supply**

Conventional high voltage DC power supplies are not suitable for pulsed power applications. Reasons like they are designed to operate at constant or near constant load conditions. Moreover it draws large amount of inrush current from the mains, when the load is capacitive in nature. Size and weight too increases with increase in output voltage and charging rate. Furthermore overall efficiency is much lesser for regulated output due to higher power loss. Regulated DC power supplies are deficient in providing charge to load if the repetition rate in kHz range. In view of aforementioned demerits conventional high voltage DC power supplies are incapable as a charging source to charge capacitive nature of loads with high repetition rate.

### **2.2.2 Switched mode power supply**

Switch-mode power supplies (SMPS) results in low power dissipation compared to conventional high voltage DC power supplies. Insulated gate bi-polar transistor (IGBT) and metal oxide semiconductor field effect transistors (MOSFET) are used as switching elements and are operated in saturation region (for ON state) and in cut off region (for off state). The other switches like bi-polar junction transistor (BJT) and silicon controlled rectifier (SCR) can be used. Though BJTs are fast enough but not used due to tail current and are not available in higher rating, on the other hand SCRs are available for higher rating but they demands for extra commutation circuits. High frequency operation reduces the component size and weight of energy storage elements and transformer in SMPS, at the same time it comes at a cost of high complexity, switching stress and interferences. Switch mode power supplies efficiency is more over conventional DC power supplies due to low losses. Due to switching limitation in the switching device one cannot increase the switching frequency beyond certain limit to make more compact system.

#### **2.2.2.1 Types of switching in SMPS**

Two types of switching are present, more commonly called as hard switching and soft switching. Most of the times load demands for sudden shutdown of power supply during operation (charging in case of capacitive nature loads). In these conditions a sudden turnoff of switching devices occurs in the power supply. At that instant of time the voltage across switching device or current through the device is not zero or at a finite value. This kind of switching called as hard switching. In hard switching the switching losses are very high and these losses are directly proportional to the switching frequency. So, the limitation in switching frequency has encountered when it is hard switching. Switching losses are very high in this case. Moreover this kind of switching introduces electromagnetic interference (EMI) into the system. To overcome or to minimize switching losses and EMI effects needed

extra compensation networks or circuits to transfer switching losses from switching device to auxiliary circuit. Such switching present in basic SMPS like boost and other isolated converters namely fly back and push-pull converters [6-7]. Switch mode power supplies efficiency largely depends on switching losses occurring in solid state switches (SSS) of inverter stage. If the switch is made to change its state from OFF to ON and vice versa, instant at which either voltage across it or current through is zero, then aforementioned shortcomings (switching losses) are minimized. Such switching action is termed as soft switching (SS). Zero-voltage-switching (ZVS) and zero current switching (ZCS) are the two types of soft switching methods.

Soft switching (ZVS or ZCS) can be achieved in different ways like adding passive auxiliary reactive components [8], adding active auxiliary circuit [9], modifying the switching strategy [10-11] and changing the converter topology (e.g. resonant converters). Merits and limitations of various soft switching methods are reviewed in [12-13]. Operation and mode boundaries of both ZVS and non-ZVS in case of series resonant converter (SRC) and parallel resonant converter (PRC) and their design procedure is presented in [14].

### **2.3 Resonant converters in DC-DC converters**

Soft switching (ZCS and ZVS) and constant current can be achieved by implementing DC to DC converters with resonant circuit. The basic DC-DC converter is shown in Figure.2.2. Different types of non-isolated and isolated DC-DC converters are reviewed in [15]. A half bridge or full bridge high frequency inverter is fed from a DC source. The inverter operated with very high frequency  $\geq 20$  kHz, which converts constant DC voltage in to a square wave with a frequency equal to switching frequency. The input source to the inverter may be either constant voltage or constant current source. Resonant converter followed by inverter, the output of resonant converter is sine wave whose frequency equal to resonant frequency, then

once again it rectified and given to the load. Before delivering to the load a high value capacitor is connected across the load to filter out ripples.

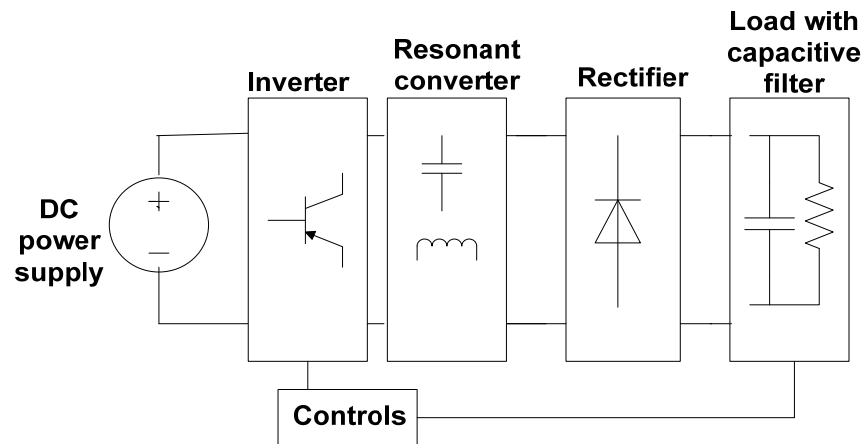


Figure.2.2: Basic schematic diagram of DC-DC converter

If operating frequency in kHz range a small value capacitor is enough to filter out ripples, but if the operating if inverter operating at fundamental frequency (i.e. 50Hz) needs high value capacitor to filter out ripples in the output voltage. In some cases, if it is a resonant converter based power supply a low value capacitor may effect on the operation of resonant conversion. In this case if a large value capacitor connected at the output it will not alter the resonant converter operation as well as it can filter all ripples in the output voltage. A voltage source in series with large inductor makes a constant voltage source into a constant currents source and is feeds to the resonant network [16-17]. Current source fed resonant converter are not so popular, because a large inductor should use at the input to maintain constant current [18-20]. Voltage source fed inverter followed by series resonant converter is a popular DC-DC converter for industrial heating applications [21-22]. Parallel load resonant converter is another attractive topology, provides load independent constant current and soft switching at  $f_s = f_r$ . Parallel resonant inverter with current source as an input source with a resonant capacitor connected in parallel with resonant inductor makes the constant current source for industrial heating applications [23-24]. A novel distributed control scheme for a soft

switching multi inverter system with LCL-resonant circuit for induction heating application is proposed and compared to a classical central control, such as improved reliability and simple adaption of the control to any number of inverter connected in parallel. A comparison of the resonant topology is done in the high voltage DC application [25]. Series-parallel resonant converter or LCC resonant converter has been the topic of extensive investigation in three element resonant network for different industrial applications [26-27]. Fourth order LCLC resonant converters are studied and implemented with output filter capacitor [28-29]. Operating at constant switching frequency and tuned to resonant frequency the LCLC DC-DC converter achieved zero switching losses.

A lot more resonant topologies previously reported for constant current and constant voltage applications. Single branch, two branch, three branch and four branch resonant topologies of second, third, fourth and even fifth order resonant converters are analyzed and reviewed for the same application in [30]. Topological structures of single, two, three and four branch resonant converter topologies are shown in Figure.2.3.

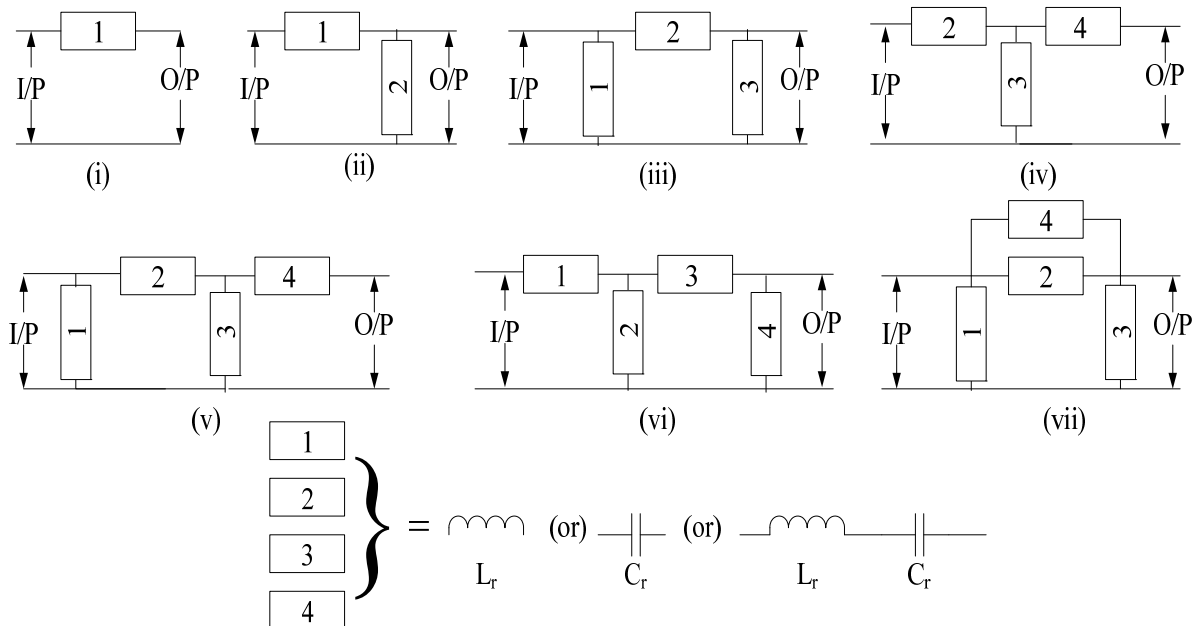


Figure.2.3: Topological structures of single, two, three and four branch resonant converter topologies

Application of resonant converters in DC-DC step up or step down converters makes the power supply efficient, smaller and controllable. Some of the common applications which are not required precise control of voltage and current are ballasts for fluorescent lamps [31-32], power factor correction [33-34], induction heating [35-36], welding [37], inductive power transfer [38] and high voltage power supply [39-40]. Reviewed other applications where current and voltage are maintained to constant throughout operation such applications are electric arc welding [41], laser diode drivers [42-43], magnet power supplies [44], illumination systems [45], battery charging [46], capacitor charging [47-49] and electrochemical processes [50].

## 2.4 Review of capacitor charging techniques

Capacitor can be charged in multiple ways, some of these techniques are reviewed in [51]. Resistive, one cycle resonant, constant current and constant power charging are the few charging methods. In ideal case the maximum efficiency is 50% in resistive charging, as a result this charging technique is utilized in the circuits where the charging rate is low, typically about at 200J/s. More over five time constants  $5RC$  is required for the capacitor to reach 98% of maximum desired voltage is shown in Figure.2.4. Medium and high power applications typically opted for one cycle resonant charging.

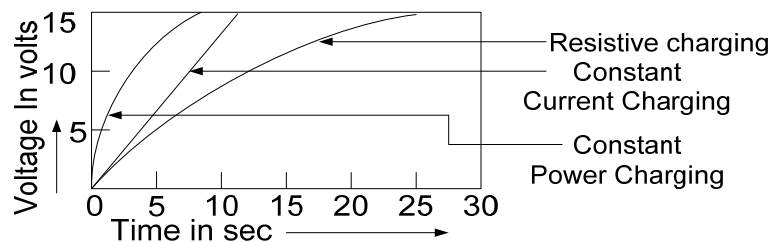


Figure.2.4: Characteristics of different charging schemes

Main drawback with this charging method is it needs an additional energy storage capacitor, inductor. The switch used in this power supply can be a simple diode or a unidirectional

closing switch like a thyatron or SCR. Constant current is another type of charging method and is more preferred charging method than all other charging methods, where minimum volume and regulation are the critical design issues. Constant current charging method limits the inrush current at the time of starting and main the same current at the end of charging (i.e. near to target voltage). During charging, it is important to limit the output current for safe operation and power supply must operate in constant current (CC) mode. Once the capacitor is charged to a required target voltage level, the charging power supply changes its mode from CC to constant voltage (CV) to maintain constant voltage across the capacitor.

In order to comply with stringent mains voltage variations, the charging power supplies are operated with so called constant-power charging techniques [25]. In the charging cycle, initially the charging current is high which progressively decrease during the charging with the same factor with which voltage increases. In this way instantaneous power delivered in the charge cycle is constant and therefore the current drawn from three phase mains also remains constant. In Figure.2.4 characteristics of three different charging schemes has been shown. Controlling both parameters like voltage and current simultaneously is unmanageable. Time taken to reach the target voltage is high in resistive charging as compared to other two. Though time taken to reach the target is less in case of constant power compared to constant current, but controlling both voltage and current simultaneously is difficult, on the other hand controlling a single parameter (current) is easy in case of constant current charging mode.

## **2.5 Capacitor charging power supply (CCPS)**

### **2.5.1 Back ground**

A power supply is required to charge a capacitor (an energy storage capacitor is a main charging element in pulsed power system), so called capacitor charging power supply (CCPS). Some of the salient features of CCPS are

1. The wide range of load conditions over which it should operate [52-53]
2. It should sustain for highly dynamic load conditions
3. It should not draw any short circuit power from mains at the beginning of the charging cycle to a very light load conditions at the end of charging cycle for a pre defined target voltage.

Capacitors used in pulsed power systems are needed to be charged prior to each repetition of energy release to the load. The rate at which the capacitor discharges is called the repetition rate. It may be a few 0.01Hz for large capacitor banks to a few kHz for certain lasers with small stored energy. After the energy storage capacitor discharges, it must recharge to a specified voltage with the capacitor charging power supply (CCPS) [15].

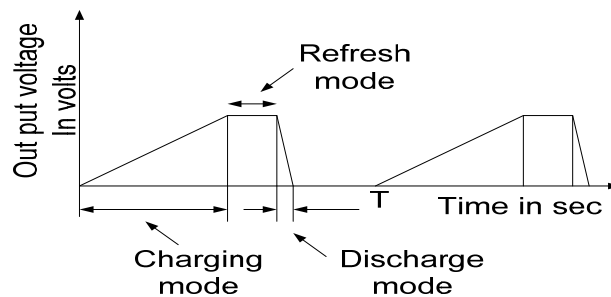


Figure.2.5: Charging pattern of CCPS ( $1/T$  is the repetition rate)

The voltage profile across energy storage capacitor connected at the output terminals of CCPS is shown in Figure.2.5. The average output voltage is decreased due to the presents of refresh mode is shown in Figure.2.5. As soon as the capacitor is charged to the particular voltage it discharges, hence per cycle time is reduced and the average output is increased. The voltage profile which is shown in Figure.2.6 has been divided in to two named charging and discharging. In discharging period, the CCPS has been disabled from the mains and rapidly discharges across the load, which is inactive in the charge mode. The discharge mode is normally much shorter than the charging period. The CCPS enters near short circuit conditions across its output terminals in charging mode. In this mode CCPS operates at its

maximum charging mode to refresh mode when the target voltage is reached and remains in this mode until load discharges the capacitor. In charging mode capacitor does not supply any energy to the load. The amount of time CCPS remains in this mode is determined by how quickly the capacitor stored energy can be discharged to the load. The output voltage may drift due to capacitor leakage and parasitic resistances.

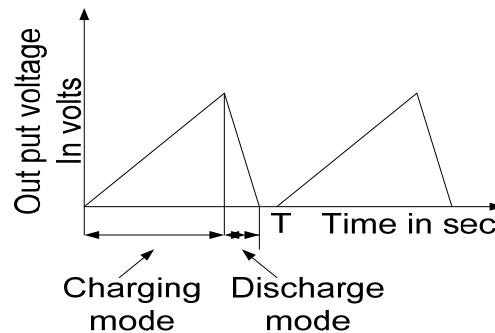


Figure.2.6: Charging pattern of CCPS without refresh time

Instantaneous output power is almost zero at the beginning of the charging mode. If the charging current is constant, the peak instantaneous output power occurs at the end of the charging mode. Refresh mode is typically a low power mode, since current is small as compared to charging mode. Average output power for a CCPS depends on the repetition rate, wherein the capacitor discharges at the end of charging, which corresponds to operation without refresh mode. Rating of CCPS is given in kJ/s instead of kW. The rating kJ/s indicates that how fast the capacitor charged to a particular load. Application of switch mode conversion achieved an improvement in efficiency, regulation and a reduction in size and weight. The same technology has been adopted in the design of CCPS by operating at high switching frequencies to reduce the size and weight of the CCPS.

Regulation can be improved through the utilization of the control techniques such as pulsed width modulation or constant on time control. These control techniques can also be employed in the “keep alive” mode, which does not exist in the other techniques presented in this paper

[54-55]. As a result, the CCPS may operate over a broad range of load repetition rates and still maintain the desired output voltage. Capacitor leakage may be replaced in a burst fashion or in a continuous fashion similar to trickle charging a battery [56].

## 2.6 CCPS in pulsed power systems

Resonant converters are adopted in CCPS to avail benefits like constant current, short circuit proof and soft switching which is already been discussed in the previous section. Second, third and fourth order resonant topologies are the attractive topologies to design charging power supply.

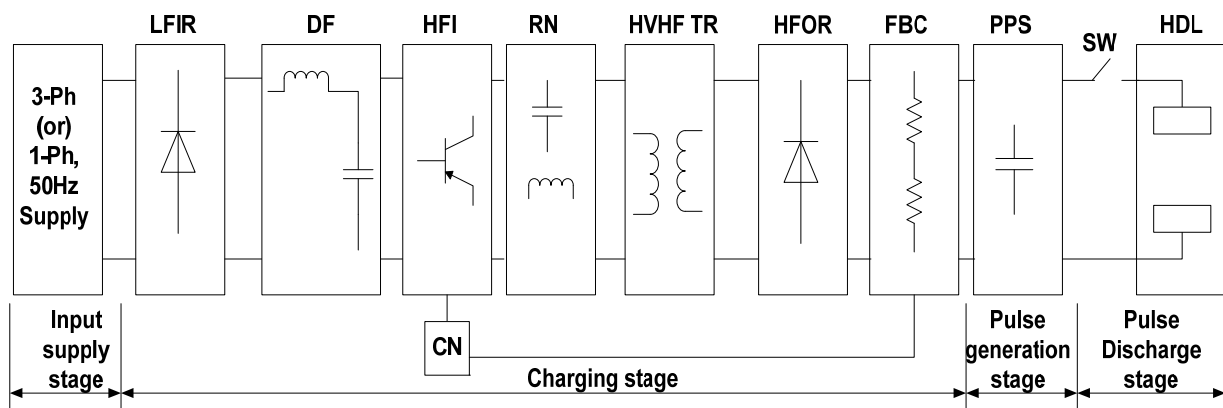


Figure.2.7. Detailed block diagram of pulsed power facility

Whereas low frequency input rectifier (LFIR), DC filter (DF), high frequency inverter (HFI), resonant network (RN), high voltage high frequency transformer (HVHF TR), high frequency output rectifier (HFOR), feedback circuit (FBC), pulsed power system (PPS), switch (SW), highly dynamic load (HDL) and control circuit (CN).

Aforementioned resonant converters provide load independent constant current and soft switching in various operating conditions. The detailed schematic diagram for pulsed power facility is shown in Figure.2.7. It has been divided in four stages, wherein first stage is supply mains, second stage comprises charging stage, third stage is pulsed generation and shaping stage and last stage is pulsed discharge stage. Second order series LC resonant converter

provides load independent constant current when operated in discontinuous conduction mode. All other resonant converter topologies achieve load independent constant current and soft switching in various operating modes. The discontinuous conduction mode operation achieved only when resonant frequency ( $f_r$ )  $\geq 2f_s$  ( $f_s$  = Switching frequency). Under this operating condition the series LC resonant converter provides load independent constant current and inherent zero current switching. Current in the discontinuous conduction mode is linear and it is constant over each half of switching cycle. Series resonant converter based charging sources are more popular for pulsed power applications. These converter characteristics have been discussed in [57].

Effect of leakage inductance on resonant components and the detailed analysis of di/dt effect were discussed in [58], wherein improvement in dynamic response have been achieved by pulsed width modulation with constant switching frequency. The design of series resonant based high wattage power supply for industrial magnetron. Series loaded resonant converter based power supplies current characteristics for industrial magnetron, power modulator and other applications have been analyzed and designed with minimum component stress are discussed in [59-61]. There are other resonant topologies such as parallel LC, combination of series LC- parallel LC and LCC resonant converters are used as constant current source to charge pulsed power systems [62]. Due to high peak currents and thermal management, series LC resonant based charging source is not preferable in high charging rates. New design procedure for three element converters is also introduced for charging applications in [63]. DC/DC power convertor operating modes at constant resonant frequency are identified and discussed. Generalized state-plane analysis of a half bridge converter performance characteristics were analyzed in [64-65]. LLC type series resonant converter operation with PWM control is presented in [66]. Series resonant converter is modified by adding an inductor in parallel with the transformer primary (or secondary) forms a LCL-type series

resonant converter and its analysis were presented in [67]. Optimum design of a LCC parallel-series inverter with resonant current mode control has been discussed in [68]. Design and development features of a repetitive capacitor charging source for pulsed power applications is presented in [69]. Dynamic nature of the capacitor charging causes a shift in the resonant frequency of the PRC. Repetitive charging sources are preferred to increase the average power delivered to load. One such charging source with LCL resonant topology has been discussed in [70]. Series- parallel load resonant converter operating at a fixed frequency is used in the design of CCPS [71-72], is a special kind of resonant circuit which does not require any kind of control circuit.

## **2.7 Controlling techniques**

Controlling is necessitated for certain pulsed power applications like some system demand for lower voltage and high repetition rate, on the other side some pulsed power systems demand for higher charging voltage with lower repetition rate. There are different ways to control voltage and current in resonant converter based DC power supplies. Some of the controlling techniques examined, and listed are clamped mode control, phase control, variable frequency control, asymmetrical duty cycle control, integral cycle control, self-sustained oscillating control, and asymmetrical voltage cancellation control. The clamped mode control, complete steady state analysis, investigation of different operating modes and mode boundaries has been extensively reported for SRC [73]. The mode boundaries for ZVS and non-ZVS operation in SRC and PRC and their design are discussed in [74]. Synthesis of phase controlled resonant converters is reported in [75] and detailed analysis of various phase-controlled topologies, namely SRC is described in greater details in [76]. The output voltage of a RC can be controlled by varying the operating frequency. However, it is difficult to optimize the design of magnetic components and filters for variable frequency operation. Operation away from the resonant frequency causes reactive power loading on the inverter

switches, thereby reducing the conversion efficiency [14]. It is unsuitable for applications with frequency locking requirements.

This control method leads to asymmetric operation of the high-side and the low-side switches and leads to unequal voltages across the leg capacitors; it has been popularly applied to power converters (resonant as well as non-resonant) due to simpler implementation and soft-switching [77]. To control the output voltage while maintaining near resonance operation, the integral cycle control was proposed [78].

The output voltage is controlled by the duty ratio of powering mode and free-resonant mode. The phase angle between the bridge output voltage and current can be controlled as a result the switching frequency is no longer externally imposed as in the conventional variable frequency control and the converter is said to be operating in so called self-sustained oscillating mode [79]. This control method [80] is generalization of the conventional clamped mode and asymmetrical duty-cycle control techniques, which is more advantageous for output voltage variations.

## **2.8 Protection**

Protection is another major criterion in the design of power supply, most of the power supplies are lagging in this regard. Regards less of load conditions the power supply should provide proper protection against open circuit, short circuit, over temp, Arc and output reverse pulsed protection. Protection is mandatory for power supply when operating with highly dynamic pulsed loads. In addition other protections have to be made to tolerate electromagnetic interference (EMI),  $dv/dt$  and  $di/dt$  against noise [81-84]. Some of the protection techniques are reviewed previously for EMI,  $dv/dt$  and  $di/dt$ . Interfacing of power supply with pulsed power systems, difficulties in interfacing and protection are discussed by Bushnell A.H. [85].

## Summary

In this chapter studied the importance of pulsed power technology and identified various applications of pulsed power systems. Study continued in search of different pulsed power systems which are used to generate high intensity pulses with short duration of time. Noticed some of the pulsed power systems like Marx based system, linear induction accelerator, inductive energy storage system, pulser and power modulator named few pulsed generators. Pulsed shaping has been done in these kinds of systems with the utilization of switches like solid state switches, magnetic switches and spark gaps. All these devices used in pulsed power systems to make pulsed with a required rise time and pulse width. Pulsed power systems are usually represented with an equivalent energy storage element, so called an energy storage capacitor. A suitable charging source required to charge the capacitor, in view of this collected some literature on power supplies. High voltage DC power supply is needed to charge capacitor. Pulsed power systems connected with highly dynamic loads like magnetron, vircator, klystron and backward wave oscillator generates noise, which intern induces into the power supply which is connected at the input of pulsed power systems. Conventional high voltage DC power supplies are not been used as charging source for pulsed power systems. More over these power supplies are less efficient and bulky.

On the other hand switched mode power supplies are popular for DC power applications over conventional DC power supplies due to higher efficiencies and compact. The main contribution of losses in SMPS is due to switching of devices with higher frequencies. Improvements in SMPS are studied in detail and observed that the auxiliary circuits and loss less snubbers are minimizing the switching losses in the switching devices. Apart from auxiliary circuits and snubbers resonant converter topologies have been found a suitable circuit to minimize switching losses in SMPS. Soft switching like zero current and zero voltage switching are achieved with resonant converters.

Second, third, fourth and even higher order resonant converters can be used to provide soft switching for switching devices in various applications with different operating conditions. Usage of 2nd, 3rd and 4th order resonant converters for various applications such as power factor correction, inductive power transfer, induction heating welding, ballasts for fluorescent lamps, and high voltage power supply are studied. Some more applications reviewed where they demands for constant voltage or constant current such applications listed as capacitor charging electric arc welding, laser diode drivers, electrochemical processes, illumination systems, battery charging, and magnet power supplies. Reviewed various charging methods and identified constant current charging method is a suitable charging method to charge a capacitor over resistive, constant power and one cycle resonant charging. Basics of capacitor charging power supply (CCPS) and their requirements for operating pulsed power systems have been studied. Applications of 2nd and 3rd order resonant converter as constant current source in the design of CCPS for pulsed power applications have been studied. In addition to above literature reviewed different controlling and protection schemes in power supplies.

## Chapter-3

# Feasibility of different resonant converter topologies

---

Resonant converters are more popular for constant current, constant voltage and soft switching applications. Power supply design engineers are focused on resonant converter to design charging source for pulsed power applications. The objective of using resonant converters in the charging source is to provide load independent constant current, short circuit proof and soft switching. Second order series LC, parallel LC and series-parallel resonant converters have already been utilized in the design of charging source for single and repetitive operation for pulsed power applications. Charging source along with pulsed power system with dynamic load has been shown in Figure.3.1.

The basic building blocks of capacitor charging power supplies are low frequency input rectifier, DC filter section, high frequency inverter, resonant network, high frequency transformer and high frequency output rectifier. The low frequency rectifier stage is operated at fundamental frequency (50Hz) and is converted the alternating voltage in to DC voltage. Ripples in the DC voltage are filter out by LC filter. Constant DC voltage is converted into high frequency square wave voltage by high frequency inverter, wherein the period of the square depends on chosen switching frequency. In the resonant converter stage the high frequency square is converter into sine and is applied to high frequency transformer. The output of high frequency transformer is rectified with high frequency diode rectifier and is applied to the capacitor. Designing all these stages becomes critical when the charging rate in multiples of 10kJ/s.

Conditions for constant current in case of 2<sup>nd</sup>, 3<sup>rd</sup>, 4<sup>th</sup> and 5<sup>th</sup> order resonant converters are already been derived in the past. While designing power supply for pulsed power applications designers often chooses series LC resonant converter.

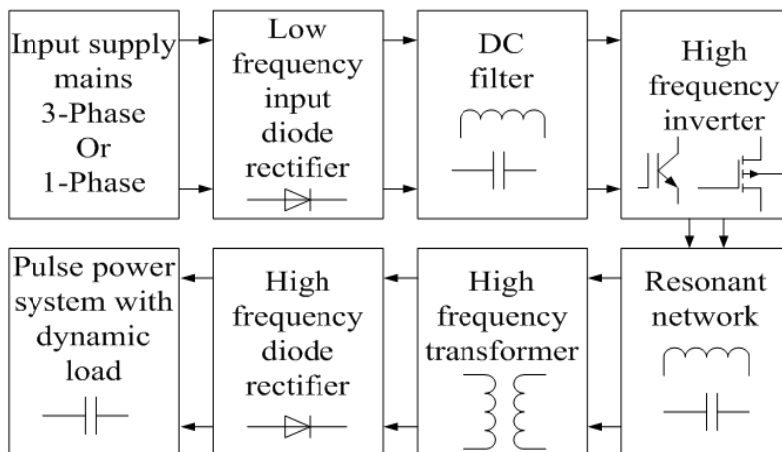


Figure.3.1: Block diagram of CCPS with pulsed power system

This converter is simple to design and provides inherent short circuit protection, load independent constant current and zero current soft switching when operated in the discontinuous conduction mode. Difficulties arise in thermal management, compatibility and lacks in reliability when operated the power supply with highly dynamic loads. Power supply experience dynamic noise when operated with pulsed power system, which leads to frequent failure of controlled switches in the inverter stage of power supply. This phenomenon frequently occurs in series LC resonant based charging source when interfaced with pulsed power system. The designers are lacking in providing protection against dynamic noise. Second order parallel LC and third order LCC, CLL, LCL and LLC topologies have been used previously to design regulated power and charging applications. In all these power supplies designers are concentrated in achieving constant current, constant voltage and soft switching, but they are fail in achieving high efficiency, DC blocking and in protection point of view. Parallel LC and LCL resonant topologies provide constant current when switching frequency equal to resonant frequency. Application of resonant converters in design of CCPS A capacitor charging power supply using high frequency inverter technology smart

modulator application are presented in [86-87]. Due to the limitations and difficulties of 2<sup>nd</sup> and 3<sup>rd</sup> order resonant converters proposed a 4<sup>th</sup> order resonant converter. The proposed 4<sup>th</sup> order resonant converters will take care of all the difficulties and a limitation of 2<sup>nd</sup> and 3<sup>rd</sup> order resonant converter, in adversely it provides protection against noise. Out of many combinations only four 4<sup>th</sup> order resonant converter topologies have been chosen and which are suitable for the design.

### 3.1 Resonant network topologies

Resonant networks such as 2<sup>nd</sup>, 3<sup>rd</sup>, 4<sup>th</sup> and other higher order are exploited to get advantages mentioned in the previous section.

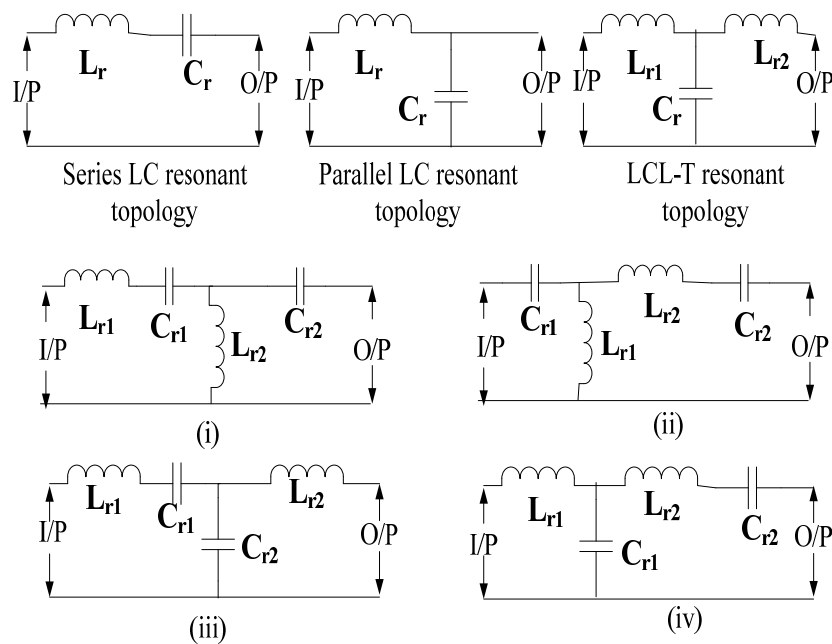


Figure.3.2: Topological structures of 2<sup>nd</sup>, 3<sup>rd</sup> and 4<sup>th</sup> order resonant networks

As the order increases circuit complexity, number of resonant frequencies and interference also increases. Energy storage elements (Inductances and capacitances) are connected in different fashion in second, third and in fourth order to achieve the goal. Series and parallel combinations are possible in second order, whereas in third and fourth T-fashion or  $\pi$ -fashion is the possible connection techniques. Topological structures of 2<sup>nd</sup>, 3<sup>rd</sup>, 4<sup>th</sup> and higher order

resonant topologies are already been discussed in the past and are reviewed in [49]. There are many other combinations in both 3<sup>rd</sup> and 4<sup>th</sup> order with three branch and four branches, but all combinations are not useful for specific applications like constant current, soft switching and DC blocking. For analysis picked only few topological structures which are suitable for CCPS applications. Topological structures shown in Figure.3.2 are used as constant current converter as a part of CCPS. Above mentioned resonant topologies provide constant current and soft switching at different operating conditions.

### 3.2 Second (2<sup>nd</sup>) order resonant analysis

#### 3.2.1 Series LC resonant network analysis

Series LC resonant converter is one of the simple more popular for constant current applications. For the analysis the load resistance ( $R_L$ ) is shifted to the primary side of high frequency transformer, whose equivalent impedance is represented by  $Z_L$ .

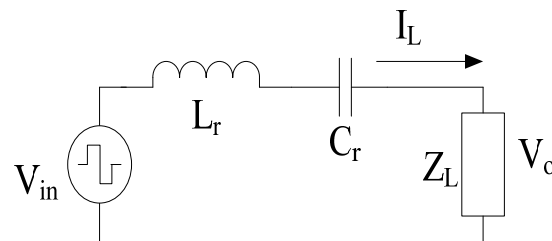


Figure.3.3: Series LC resonant converter for mathematical analysis

The equivalent circuit of series LC resonant based converter with equivalent load is shown in Figure.3.3. The input to the converter is a simple square wave generator followed by resonant network then followed by equivalent load.

$$\text{The total impedance } Z_{TOT} = Z_L + j \left\{ \omega L_r - \left( \frac{1}{\omega C_r} \right) \right\} \dots (3.1)$$

The circuit has a resonant frequency when the imaginary part of  $Z_{TOT}$  equal to zero and it is given by

$$\omega_o = \frac{1}{\sqrt{L_r C_r}} \quad \dots (3.2)$$

The resonant frequency is independent of  $Z_L$  and the current at this time of instant is given by

$$I_L = \frac{V_{in}}{Z_L} \quad \dots (3.3)$$

Where

$V_{in}$  – The RMS voltage of input source

$I_L$  – Load current

If the value of load changes the current drawn from the source are also changes when it operated at resonant frequency, it means the series LC resonant converter is not providing constant current at resonant frequency. Particularly if the load is a capacitor then the impedance seen by the source at resonant frequency is almost zero, in that case the current drawn from the source is nearly equal to infinity. These conditions so called short circuit conditions.

Resonant frequency =  $\omega_o = \frac{1}{\sqrt{L_r C_r}}$ , the characteristic impedance of the circuit is represented

with  $Z_n$  and is given by

$$Z_n = \sqrt{\frac{L_r}{C_r}} \quad \dots (3.4)$$

Quality factor of the circuit is represented with Q and is given by

$$Q = \frac{\omega_o L_r}{R_L} = \frac{1}{\omega_o C_r R_L} = \frac{Z_n}{Z_L} \quad \dots (3.5)$$

The magnitude of characteristic impedance ( $Z_n$ ) of the circuit is a function of frequency with Q as parameter, keeping  $Z_L$  constant.  $Z_n$  is pure resistance when  $\omega_s = \omega_o$ , but inductance impedance dominates when operated below resonant frequency ( $\omega_o$ ) where as capacitive

impedance dominates when operated above resonant frequency ( $\omega_o$ ). The load current characteristics vs normalized frequency ( $\omega_n$ ) has been shown in Figure.3.4.

Operating a series LC resonant converter below resonant frequency leads to discontinuous conduction mode (DCM). The normalized frequency ( $\omega_n$ ) is the ratio between switching frequency ( $\omega_s$ ) to the resonant frequency ( $\omega_o$ ). The abbreviation of DCM is discontinuous conduction mode. It means any continuous waveform, if it encounters zero state and stays in that state for some time then it is called as discontinuous waveform. In series loaded resonant converters the current waveform attains positive and negative values for certain time and reaches to zero. This mode of operation is called as discontinuous conduction mode (DCM) of operation.

Series loaded LC resonant converter can be operated in two modes; the one is continuous conduction mode (CCM) and discontinuous conduction mode. It is achieved on the ratio between switching frequency ( $f_s$ ) to resonant frequency ( $f_o$ ). Under the condition when  $f_s \leq 0.5f_o$  the current in the circuit becomes discontinuous due to resonant inductor. The current in the resonant inductor becomes maximum it does not allow any current to flow through it and at the same time voltage across resonant capacitor becomes two times of input voltage.

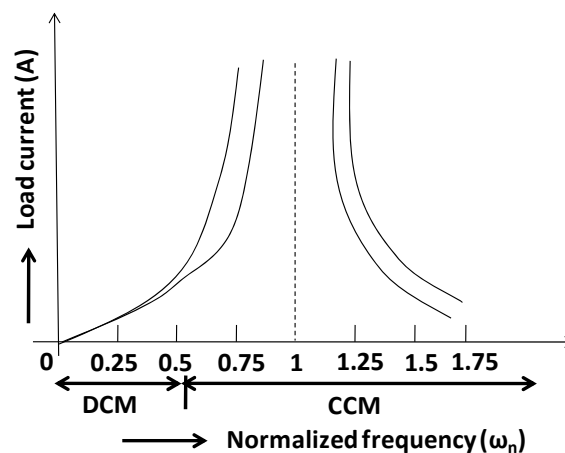


Figure.3.4. Load current vs normalized frequency characteristics of series LC resonant converter.

So, the energy of both these elements dissipates across the load till the energy becomes zero. The current at this moment becomes zero and the switching action takes place in the inverter stage, that why it is called zero current switching (ZCS). The other type of switching (i.e. zero voltage switching) achieved by making voltage across the switch which is going to be turned on. This type switching action can be achieved by operating in continuous conduction mode. It is achieved when it is operated at  $f_s \geq 0.5f_o$  one can achieve CCM of operation. It is clear from the graph that current is linear in the region when  $2\omega_s \leq \omega_o$ . This mode of operation is called discontinuous conduction mode, in addition in this mode series LC provide inherent zero current switching. So, this is the reason why the designers always operate series LC resonant converter below the half of resonant frequency. In this operating mode the current is linear and is constant.

#### Advantages

1. It provides inherent short circuit protection
2. Constant current and soft switching in discontinuous conduction mode
3. The tank current varies with load, therefore offers higher efficiency at light load
4. Simple comparatively all resonant topologies

#### Disadvantages

1. Cannot be operated at no load
2. Poor cross regulation in multi output power supplies
3. High peak currents, so the thermal management and paralleling operating needed for higher rating.

### 3.2.2 Parallel resonant network analysis

Analysis of parallel resonant converter for constant current application has been done in this section. Circuit of parallel LC resonant based converter with equivalent load is shown in Figure.3.5. The input to the converter is a simple square wave generator followed by resonant network then followed by equivalent load.

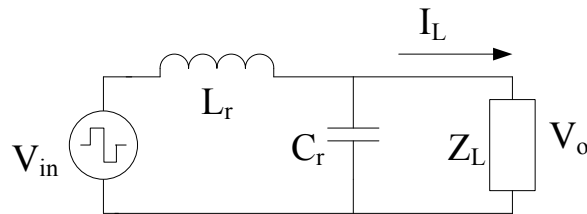


Figure.3.5: Parallel LC resonant converter for mathematical analysis

The AC equivalent load resistance referred to the primary side of high frequency transformer and rms voltage of input voltage square wave is given by

$$Z_L = \frac{\pi^2 R_L}{8n^2} \quad \dots (3.6)$$

$$\text{RMS value of square wave voltage} = V_{\text{rms}} = \frac{2\sqrt{2}V_{\text{DC}}}{\pi} \quad \dots (3.7)$$

Where  $V_{\text{DC}}$  is DC input voltage,  $R_L$  is the load resistance,  $n$  is the turns ratio,  $Z_L$  is the AC equivalent resistance at the primary side of high frequency transformer and  $V_{\text{rms}}$  is the RMS voltage of square wave voltage at the input.

$$Z_{\text{TOT}} = \frac{Z_L}{j\omega C_r Z_L + 1} + j\omega L_r \quad \dots (3.8)$$

Rationalizing and on minimizing the total impedance it become

$$Z_{\text{TOT}} = \frac{Z_L + j(\omega^3 L_r C_r^2 Z_L^2 - \omega C_r Z_L^2 + \omega L_r)}{\omega C_r^2 Z_L^2 + 1} \quad \dots (3.9)$$

By equating imaginary to zero, the circuit has resonant frequencies

$$\omega_o = 0 \quad \dots (3.10)$$

$$\omega_2 = \sqrt{\frac{C_r Z_L^2 - L_r}{L_r C_r^2 Z_L^2}} \quad \dots (3.11)$$

In contrast to the series LC, this resonant frequency depends on load

$$I_L = \frac{V_{in} X_2}{Z_L X_1 + Z_L X_2 + j X_1 X_2} \quad \dots (3.12)$$

Where  $X_1 = sL_r$  and

$$X_2 = \frac{1}{sC_r}$$

The load current still dependent on the load ( $Z_L$ ), but one can make the load current independent of load by choosing  $X_1 = -X_2$ . This can be achieved at a particular frequency so called resonant frequency ( $\omega_0$ ). It is given by  $\omega_0 = \frac{1}{\sqrt{L_r C_r}}$ .

$$\omega_2 = \sqrt{\omega_0^2 - \frac{1}{C_r^2 Z_L^2}} \quad \dots (3.13)$$

Hence constant current operation could be achieved in this circuit at the frequency, where  $X_1 = -X_2$ , but this frequency would not be a resonant frequency of the circuit unless  $Z_L$  was very large.

#### Advantages

1. It provides constant current under variable load conditions
2. Low Q value makes parallel resonant converter attractive constant current source with simpler control and soft switching can be achieved.

#### Disadvantages

1. It suffers from high circulating currents
2. Poor part load efficiency
3. A large variation in switching frequency is demanded for wider conversion range

### 3.3 Third (3<sup>rd</sup>) LCL-T resonant network analysis

Two inductors and one capacitor connected in the T-fashion to form LCL-T resonant network. LCL-T network with input and equivalent load impedance is shown in Figure.3.6.

The total impedance offered by the circuit is given by

$$Z_{TOT} = \frac{(j\omega L_{r2} + Z_L)}{-\omega^2 L_{r2} C_r + j\omega C_r Z_L + 1} + j\omega L_{r1} \quad \dots (3.14)$$

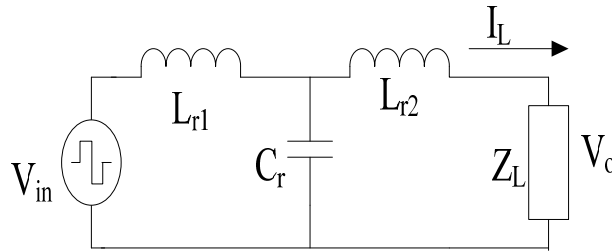


Figure.3.6: LCL-T resonant converter for mathematical analysis

On rationalizing the above equation then the total equivalent impedance becomes

$$Z_{TOT} = \frac{Z_L + j(\omega^5 L_{r1} C_r^2 L_{r2}^2 - 2\omega^4 L_{r1} C_r L_{r1} + \omega^4 L_{r1} C_r^2 Z_L^2 + \omega^4 C_r L_{r2}^2 + \omega^2 L_{r1} + \omega^2 L_{r2} + \omega^2 C_r^2 Z_L^2)}{\omega^4 C_r^2 L_{r2}^2 - 2\omega^2 C_r L_{r2} + \omega^2 C_r^2 Z_L^2 + 1} \quad \dots (3.15)$$

On making imaginary part of  $Z_{TOT}$  equal to zero, one can obtain number of resonant frequency as well as soft switching. In this particular resonant converter there are three resonant frequencies and they are

$$\omega_0 = 0,$$

$$\omega_1 =$$

$$\sqrt{\frac{(2L_{r1} C_r L_{r1} - L_{r1} C_r^2 Z_L^2 + C_r L_{r2}^2) + \sqrt{[(-2L_{r1} C_r L_{r1} + L_{r1} C_r^2 Z_L^2 - C_r L_{r2}^2)^2 - 4L_{r1} C_r^2 L_{r2}^2 (L_{r1} + L_{r2} - C_r^2 Z_L^2)]}}{2L_{r1} C_r^2 L_{r2}^2}}$$

$$\dots (3.16)$$

$$\omega_2 =$$

$$\sqrt{\frac{(2L_{r1}C_rL_{r1}-L_{r1}C_r^2Z_L^2+C_rL_{r2}^2)-\sqrt{[(-2L_{r1}C_rL_{r1}+L_{r1}C_r^2Z_L^2-C_rL_{r2}^2)^2-4L_{r1}C_r^2L_{r2}^2(L_{r1}+L_{r2}-C_r^2Z_L^2)]}}{2L_{r1}C_r^2L_{r2}^2}} \dots (3.17)$$

The current through the load at any of the three resonant frequencies is given by

$$I_2 = \frac{V_{in}X_3}{X_1X_2+X_2X_3+Z_L(X_1+X_3)} \dots (3.18)$$

The load current becomes independent load when  $Z_L(X_1 + X_3)$  becomes zero. This can be achieved by choosing  $X_1 = X_2 = -X_3$  at this condition the resonant frequency of the circuit obtained as

$\omega_o = \frac{1}{\sqrt{L_rC_r}}$ , where the resonant frequency is independent of load and is the frequency at which constant current achieved.

#### Advantages

1. Circulating currents are less compared to second order resonant topologies
2. The circuit impedance is high, which enables the current drawn from the source limited even the load is shorted
3. Soft switching achieved when resonant frequency equal to resonant frequency

#### Disadvantages

1. Lacking with DC blocking for high voltage frequency transformer leads to the saturation of transformer core
2. Number of resonant frequencies are increased

Due high peak and circulating currents, poor part load efficiencies at light load conditions and lack of DC blocking of second order (Series LC and parallel LC) and third order (LCL-T)

resonant converters not been the attractive topological structures for constant current application as charging source for pulsed power systems.

Introduced a novel fourth (4<sup>th</sup>) resonant converter and has been used as a constant current converter for pulsed power applications and it has the ability to overcome above mention disadvantages. All 4<sup>th</sup> order resonant topologies are not fit for pulsed power applications as a constant current converter. Only four resonant structures have been chosen for analysis and they are shown in Figure.3.2. Analysis of those four resonant structures (iv to vii of Fgiure.3.2.) is discussed in the further sections.

### 3.4 Fourth (4<sup>th</sup>) order LCLC resonant network analysis

In the proposed converter scheme  $L_{r1}$ ,  $C_{r1}$ ,  $L_{r2}$  and  $C_{r2}$  are connected in T structure is shown in Figure.3.7.

Inductance  $L_{r1}$  and capacitor  $C_{r1}$  are connected in series and forms an equivalent reactance of  $X_1$ , inductance  $L_{r2}$  forms reactance  $X_2$  and capacitor  $C_{r2}$  forms reactance  $X_3$ .

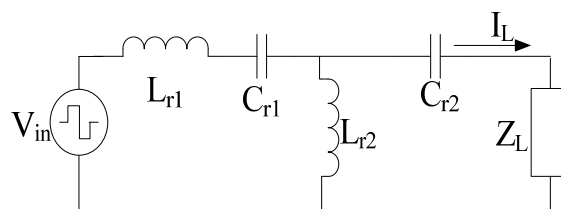


Figure.3.7: LCLC-T resonant converter for mathematical analysis

$$X_1 = \frac{1-\omega^2 L_{r1} C_{r1}}{j\omega C_{r1}}, X_2 = \omega L_{r2}, X_3 = \frac{1}{j\omega C_{r2}} \text{ and } Z_L = \frac{8R_L}{n^2 \pi^2}$$

The total circuit impedance offered by the network shown in Figure.3.7 is given by

$$Z_{TOT} = \frac{X_1 X_2 + X_1 X_3 + X_2 X_3 + Z_L (X_1 + X_2)}{X_2 + X_3 + Z_L} \dots (3.19)$$

By substituting the values of  $X_1$ ,  $X_2$  and  $X_3$  then on rationalizing the above equation

Real part of  $Z_{TOT}$  becomes

$$Z_{TOT} =$$

$$\frac{\{\omega Z_L C_{R2}(1-\omega^2 L_{R1} C_{R1})(C_{R1}+C_{R2}-\omega^2 C_{R1} C_{R2} L_{R2})-\omega Z_L C_{R1} C_{R2}(1+\omega^4 L_{R1} L_{R2} C_{R1} C_{R2}-\omega^2(L_{R1} C_{R1}+L_{R2} C_{R2}+L_{R1} C_{R2}))\}}{\omega[(C_{R1}+C_{R2}-\omega^2 L_{R2} C_{R1} C_{R2})^2+(\omega^2 Z_L^2 C_{R1}^2 C_{R2}^2)^2]} \dots (3.20)$$

And the imaginary part of  $Z_{TOT}$  will becomes

$$Z_{TOT} =$$

$$\frac{-j\{(C_{R1}+C_{R2}-\omega^2 C_{R1} C_{R2} L_{R2})(1+\omega^4 L_{R1} L_{R2} C_{R1} C_{R2}-\omega^2(L_{R1} C_{R1}+L_{R2} C_{R2}+L_{R1} C_{R2}))+\omega^2 Z_L^2 C_{R1} C_{R2}^2(1-\omega^2 L_{R1} C_{R1})\}}{\omega[(C_{R1}+C_{R2}-\omega^2 L_{R2} C_{R1} C_{R2})^2+(\omega^2 Z_L^2 C_{R1}^2 C_{R2}^2)^2]} \dots (3.21)$$

By equating imaginary part of  $Z_{TOT}$  is zero at  $\omega_0$

$$1+x = xy \text{ (Where } x = \frac{L_{R2}}{L_{R1}} \text{ and } y = \frac{C_{R2}}{C_{R1}} \text{)} \dots (3.22)$$

On applying voltage divider rule, then the voltage across  $X_2$  is given by

$$V_{X_2} = \frac{X_2(Z_L+X_3)V_{in}}{X_1X_2+X_1X_3+X_2X_3+Z_L(X_1+X_2)} \dots (3.23)$$

Then the current through load is expressed by

$$I_{Load} = \frac{V_{X_2}}{Z_L+X_3} \dots (3.24)$$

$$I_{Load} = \frac{X_2 V}{X_1X_2+X_1X_3+X_2X_3+Z_L(X_1+X_2)} \dots (3.25)$$

Solving the above equation after substituting the values  $X_1$ ,  $X_2$ , and  $X_3$  make the coefficient

of  $Z_L$  equal to zero, then the load current  $I_L$  becomes independent of  $Z_L$  at  $\omega_0 = \frac{1}{\sqrt{(1+x)L_{R1}C_{R1}}}$  at

$$y = \frac{1+x}{x} \quad \dots (3.26)$$

$$\text{Normalized frequency } \omega_n = \frac{\omega_s}{\omega_0} \quad \dots (3.27)$$

Characteristic impedance of the resonant circuit and quality factor Q are given by

$$Z_n = \sqrt{\frac{L_{r1}}{C_{r1}}} \text{ and } Q = \frac{n^2 \omega_0 L_{r1}}{Z_L} \quad \dots (3.28)$$

$$\text{Current gain} = H = \frac{nI_0}{V_d/Z_n}, \text{ voltage gain} = M = \frac{V_0/n}{V_d}$$

$$H = \frac{xy\omega_n^3(\sqrt{1+x})}{-\frac{1}{Q}\omega_n y(1+x)(1-\omega_n^2) + j\frac{\pi^2}{8}[(1-\omega_n^2)(1+x)^2 - \omega_n^2 xy(1+x-\omega_n^2)]} \quad \dots (3.29)$$

$$M = \frac{\omega_n^3 xy}{-\omega_n y(1+x)(1-\omega_n^2) + jQ\frac{\pi^2}{8}\{(1+x)^2(1-\omega_n^2) - \omega_n^2 xy(1+x-\omega_n^2)\}} \quad \dots (3.30)$$

Normalized current through and voltage across inductor  $L_{r1}$  ( $I_{L_{r1}}, V_{L_{r1}}$ ),  $L_{r2}$  ( $I_{L_{r2}}, V_{L_{r2}}$ ),  $C_{r1}$  ( $I_{C_{r1}}, V_{C_{r1}}$ ) and  $C_{r2}$  ( $I_{C_{r2}}, V_{C_{r2}}$ ) are derived with base voltage  $V_d$  and  $V_d/Z_n$  are as follows

$$I_{L_{r1},N} = I_{C_{r1},N} = \frac{I_{L_{r1},rms}}{V_d/Z_n} = \frac{I_{C_{r1},rms}}{V_d/Z_n} = \frac{\pi\sqrt{1+x}\left\{\omega_n Q(1+x-\omega_n^2) + j\frac{y8\omega_n^2}{\pi^2}\right\}}{2\sqrt{2}\left[y\omega_n(1+x)(1-\omega_n^2) + j\frac{\pi^2 Q\{xy\omega_n^2(1+x-\omega_n^2) - (1+x)^2(1-\omega_n^2)\}}{8}\right]} \quad (3.31)$$

$$I_{L_{r2},N} = \frac{I_{L_{r2},rms}}{V_d/Z_n} = \frac{\pi\sqrt{1+x}\left\{\omega_n Q(1+x) + j\frac{y8\omega_n^2}{\pi^2}\right\}}{2\sqrt{2}\left[y\omega_n(1+x)(1-\omega_n^2) + j\frac{\pi^2 Q\{xy(1+x-\omega_n^2) - (1+x)^2(1-\omega_n^2)\}}{8}\right]} \quad \dots (3.32)$$

$$I_{C_{r2},N} = \frac{I_{C_{r2},rms}}{V_d/Z_n} = \frac{\pi xy\omega_n^3(\sqrt{1+x})}{2\sqrt{2}\left[-\frac{1}{Q}\omega_n y(1+x)(1-\omega_n^2) + j\frac{\pi^2}{8}\{(1-\omega_n^2)(1+x)^2 - \omega_n^2 xy(1+x-\omega_n^2)\}\right]} \quad \dots (3.33)$$

$$V_{L_{r1},N} = \frac{V_{L_{r1},rms}}{V_d} = \frac{-\pi\left\{\omega_n^2 Q(1+x-xy\omega_n^2) + j\frac{8\omega_n^3 y}{\pi^2}\right\}}{2\sqrt{2}\left[\frac{\pi^2}{8}Q\{(1+x)^2(1-\omega_n^2) - xy\omega_n^2(1+x-\omega_n^2)\} + j\omega_n y(1-\omega_n^2)(1+x)\right]} \quad \dots (3.34)$$

$$V_{Lr2,N} = \frac{V_{Lr2,rms}}{V_d} = \frac{-\pi\omega_n^2 x \left\{ (1+x)Q + j\frac{8y\omega_n}{\pi^2} \right\}}{2\sqrt{2} \left[ \frac{\pi^2}{8} \{ (1+x)^2 (1-\omega_n^2) - xy\omega_n^2 (1+x-\omega_n^2) \} + jy\omega_n (1+x) (1-\omega_n^2) \right]} \quad \dots (3.35)$$

$$V_{Cr1,N} = \frac{V_{Cr1,rms}}{V_d} = \frac{\pi(1+x) \left[ Q(1+x-xy\omega_n^2) + j\frac{8y\omega_n}{\pi^2} \right]}{2\sqrt{2} \left[ \frac{Q\pi^2}{8} \{ (1-\omega_n^2)(1+x)^2 - xy\omega_n^2 (1-\omega_n^2) \} + jy\omega_n y (1+x) \right]} \quad \dots (3.36)$$

$$V_{Cr2,N} = \frac{V_{Cr2,rms}}{V_d} = \frac{-\pi x (1+x) \omega_n^2}{2\sqrt{2} \left[ \frac{\pi^2}{8} \{ (1-\omega_n^2)(1+x)^2 - xy\omega_n^2 (1+x-\omega_n^2) \} + j\frac{y(1+x)\omega_n}{Q} \right]} \quad \dots (3.37)$$

The proposed topology provides load independent constant current when  $\omega_n = 1$  and it is shown in Figure.3.8.

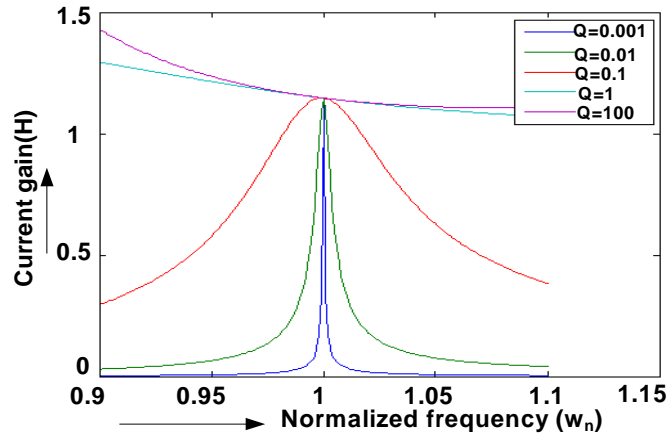


Figure.3.8: Current gain (H) vs normalized frequency ( $\omega_n$ )

Where  $\omega_n$  is the normalized frequency is the ratio between  $\omega_s$  and  $\omega_o$ . In the mathematical analysis it is already showed that current is independent of load (i.e. independent of Q). When  $\omega_n = 1$  then the current gain (H) will become constant at any value of Q. Other than  $\omega_n = 1$  the current gain vary with respect to Q.

Condition for load independent constant current, condition for zero current switching, voltage gain, current gain and relationship between resonant components (i.e. Between  $LL_{r1}$  and  $L_{r2}$  and  $C_{r1}$  and  $C_{r2}$ ) have been derived mathematically and summarized in a table shown below.

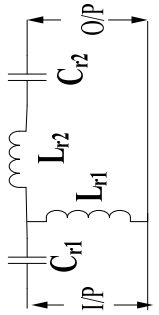
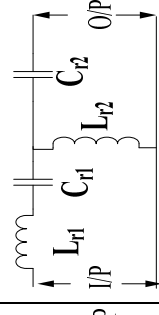
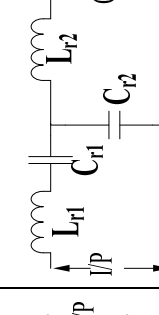
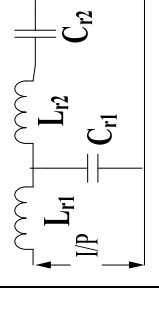
					
Condition for constant current		$\omega_0 = \sqrt{\frac{2xy}{L_{r1}C_{r1}}}$	$y = \frac{1}{1+x}$	$L_{r2} = L_{r1}$	$C_{2r} = 0.5C_{r1}$
Condition for ZCS		$\omega_0 = \sqrt{\frac{1}{(1+x)L_{r1}C_{r1}}}$	$1 + x = y$	$L_{r2} = L_{r1}$	$C_{r2} = 2C_{r1}$
Condition for ZVS		$\omega_0 = \sqrt{\frac{1+y}{yL_{r1}C_{r1}}}$	$x = \frac{1+y^2}{y+2y^2+y^3}$	$L_{r2} = 0.5L_{r1}$	$C_{r2} = C_{r1}$
Condition for constant voltage		$\omega_0 = \sqrt{\frac{xy}{2L_{r1}C_{r1}}}$	$1 + y = xy$	$L_{r2} = 2L_{r1}$	$C_{r2} = C_{r1}$
Condition for ZVS					

Table.3.1: Summarized table 1

Where  $x = \frac{L_{r2}}{L_{r1}}$  and  $y = \frac{C_{r2}}{C_{r1}}$

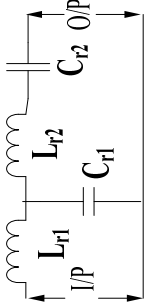
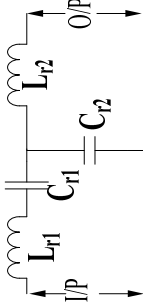
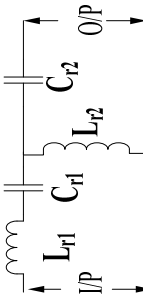
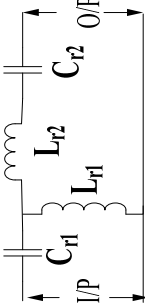
Topology	Current Gain	Voltage Gain
	$\frac{I_o}{I_{in}} = \frac{S C_{r2}}{S^3 L_{r2} C_{r1} C_{r2} + Z S^2 C_{r1} C_{r2} + S C_{r2} + 1}$	$\frac{V_o}{V_{in}} = \frac{Z S C_{r2}}{S^4 L_{r1} L_{r2} C_{r1} C_{r2} + Z S^3 L_{r1} C_{r1} C_{r2} + S^2 (L_{r1} C_{r1} + L_{r2} C_{r2}) + Z S C_{r2} + 1}$
	$\frac{I_o}{I_{in}} = \frac{1}{S^2 L_{r2} C_{r2} + Z S C_{r2} + 1}$	$\frac{V_o}{V_{in}} = \frac{Z S C_{r1}}{S^4 L_{r1} L_{r2} C_{r1} C_{r2} + Z S^3 L_{r1} C_{r1} C_{r2} + S^2 (L_{r2} C_{r1} + L_{r2} C_{r2}) + Z S (C_{r1} + C_{r2}) + 1}$
	$\frac{I_o}{I_{in}} = \frac{S^2 L_{r2} C_{r2}}{S^2 L_{r2} C_{r2} + Z S C_{r2} + 1}$	$\frac{V_o}{V_{in}} = \frac{Z S^3 L_{r2} C_{r1} C_{r2}}{Z S^3 (L_{r1} C_{r1} C_{r2} + L_{r2} C_{r1} C_{r2}) + S^2 (L_{r1} C_{r1} + L_{r2} C_{r2}) + Z S C_{r2} + 1}$
	$\frac{I_o}{I_{in}} = \frac{S^2 L_{r1} C_{r2}}{S^2 (L_{r2} C_{r2} + L_{r1} C_{r2}) + Z S C_{r2} + 1}$	$\frac{V_o}{V_{in}} = \frac{Z S^3 L_{r1} C_{r1} C_{r2}}{S^4 L_{r1} L_{r2} C_{r1} C_{r2} + Z S^3 L_{r1} C_{r1} C_{r2} + S^2 (L_{r1} C_{r1} + L_{r2} C_{r2}) + Z S C_{r2} + 1}$

Table.3.2: Summarized table 2

The relationship between input current to the resonant converter with the resonant components (Either  $L_{r1}$  or  $C_{r1}$ ) is given by

$$I_{Lr1,rms} = \frac{V_{rms}}{\omega_0 L_{r1}} = V_{rms} \omega_0 C_{r1} \quad \dots (3.38)$$

The equation is important in finding the one of the resonant component value in the resonant network. By using condition for load independent constant current formulae one can find the other resonant component value. All four 4<sup>th</sup> order resonant converters which are already been discussed in the above two tables are having their significant role in the design of capacitor charging power supply for pulsed power applications in the next chapter.

### Summary

In this chapter first discussed the basic block diagram of charging source of pulsed power systems, later discussed the important blocks of capacitor charging power supply. Identified various 2<sup>nd</sup>, 3<sup>rd</sup> and 4<sup>th</sup> order resonant converter topologies which provides basic requirements (Inherent short circuit proof, load independent constant current and soft switching) of charging source for pulsed power applications. Conditions for load independent constant current and soft switching have been derived mathematically and discussed them in detail in case of 2<sup>nd</sup>, 3<sup>rd</sup> and 4<sup>th</sup> order resonant converters. In case of series LC, the load independent constant current and inherent zero current switching obtained when it operated in discontinuous conduction mode. But, in case of parallel LC, LCL-T and other 4<sup>th</sup> order resonant converters (Shown are in Figure.3.2.) provides load independent constant current and zero current switching when switching frequency ( $f_s$ ) equal to the resonant frequency ( $f_r$ ). Advantages and disadvantages of 2<sup>nd</sup> and 3<sup>rd</sup> order resonant converters has been discussed simultaneously discussed how 4<sup>th</sup> order resonant converter have overcome disadvantages of 2<sup>nd</sup> and 3<sup>rd</sup> order resonant converters. Conditions for load independent constant current, ZCS,

current gain, voltage gain and relationship between resonant components for the chosen 4<sup>th</sup> order resonant converters are summarized and presented in a table.

# Chapter-4

## Simulation and development features

---

In this chapter discussed the development features of four 4<sup>th</sup> order resonant topologies for different pulsed power. First we have used one of the four 4<sup>th</sup> order resonant topologies to verify the basic operation like load independent constant current and soft switching (i.e. Zero current switching and zero voltage switching).

### 4.1 Development features

#### 4.1.1 Input parameters

Output voltage	200V
J/s rating	20J/s
Load capacitor	100 $\mu$ F
Charging time	100ms

Table.4.1: Rating of 20J/s CCPS

From the given input data the load current is given by

$$V_{\text{rms}} = \frac{2\sqrt{2}V_d}{\pi}, V_d=75V, V_{\text{rms}}= 67.54V,$$

$$I_{\text{Load avg}} = C_L \frac{dv}{dt},$$

$$t_c = \text{charging time} = 100\text{ms},$$

For charging the capacitor up-to 200V the current required,

$$I_{\text{Load avg}} = 0.2A = 200\text{mA}$$

The load current equivalent to the source current, condition for the same has been derived mathematically for this topology in the previous chapter.

$$\text{So, } I_L = I_{Lr1}$$

RMS value of current flowing through resonant inductor  $L_{r1}$  is given by

$$I_{Lr1rms} = 1.11I_{Lr1}$$

$$I_{Lr1rms} = 222\text{mA}$$

$$I_{Lr1rms} = \frac{V_{rms}}{\omega_0 L_{r1}}$$

$$L_{r1} = \frac{67.54}{2 \times 3.14 \times 25000 \times 222 \times 10^{-3}}$$

Value of resonant inductor  $L_{r1} = 862\mu\text{H}$

For this topology the relation between resonant components are given by

$$L_{r2} = L_{r1} \text{ and } C_{r2} = 2C_{r1}$$

Zero current achieved when

$$\omega_0 = \frac{1}{(\sqrt{1+x})(\sqrt{L_{r1}C_{r1}})} \text{ Where } f_r = \frac{1}{2\pi(\sqrt{1+x})(\sqrt{L_{r1}C_{r1}})}$$

$$\text{Where } x = \frac{L_{r2}}{L_{r1}} \text{ and } y = \frac{C_{r2}}{C_{r1}}$$

From the above relation the resonant capacitor  $C_{r1}$  obtained as 23.5nF.

$$L_{r2} = L_{r1} = 862\mu\text{H},$$

$$C_{r1} = 23.5\text{nF} \text{ and } C_{r2} = 47\text{nF}$$

#### 4.1.2 Operation

The circuit diagram of the proposed capacitor charging power supply is shown in Figure.4.1 where it utilized a high frequency half bridge inverter to provide square wave output. Switches are operated in the inverter with a switching frequency 25 kHz.

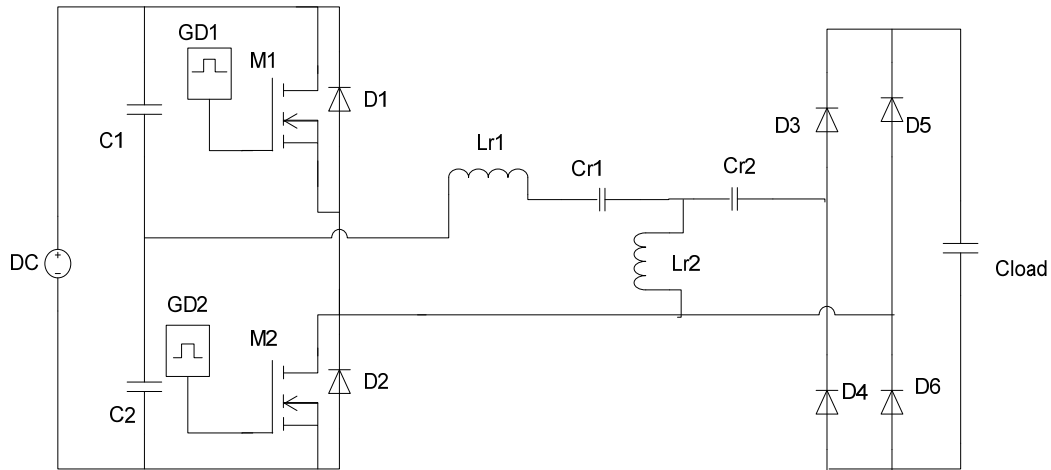


Figure.4.1: Circuit diagram of half bridge inverter based CCPS with LCLC resonant topology

Other components which are used in the development of CCPS are listed in Table.4.2.

Components	No's	Components	No's
MOSFETs (IRF 840)	2	Input rectifier module	1
DC link capacitor ( $C_{DC1}=C_{DC2}=2.2\text{mF}$ )	2	Current transformer (Ferrite core based)	1
Output rectifier diodes (BYV 26E)	4	Gate driver power supply	1
Gate drivers (Indigenous)	2	Load capacitor ( $100\mu\text{F}$ )	1
Single phase variac	1	Resonant inductors ( $862\mu\text{H}$ )	2
PWM controller card	1	Resonant capacitors ( $23.5\text{nF}$ and $47\text{nF}$ )	1

Table.4.2: Components list of 20J/s CCPS

In the circuit operation first the DC link capacitors are charged to the 37.5V each, in the first half of resonant cycle DC link capacitor ( $C_{DC1}$ ), resonant network, MOSFET ( $M_1$ ), diode ( $D_3$ ),  $C_L$  ( $100\mu\text{F}$ ) and diode ( $D_6$ ) comes into the picture as shown in Figure.4.2a. In the second half of resonant cycle DC link capacitor ( $C_{DC2}$ ), resonant network, MOSFET ( $M_2$ ), diode ( $D_4$ ),  $C_{load}$  ( $100\mu\text{F}$ ) and diode ( $D_5$ ) comes into the picture as shown in Figure.4.2b.

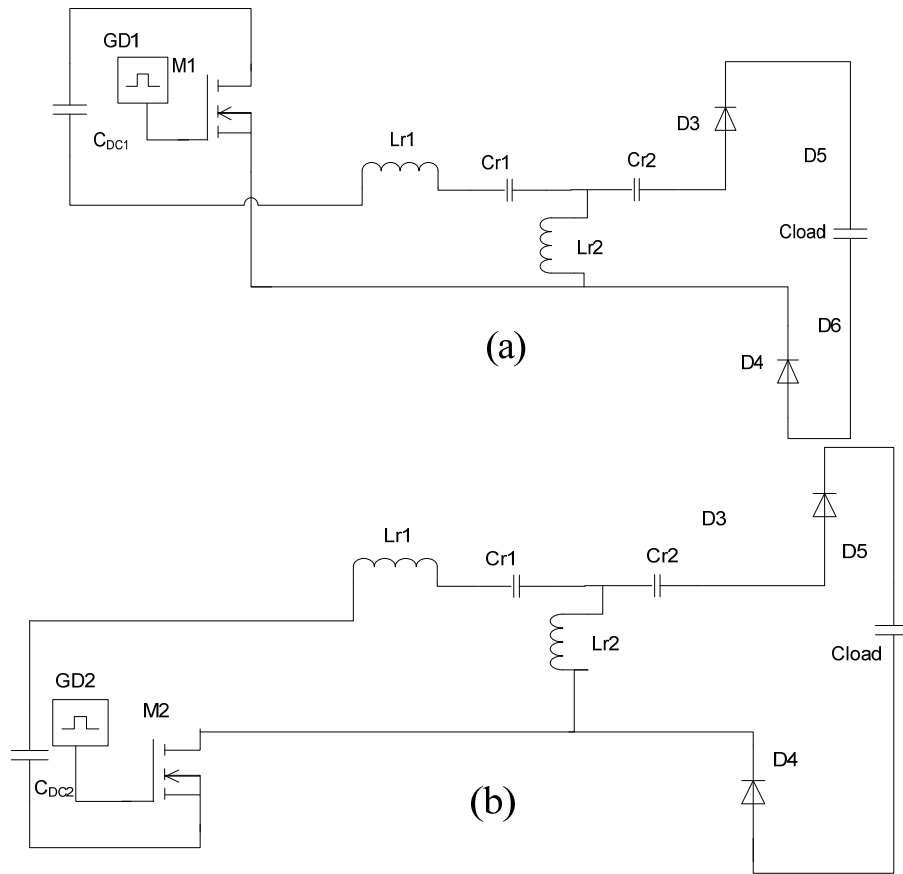


Figure.4.2: Equivalent circuits in each of cycle of switching period (a) +ve half cycle and (b) –ve half cycle

In both the half cycle the current flowing through the load is not going to change, nothing but the load capacitor charges linearly. The soft switching techniques zero current and zero voltage are main concern in the operation is explained in further section. Dc link capacitors =  $C_{DC1} = C_{DC2} = 2.2\text{mF}$  (DC link capacitor is much higher than the first resonant capacitor i.e. it should not alter the operation of resonant network). The experimental set up has showed in Figure.4.3. Developed own gate drivers and gate power supply in the lab to run inverter switches.

Switching devices are MOSFETs (IRF840) is chosen, because the prototype designed to carry 6A peak current. MOSFET (IRF840) can carry continuous drain current of 8A, the peak current flowing through each device is about 2.6A at the end of charging. Output rectifier

developed using high frequency fast diodes (BYM 26E) and discharge resistor bunch has been used for discharging the load capacitor manually.

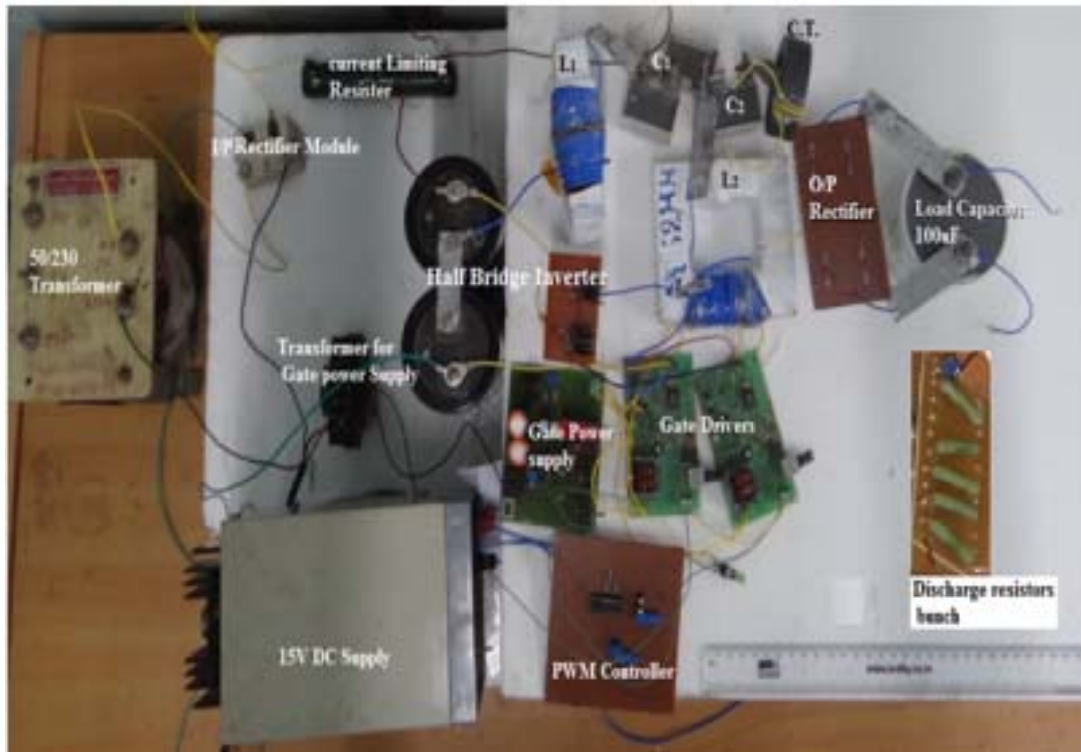


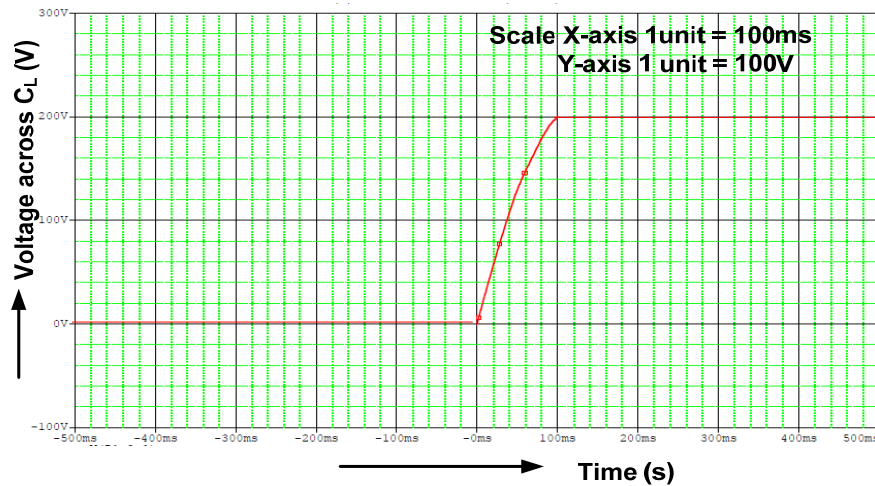
Figure.4.3: Experimental setup of proposed CCPS with LCLC resonant topology

Component ratings are not exactly equal to the design values.

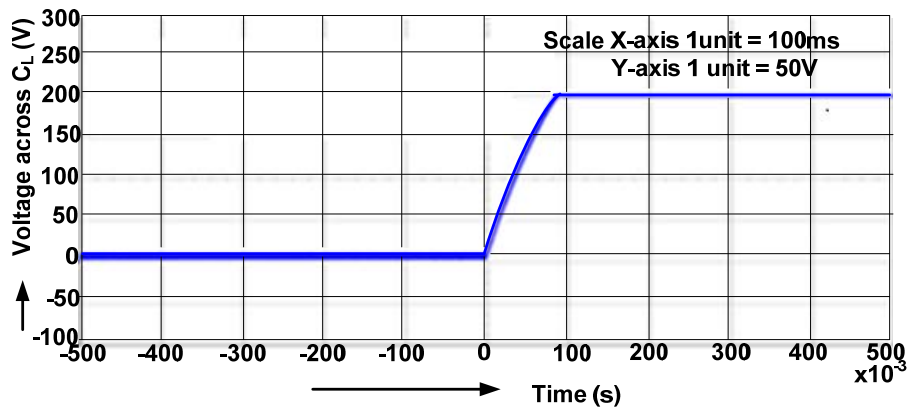
#### 4.1.3 Results

Simulation has been done in ORCAD spice simulation tool and observed the voltage across load ( $100\mu\text{F}$ ) capacitor, current through load capacitor and current through resonant inductor ( $L_{r1}$ ). Current through resonant inductor is monitored to see the peak current carried by by controlled switch in the inverter stage, where as the current monitored through the load is to ensure the load independent constant current. In addition to this monitored the voltage profile across load to ensure the targeted voltage.

Experimental results are presented in this section to cross verification with simulation results. In Figure.4.4 presented the voltage profile of load capacitor, in which the load capacitor is charged to 200V.



(a)



(b)

Figure.4.4: Voltage profile across load capacitor ( $100\mu\text{F}$ ) (a) Simulation (b) experimental

It is observed that the load capacitor ( $100\mu\text{F}$ ) charged to 200V in 100ms. Simulation result has been presented in Figure.4.4a and experimental result is presented in Figure.4.4b.

It is already been discussed in the previous chapter that when it operated at a constant switching frequency which is also equal to the resonant frequency provides constant current and soft switching. It is explained with the help of current gain plot in the previous chapter.

Current flowing through load is constant (200mA) from starting to the end of charging is shown in Figure.4.5.

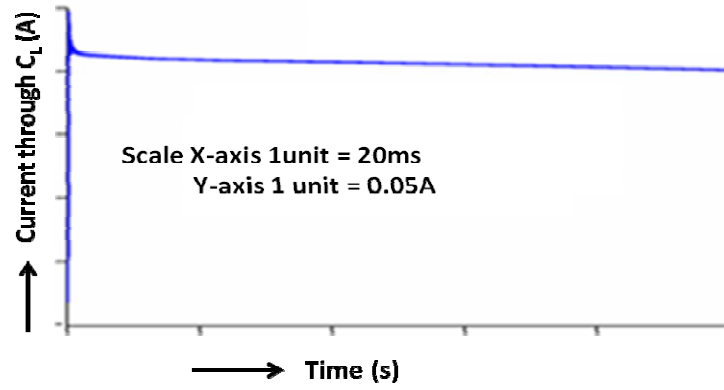
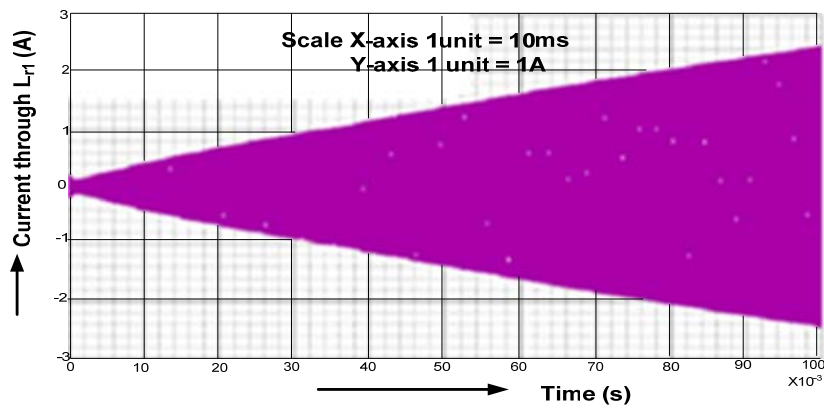
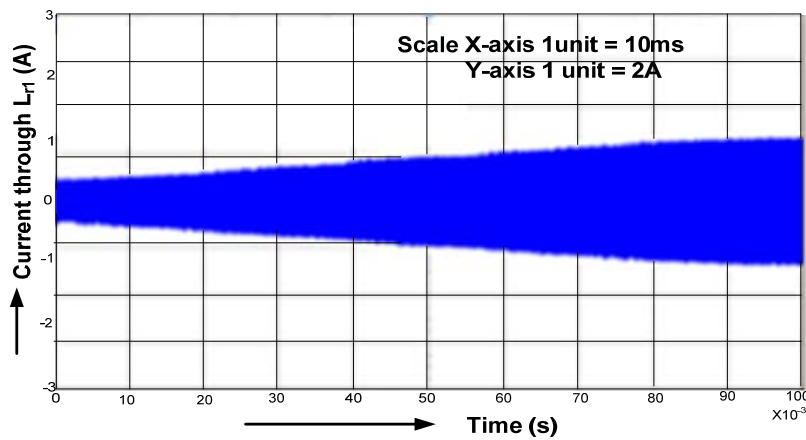


Figure.4.5: Current through load capacitor (100 $\mu$ F)



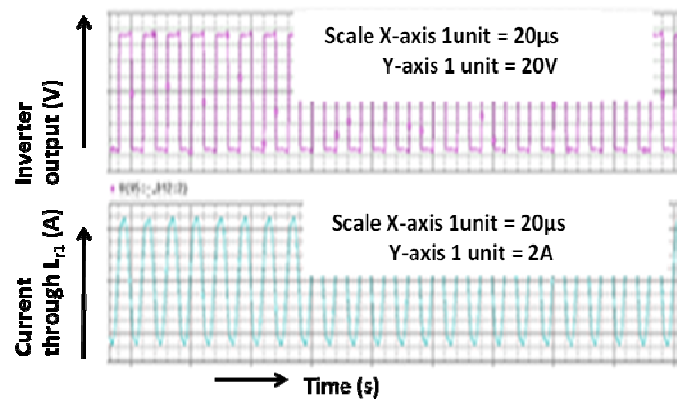
(a)



(b)

Figure.4.6: Current through resonant inductor ( $L_{r1}$ ) (a) Simulation, (b) Experimental

This current will not change for any load capacitor, unless the load capacitor is comparable with second resonant capacitor value (47nF). The load capacitor value is at least 10 times greater than 47nF. Current profile through resonant inductor  $L_{r1}$  is shown in Figure.4.6 to verify the peak current both in simulation as well as in experimental.



(a)



(b)

Figure.4.7: Inverter output voltage vs current through  $L_{r1}$  to verify ZCS

(a) Simulation (b) Experimental

A current transformer (CT) with turn's ratio 10 has been used to measure current through  $L_{r1}$ , wherein 10 $\Omega$  resistor burden has been used. The voltage obtained across burden is 2.4V (shown in Figure.4.6b). So, the current through burden becomes 0.24A, but when it referred to primary it is equivalent to 2.4A. This is the current flowing through  $L_{r1}$  is in comparable with 2.5A which is obtained from simulation (shown in Figure.4.6a).

The current obtained in the experimental is not exactly equal to simulation due to the presence of lead inductance. Zero current switching (ZCS) is nothing but turn off action in controlled switch of inverter stage of CCPS is takes place when current through the switch is zero. Device conduction during +ve half cycle and –ve half cycle is shown in Figure.4.2.The current becomes zero in the circuit when switching frequency equal to resonant frequency. At this condition the circuit becomes resistive in nature, so the inverter output voltage and current through the resonant inductor ( $L_{r1}$ ) are in same phase. In the design the switching frequency has been chosen as 25 kHz and its time period becomes  $40\mu s$ , so the current becomes zero after every  $20\mu s$ . For every  $20\mu s$  switches will get turn on and turn off. Simulation and experimental results were shown in Figure.4.7. Zero voltage switching obtained by making the current to flow through the anti parallel diodes of MOSFET switches  $M_1$  and  $M_2$  and the operation explained on the basis of current wave form is shown in Figure.4.9.

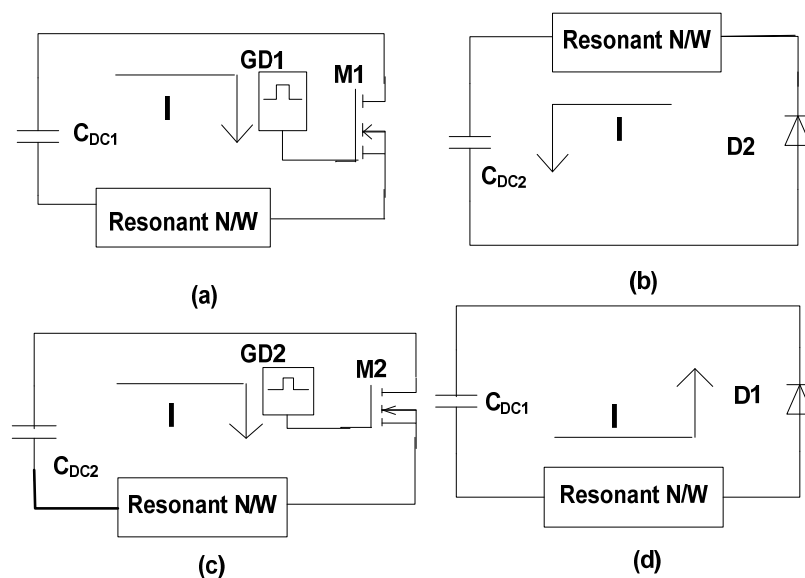


Figure.4.8: Current direction in each mode of ZVS

During time  $t_1$  MOSFET  $M_1$  is switched on and the current direction through the load is shown in Figure.4.8a. When the switch  $M_1$  is turned off current still in the same direction but

the circuit completes through  $C_{DC2}$  and diode ( $D_2$ ) and resonant network (shown in Figure.4.8b) by adjusting the dead time between  $M_1$  and  $M_2$ . During the time  $t_3$  when MOSFET  $M_2$  is switched on and the current direction through the resonant network is reversed as shown in Figure.4.8c, during the time  $t_4$  diode ( $D_1$ ) of MOSFET ( $M_1$ ) get forward biased after turning off the switch  $M_2$  the current through the resonant network is still in same direction and circuit completes through load  $C_{DC1}$ , resonant network and diode ( $D_1$ ) (shown in Figure.4.8d) in the dead time period.

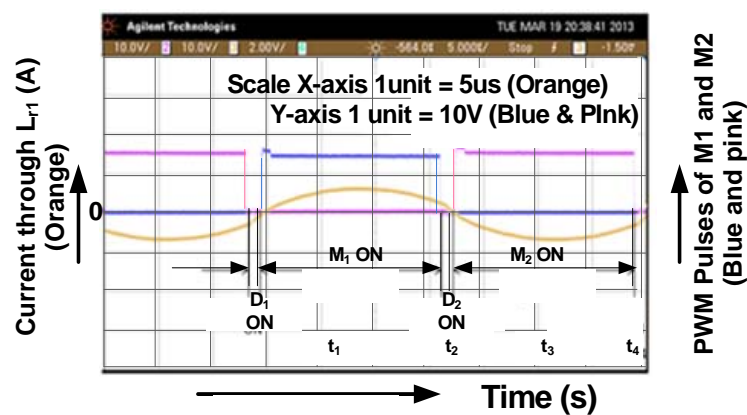


Figure.4.9: PWM signals for switches in the inverter stage vs current through  $L_{r1}$  to verify

### ZVS

Figure.4.9 describes zero voltage switching (ZVS), it can be explained by comparing PWM pulses for MOSFET switches and current flowing through  $M_1$ ,  $M_2$ ,  $D_1$  and  $D_2$  with respect to time. Switching action takes place in inverter switches when the voltage across the switch is zero is shown in Figure.4.9.

Explanation is as follows, when the switch  $M_1$  is turned off the current will not become zero immediately it tried to flow in same direction, then it chooses the path resonant network –  $D_2$  –  $C_{DC2}$ . In the very next instant of time, when switch  $M_2$  about to start the voltage across the switch is zero due to the conduction of anti parallel diode  $D_2$  (i.e. the switch  $M_2$  turned on at zero voltage). On the other hand when switch  $M_2$  is turned off the current will not become

zero immediately it tried to flows in the same direction, then it chooses the path resonant network –  $D_1 - C_{DC1}$ . In the very next instant of time, when switch  $M_1$  about to start the voltage across the switch is zero due to the conduction of anti parallel diode  $D_1$  (i.e. the switch  $M_2$  turned on at zero voltage).

#### **4.2 Development of control circuit**

Control circuit design plays important role in charging applications, wherein energy storage capacitors are charged to target voltage in a specified duration of time and discharges to the load for a very short duration of time. Since capacitor charging power supply with resonant network provides load independent constant current will charges the load capacitor beyond its rated value if there is no control. If the load capacitor value changes then charging time also changes proportionately, because the current supplied to the load is constant. In absence of control circuit the constant current leads to failure of load capacitors due to over voltages.

In the present section the design and development features of a generalized control circuitry has been presented, which provides control signals for semi conductor controlled switches (IGBTs or MOSFETs etc). Energy has been transferred from source to load via high frequency inverter circuit, so our target is to provide control signals to switches in the inverter stage such that they should be in turned on position till the target voltage reaches. The block diagram of the proposed control circuit is shown in Figure.4.10.

Two micro controllers, ADC (Analog to digital converter), DAC (Digital to analog converter, comparator, PWM controller, Max232, SMPS (24V, 15V and 5V), MOXA (Electrical to optical and vice versa) and industrial PC has been used in the development of control circuit. Initially a program has been dumped in to the master and slave micro controller. A ladder program runs on industrial PC with three controlled variables and one measurement variable.

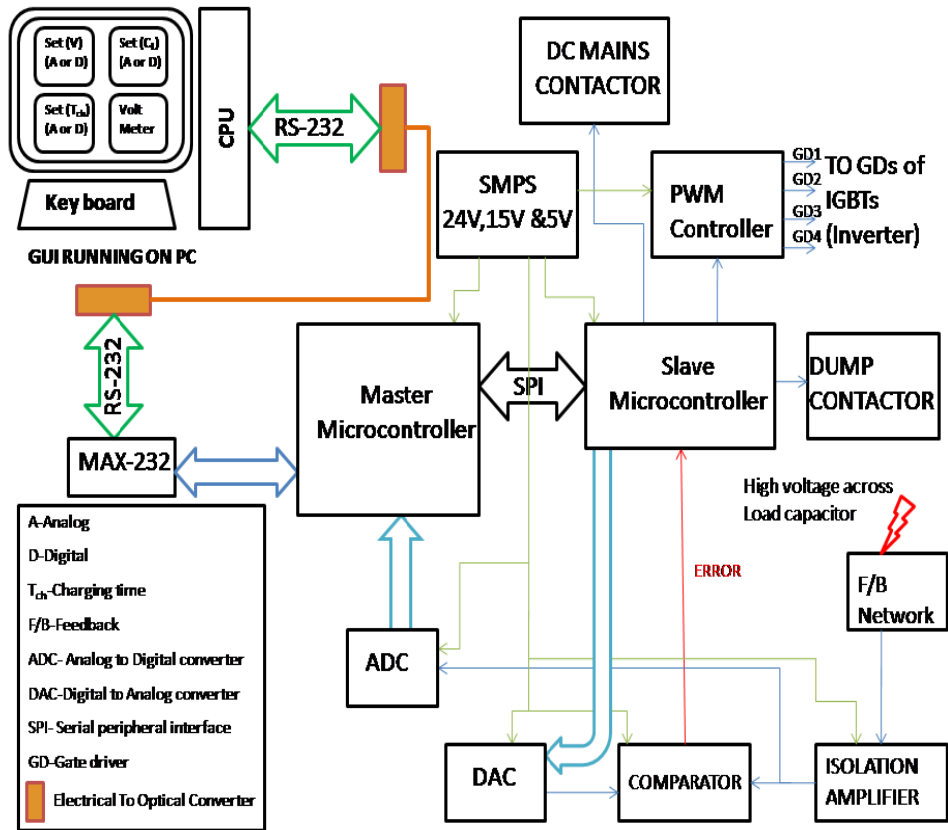


Figure.4.10: Block diagram of control circuit

These control variables are set voltage [Set (V)], set charging time [Set ( $T_{ch}$ )] and set load capacitor value [Set ( $C_L$ )]. Measurement variable (Voltmeter) used to monitor the voltage across load capacitor. Max232 is a communication IC which interfaces between MOXA and Master controller.

#### 4.2.1 Operation

At the initial stage one has to set the value of load capacitor either in analog or in digital and then set the charging time the target voltage is automatically get updated. In the other case if we set load capacitor and target voltage then charging time automatically updated based on these two values. These two set values are first converted in to optical signal by MOXA (electrical to optical converter) and then transmitted through optical cable. Optical signal then converted in to electrical signal by MOXA (optical to electrical converter) and given to the

master controller through MAX232 IC. The pre loaded programmed in the master controller runs and generates two signals, one is for PC the other is for slave controller. The preloaded programme in slave controller generates four signals, one is for PWM IC, second is for DAC IC, third for dump contactor and fourth for mains contactor. Signal for mains contactor will enables the contactor to close and the power flows from input mains. The signal generated for PWM IC is a timing signal which is directly given on shut down pin of PWM IC. The free running PWM IC generate pulses with time period equal to switching frequency for time duration specified on shut down pin. The signal which generated for dump contactor enables the dump contactor to dump the energy stored in load capacitor to dummy load in emergency. The signal generated for DAC will set the value of target voltage obtained from slave controller in digital form.

Comparator block consist of a differential amplifier which takes the signal from DAC and isolation amplifier and compares. The generated error is given to both master and slave controller simultaneously. Isolation amplifier provides isolation between feedback network and low power electronics. Feedback network obtain the signal from lower arm resistor of voltage divider circuit through isolation amplifier. Analog to digital converter (ADC) IC will get the signal from isolation transformer and converted into digital, which continuously poles to master controller. Master controller senses this digital signal and it gives the signal to PC to display the charged voltage in voltage meter.

The loop continues till the error generated by the comparator is zero, it means that the voltage across load capacitor reaches to the target voltage the loop continues. In this loop slave controller, PWM controller, comparator, DAC, isolation amplifier and feedback network are working simultaneously. The generated PWM signals are used to turn on and turn off the controlled switches in the inverter stage. The energy transferred to the load from source

happens in each switching cycle. As an when voltage across load capacitor reaches to target voltage PWM signals for switches in the inverter stage got removed.

### **Summary**

The first 4<sup>th</sup> order resonant topology shown in Figure.3.2 has been chosen to verify the basic operation of 4<sup>th</sup> order resonant topology for constant current application. A prototype based 20J/s capacitor charging power supply has been developed and tested with 100  $\mu$ F capacitor. A half bridge inverter has been utilized to get square wave voltage with switching frequency of 25 kHz. The proposed topology achieved load independent constant current and soft switching when switching frequency is equal to the resonant frequency. Zero voltage switching and zero current switching achieved experimental at 26 kHz. The test set up has been tested for a voltage of 200V with 75V DC input. A generalized control scheme has been developed to provide control signals for switches in the high frequency inverter stage of capacitor charging power supply. Input signals obtained from human interface (HMI), such as set voltage, set charging time and set load capacitor value. Micro controller generates the timing signal to free running pulsed width modulator (PWM) based on the given values in HMI. The PWM IC provides ON/OFF signals for switches in the inverter stage to transfer energy from input to output with cycle time equivalent to switching frequency. In addition controller takes the interrupts from feedback and generates timing signal according to the error generated at the output of differential amplifier.

# Chapter-5

## Validation with various pulsed power systems

---

The development features of different rated CCPS are implemented with 4<sup>th</sup> order resonant converters and validated with experimental results.

### 5.1 Development of CCPS for power modulator applications to study spark gap recovery times

Highly pressurized spark gaps are adopted in the area of pulsed power technology to generate high intensity pulses. The main limitation with spark gap technology is its repetition rate. Spark gap recovery times varies from gas to gas, even if they recovered fast the limitation comes at the source end.

#### 5.1.1 Design features

A fourth order CLCL resonant converter topology has been utilized to design a charging power supply for power modulator application.

Input voltage	200V
Output voltage	1 kV
J/s rating	500J/s
Load capacitor	100 $\mu$ F
Charging time	100ms

Table.5.1: Rating of 500J/s CCPS

In the present design a high voltage high frequency transformer has been used to increase voltage from 200V to 1kV. The chosen resonant converter provides constant current and soft switching when switching frequency equal to resonant frequency. A 1kV and 500J/s constant current charging source has been developed and tested with 100 $\mu$ F capacitor.

The block diagram of 4<sup>th</sup> order LCLC resonant based CCPS is shown in Figure.5.1.

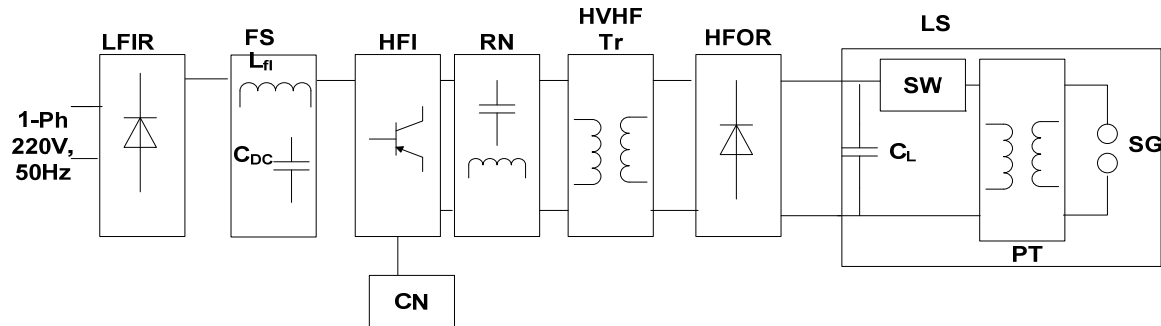


Figure.5.1: Block diagram of proposed CCPS with power modulator

In the above figure low frequency input rectifier (LFIR), filter section (FS), high frequency inverter (HFI), resonant network (RN), high voltage high frequency transformer (HVHF Tr), high frequency output rectifier (HFOR), load section (LS), switch (SW), pulsed transformer (PT), spark gap (SG) and control circuitry (CN). The detailed circuit diagram of power supply with power modulator is shown in Figure.5.2.

In the present design a high voltage high frequency transformer is utilized to step up voltage from 200V to 1kV. Effect of transformer parameters like leakage inductance and distributed capacitance have been studied in the next section.

### 5.1.2 Development features

The design parameters are calculated based on the equations derived in the previous section.

Input voltage =  $V_{dc} = 200V$

Switching frequency =  $f_s = 25 \text{ kHz}$

Charging voltage =  $V_{load} = 1000V$

$$C_{\text{load}} = 100\mu\text{F}$$

$$\text{J/s rating} = 500\text{J/s}$$

The circuit diagram of CCPS with HVHF transformer is shown in Figure.5.2.

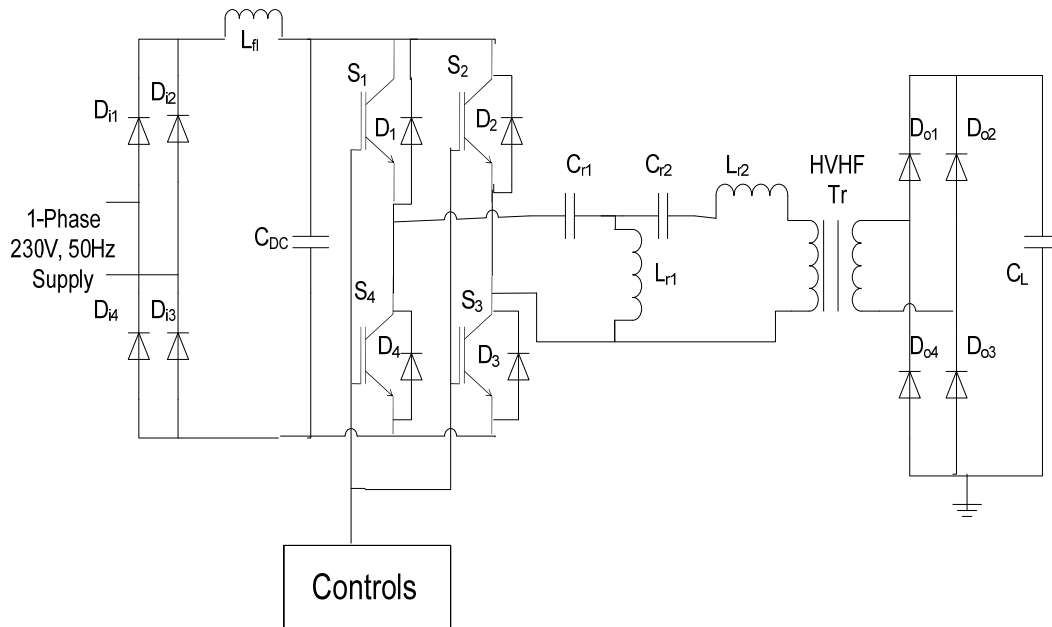


Figure.5.2: Basic schematic circuit diagram of 4<sup>th</sup> order CLCL resonant based CCPS with feedback

$$I_{r1} = V_{\text{rms}}\omega_0 C_{r1} \text{ (Where } V_{\text{rms}} = 255\text{V)}$$

$$I_{\text{Load avg}} = C_L \frac{dV}{dt},$$

$$t_c = \text{charging time} = 100\text{ms}$$

For charging the capacitor up-to 1000V the current required,

$$I_{\text{Load avg}} = 1,$$

$$\frac{I_{\text{rms}}}{I_{\text{avg}}} = 1.11,$$

$$n = \frac{V_2}{V_1} = \frac{1000}{200}$$

$$n = \frac{V_2}{V_1} = 5 = \frac{I_1}{I_2}$$

Components	No's	Components	No's
IGBTs (IRG4ph40KD)	4	Input rectifier module	1
DC link capacitor ( $C_{DC}=4.7mF$ )	1	Current transformer (Ferrite core based)	1
Output rectifier diodes (RHRP30100)	4	SMPS (15V and 5V)	1
Gate drivers (Indigenous)	4	Load capacitor (100 $\mu$ F)	1
Single phase variac	1	Resonant inductors (406 $\mu$ H) and 203 $\mu$ F	1
PWM controller card	1	Resonant capacitors (200nF)	2

Table.5.2: Components list of 500J/s CCPS

$$I_{r1} = V_{rms}\omega_0 C_{r1} = 5.55$$

$$C_{r1} = 138nF,$$

Due to non availability of exact value of capacitor (138nF) chosen a 200nF.

$$C_{r1} = C_{r2} = 200nF \text{ and}$$

$$\omega_0 = \sqrt{\frac{1+y}{yL_{r1}C_{r1}}}$$

$$\text{Where } y = 1, (x = \frac{L_{r2}}{L_{r1}} \text{ and } y = \frac{C_{r2}}{C_{r1}})$$

$$\text{Then } L_{r1} = 406\mu H \text{ and}$$

$$L_{r2} = 0.5L_{r1}$$

$$L_{r2} = 203\mu H$$

### 5.1.3 Experimental set up

Developed a HVHF Tr with a turns ratio of 5, wherein a ferrite based toroidal core whose maximum flux density is 0.2wb/m<sup>2</sup>. The input to the transformer is 200V and corresponding output is 1kV.

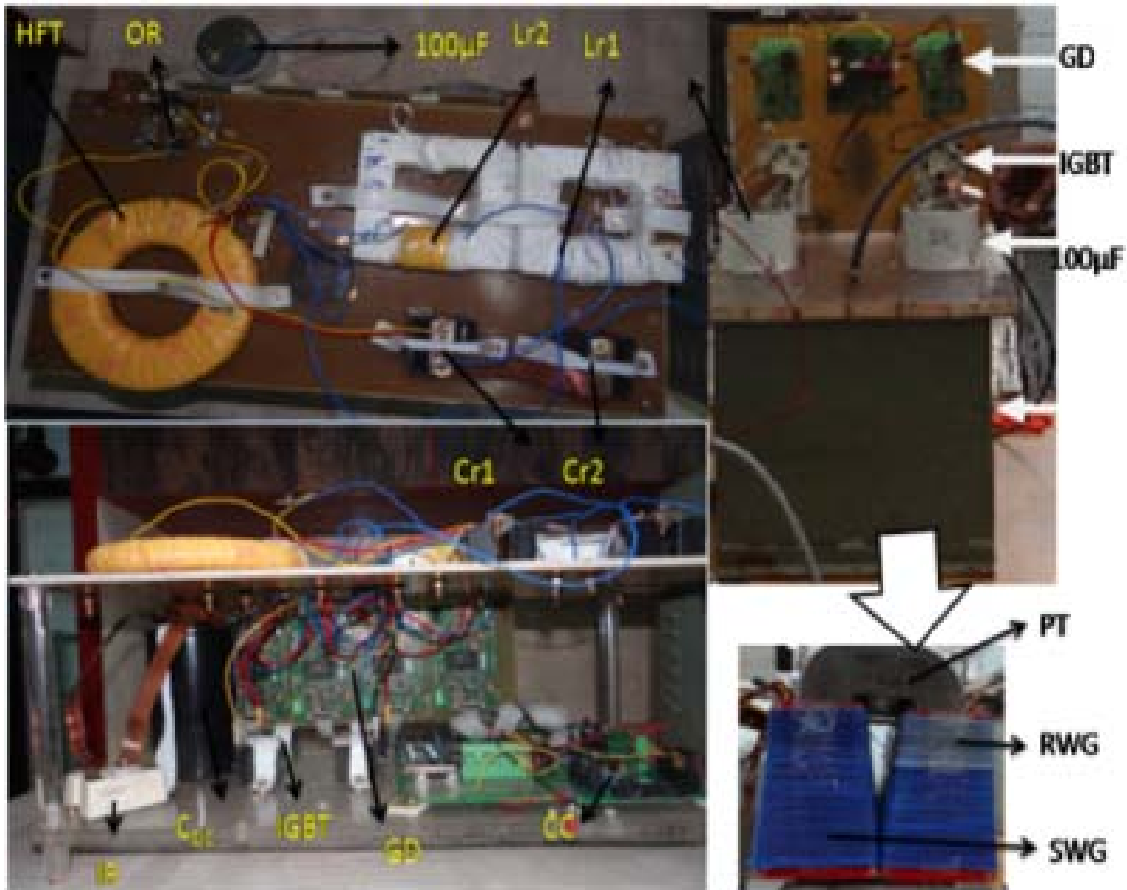


Figure.5.3: Experimental setup of 4<sup>th</sup> order LCLC resonant topology with power modulator

The second resonant inductor has to be adjusted such that the whole inductance in that branch should not increase  $203\mu\text{H}$  (After adding the leakage inductance of high frequency transformer to  $L_{r2}$ ). A current transformer also developed to measure the current through first resonant inductor. Experimental set up is shown in Figure.5.3. The proposed power supply is designed to charge  $0.5\mu\text{F}$  capacitor, but due to non availability of this rating capacitor tested with  $100\mu\text{F}$  capacitor.

#### 5.1.4 Results

In this section presented both simulation and experimental results to verify current flowing through the IGBT switch, charging voltage profile across load capacitor ( $100\mu\text{F}$ ). This current charges the load capacitor ( $100\mu\text{F}$ ) to  $1\text{kV}$  in  $100\text{ms}$ . The load capacitor charged to  $1\text{kV}$  both in simulation and experimental in  $98\text{msec}$  and is shown in Figure.5.4.

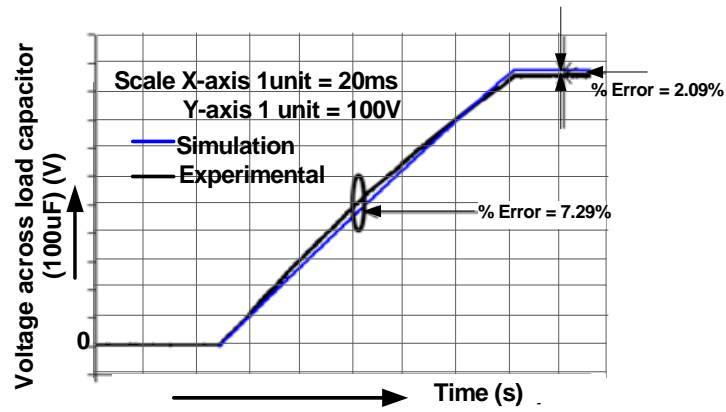


Figure.5.4: Voltage profile across load capacitor (100µF)

There is an error of 7.29% in the transient period and 2.09% in the steady state period. An extra lead inductance and coupling capacitance make the 4<sup>th</sup> order CLCL resonant network not been operated exact resonant frequency (25 kHz). The load current (1A average) has been found mathematically in the previous section and is shown in Figure.5.5. There is some error linearity error in transient period due to lead inductance and other reasons.

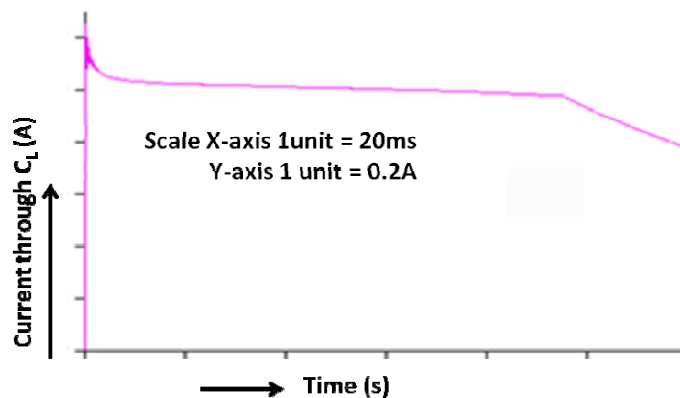


Figure.5.5: Current through load capacitor (100µF)

Current measured through the resonant capacitor ( $C_{r1}$ ) to verify the peak current flowing through the IGBT switch in the inverter stage of power supply. Measurement of  $I_{Lr}$  is so important in choosing IGBT rating of high frequency inverter. If the rating in multiples of 10kJ/s, peak current consideration becomes essential in choosing IGBT switch. The maximum current observed from simulation and experimental (Figure.5.6.) is almost same and is nearly equivalent to 8A.

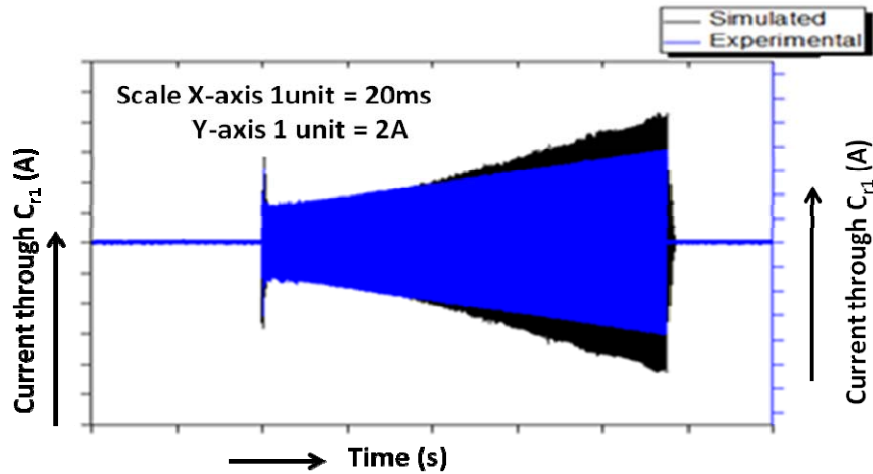


Figure.5.6: Current profile observed through  $L_{r1}$

This is because of the first resonant inductor ( $L_{r1}$ ) and capacitor ( $C_{r1}$ ) value. There is a large difference between simulation and experimental results, because the calculated values can be used in simulation but they are not achieved in experimental. So, the characteristic impedance is differing in simulation from experimental.

## 5.2 Development of CCPS for solid state pulser application

Designing a high repetitive (9 kHz) constant current charging source for pulsed power system is a challenging task for designers. A 4kV and 9 kHz repetitive charging source based on forth order LCCL resonant topology has been designed and developed for pulser application. A 4<sup>th</sup> order LCCL resonant topology has been utilized to provide constant current, zero current switching when switching frequency equal to the resonant frequency (i.e.  $f_s=f_r$ ).

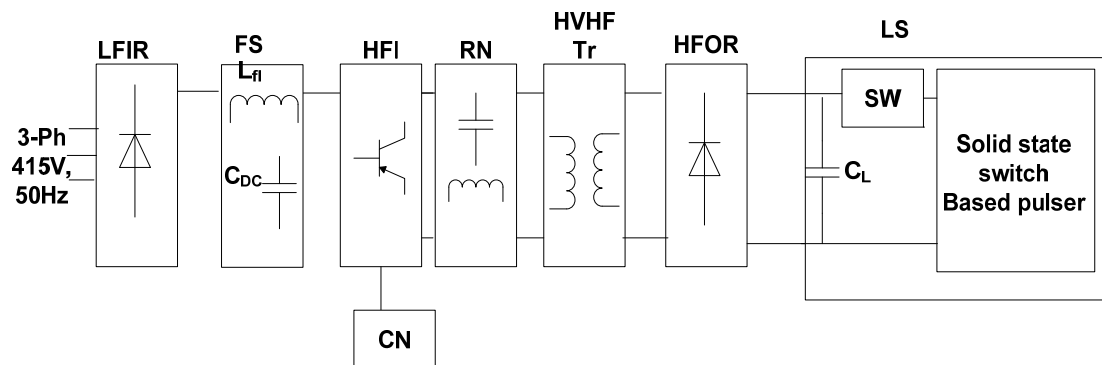


Figure.5.7: Basic block diagram of charging source with pulser

The basic block diagram for the design is shown in Figure.5.7. In the above figure LFIR is low frequency input rectifier, FS filter section, HFI is high frequency inverter, RN is resonant network, HVHF Tr is high voltage high frequency transformer, HFOR is high frequency output rectifier, LS is load section, SW is switch and CN is control circuitry. The detailed circuit diagram of power supply with power modulator is shown in Figure.5.7. HVHF transformer leakage inductance has been utilized as a part of one of resonant inductor  $L_{r2}$ .

### 5.2.1 Development features

Development features consists various calculations to find power and resonant component values to develop power supply. In development feature first step is to decide the load parameters, which will be given by end user.

Input voltage	500V
Output voltage	4 kV
J/s rating	3.7 kJ/s
Load capacitor	47nF
Repetition rate	9 kHz

Table.5.3: Rating of 3.7 kJ/s CCPS

Switching frequency =  $f_s = 25$  kHz

It is generally equivalent or more than audible range would be chosen

Charging voltage = 4 kV

Repetition rate = 9 kHz

Average voltage =  $V_{DC} = 500V$  (assumed)

Load capacitor =  $C_L = 47nF$

$$\text{Total time} = T_{\text{Total}} = \frac{1}{\text{Repetitionrate}} = \frac{1}{9000} = 111\mu\text{s}$$

$$\text{Total time } T = T_{\text{charging}} + T_{\text{refresh}} + T_{\text{discharge}}$$

$$T_{\text{discharge}} = 1\mu\text{s}, T_{\text{refresh}} = 10\mu\text{s}, T_{\text{charging}} = 100\mu\text{s}$$

$$\text{Energy stored in the load capacitor} = \frac{1}{2C_L V_L^2} = 0.376\text{J}$$

$$\text{J/s rating of power supply becomes} = \text{energy stored} / T_{\text{charging}} = \frac{0.376}{100 \times 10^{-6}} = 3.7 \text{ kJ/s}$$

Data obtained from the above calculation and the current through the load capacitor is given by

$$I_{\text{Load avg}} = C_L \frac{dV}{dt} = 1.9\text{A}$$

$$\text{Turns ratio} = \frac{V_{\text{sec}}}{V_{\text{pri}}} = \frac{4000}{500} = 8.$$

Circuit diagram of CCPS with 4<sup>th</sup> order resonant converter is shown in Figure.5.8.

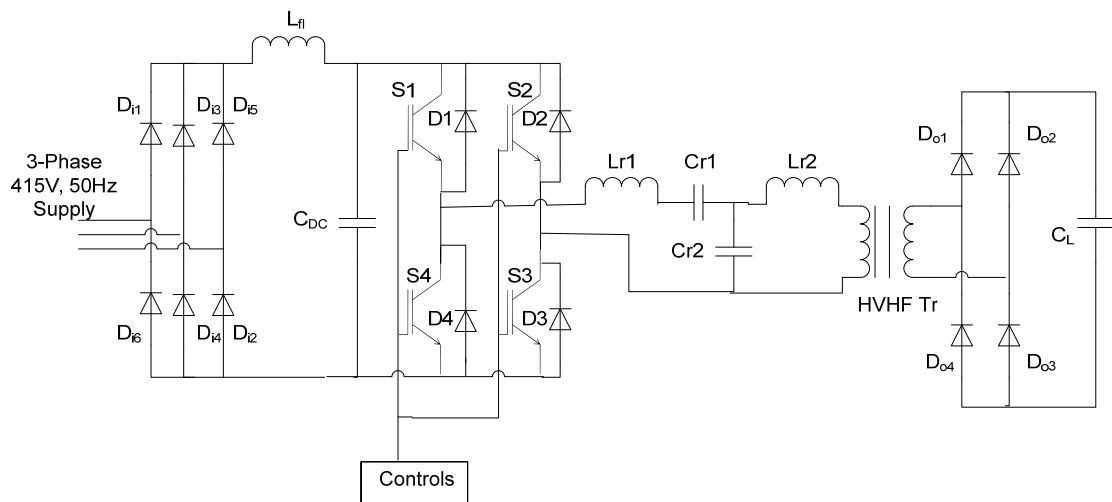


Figure.5.8: Typical circuit diagram of LCCL resonant based charging source

Three stage conversions have been done to transfer energy form source to the load. In the first stage of conversion the alternating power converter to DC power by input diode rectifier, then the DC power converted to alternating power by resonant converter and finally alternating power converted to DC power by fast recovery high frequency diode rectifier is shown in Figure.5.8.

$$\text{The reflected current at the primary of the high frequency transformer} = 8 \times 1.9 = 15.2\text{A}$$

$$I_{\text{rms}} = 1.1 I_{\text{Load avg}} \text{ (Reflected primary current)}$$

$$I_{Lr1} = 1.11 * 15 = 16.9A$$

From the equation 3.26 the resonant capacitor value found to be =  $C_{r1} = 170nF$

Due to non availability of exact value chosen the capacitor value is 200nF, which intern increases the current through resonant inductor.

$$\text{Then } C_{r1} = C_{r2} = 200nF$$

The resonant inductor value becomes =  $L_{r1} = 406\mu H$ ,

$$L_{r2} = 0.5L_{r1}, L_{r2} = 203\mu H$$

Components	No's	Components	No's
IGBTs (IRG4ph40KD)	4	Input rectifier module	1
DC link capacitor ( $C_{DC} = 4.7mF$ )	1	Current transformer (Ferrite core based)	1
Output rectifier diodes (RHRP30100)	16	SMPS (15V and 5V)	1
Gate drivers (Indigenous)	4	Load capacitor (100 $\mu F$ )	1
Discharge resistors	5	Resonant inductors (406 $\mu H$ and 135 $\mu H$ )	1
Current limiting resistor	1	Resonant capacitors (200nF)	2
Single phase variac	1	PWM controller card	1

Table.5.4: Components list of 3.7 kJ/s CCPS

Development of resonant inductors and HVHF transformer are crucial in the design. Transformer parameters like leakage inductance and the distributed capacitance may alter the actual operation of resonant based charging source. Distributed capacitance should be as less as possible while developing HVHF Tr, where as leakage inductance can be adjusted as a part of resonant inductor. Components are to be chosen based on current carried by them and voltage developing across them. Components used for the development of CCPS for the current design are listed in Table.5.4.

## 5.2.2 Experimental set up

A table top setup has been developed to test the high voltage solid state based.

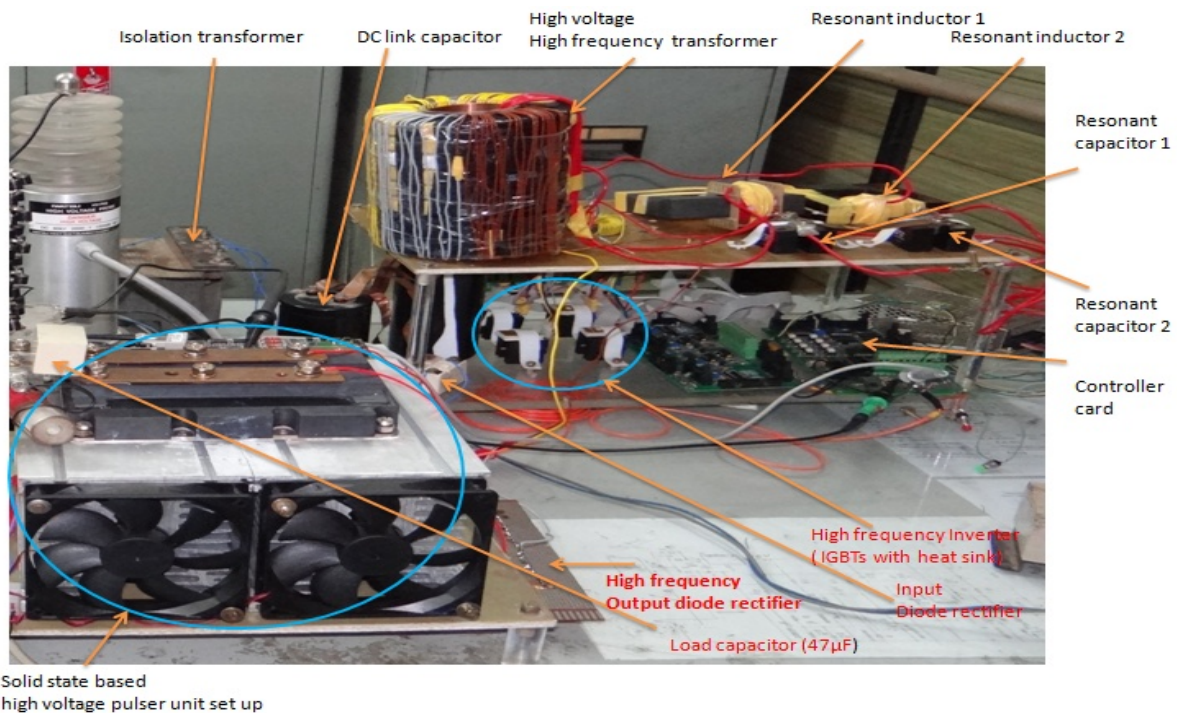


Figure.5.9: Experimental setup with high voltage pulser

Experimental setup consisting of input rectifier, DC link capacitors, high frequency inverter and resonant network consisting of two resonant inductors ( $L_{r1} = 406\mu\text{H}$  and  $L_{r2} = 135\mu\text{H}$  after deducting leakage inductance  $70\mu\text{H}$  of high frequency transformer) and two resonant capacitors (Each of  $200\text{nF}$ ) is shown in Figure.5.9. Followed by high frequency transformer, then high frequency fast diode rectifier unit, finally load capacitor. In this case the load is not been grounded. Experimental set up of  $3.7\text{ kJ/s}$  CCPS with solid state switch based pulser has been shown in Figure.5.9. Switching signals for IGBT switches in the inverter circuit are generated by micro controller and other peripheral ICs. The charging time is preloaded into the controller then controller provides the timing signal to PWM generator. The free running PWM IC generates pulsed based on switching frequency for a specified duration of time. These PWM signals are used to provide turn on and turn off the IGBT switches in the full bridge inverter circuit.

### 5.2.3 Results

Results which are shown in this section is to verify the peak current flowing through the IGBT switch, charging and discharging voltage profile load capacitor (47nF) with a repetition rate (9 kHz).

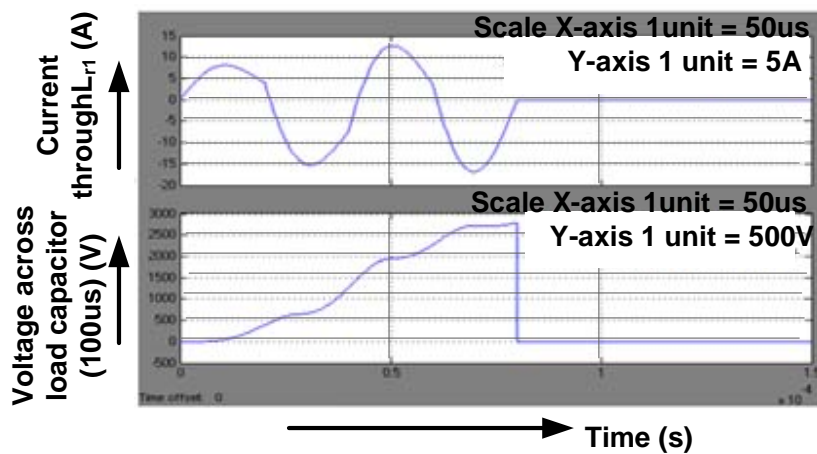


Figure.5.10: Simulation results of charging voltage and current through resonant inductor

In addition discussed the various modes of operation in which zero current and zero voltage switching is occur. The chosen load capacitor 47nF (experimental) voltage rating is only 3kV, so restricted to charge a load capacitor with a charging time up to 80 $\mu$ s.

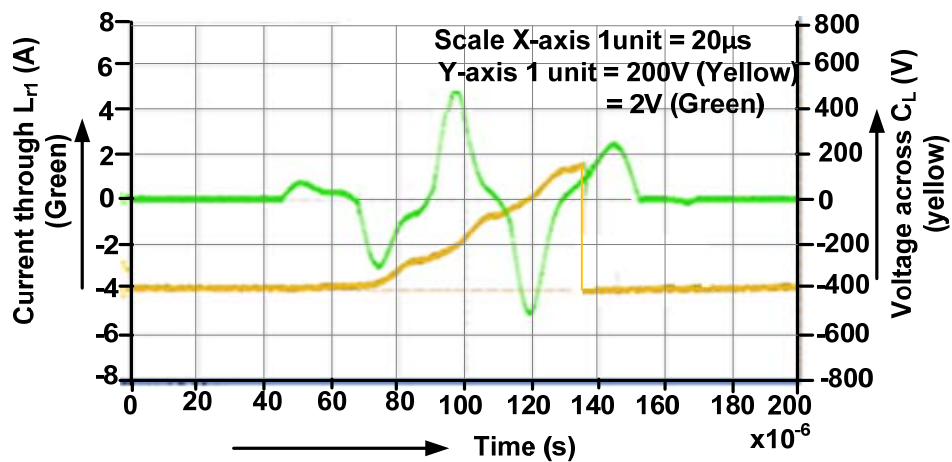


Figure.5.11: Experimental results of charging voltage and current through resonant inductor

Peak current through IGBT switch and voltage across load capacitor are shown in Figure.5.10 and 5.11. The time taken to charge load capacitor (47nF) up to 3kV will take only 80μs and it completes it in just two cycles. Because the switching frequency is 25 kHz and equivalent time period becomes 40μs.

The peak current flowing through IGBT switch is about 13.8A (Simulation Figure.5.10.) and 14A (Experimental Figure.5.11. i.e.  $2.8 \times 5$  (CT turns ratio) = 14.1A) are in comparable with mathematical value (for 80μs charging time and 3kV charging voltage the peak current is about 14A). The charging voltage across load capacitor is 2.8kV (experimental) is almost in comparable with simulation and mathematical value 3kV is shown in Figure.5.10b and in 5.11.

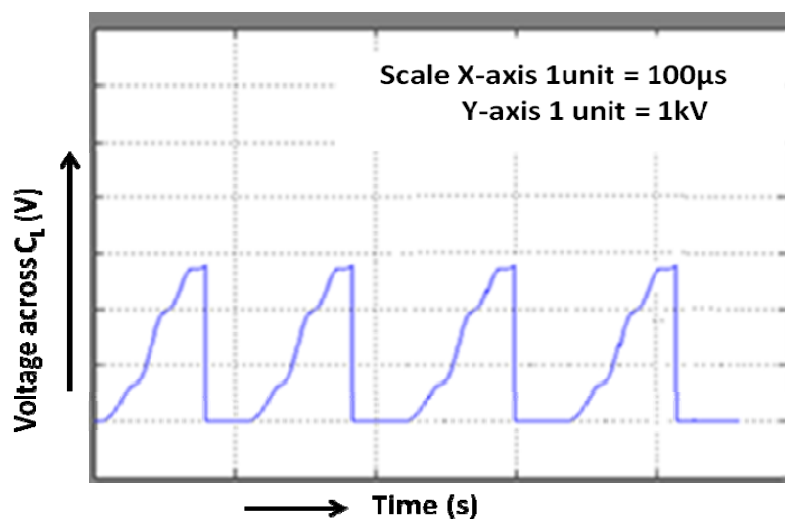


Figure.5.12: Simulation results of charging voltage with 9 kHz repetition rate

Charging and discharging of load capacitor has been shown in Figure.5.12 to ensure the repetition rate 9 kHz. The 9 kHz frequency time period becomes = 111μs (This includes charging, holding and discharge timings) whose simulation result is shown in Figure.5.12. The same wave form with 9 kHz repetition rate has been observed experimentally and is shown in Figure.5.13.

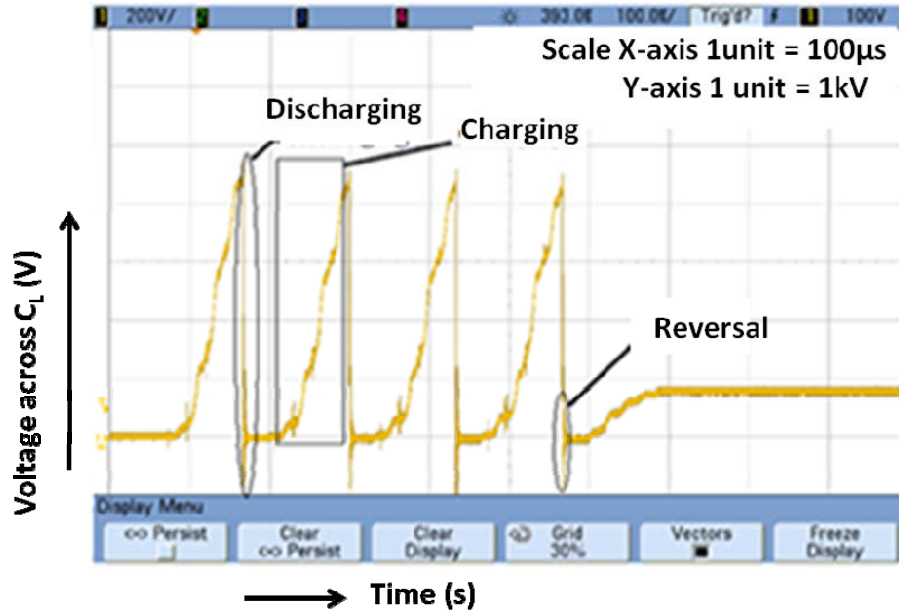


Figure.5.13: Experimental results of charging voltage and with 9 kHz repetition rate

Charging and discharging voltage profile across load capacitor (47nF) experimentally has been shown in Figure.5.13. Discharging profile of load capacitor is not exactly same as that of simulation result, because when it is discharges across load a reversal getting across load capacitor (47nF) is shown in Figure.5.13.

### 5.3 Development of CCPS for 1kJ Marx based repetitive pulsed power system

Designing a reliable and compatible power supply for pulsed power applications is always a tricky job when charging rate in multiples of 10kJ/s. A  $\pm 50\text{kV}$  and 45kJ/s capacitor charging power supply based on 4<sup>th</sup> order LCLC resonant topology has been designed and developed for repetitive Marx based system.

The typical circuit diagram of capacitor charging power supply is shown in Figure.5.14. Number of stages involved in the power supply, schematic circuit diagram is shown in Figure.5.14. Stage (S-1) consists of low frequency rectifier (LFIR) to convert AC to DC.

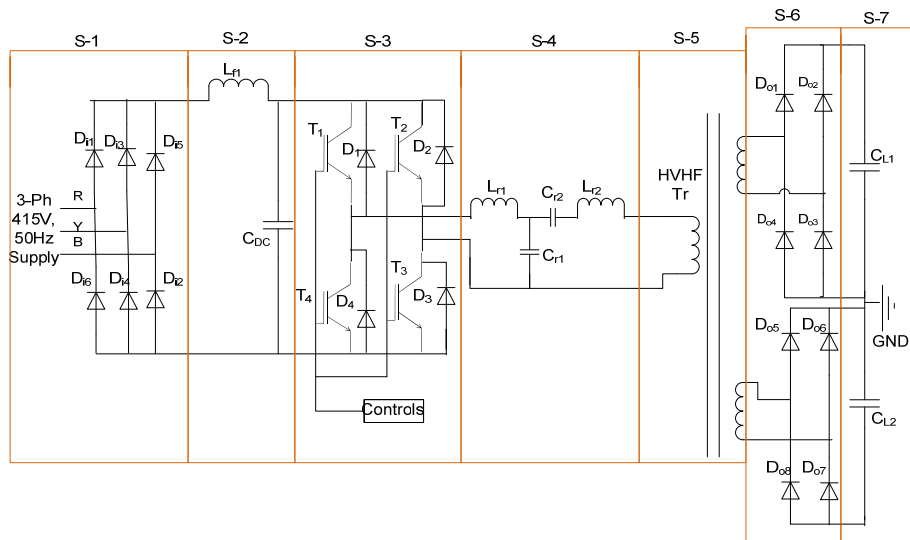


Figure.5.14. Typical circuit diagram of LCCL resonant based charging source

In S-2 ripples are filter out in filter section (FS) by DC link capacitor and inductor, where as in S-3 the constant DC is converted into a square wave by high frequency inverter (HFI) with a switching frequency 25 kHz. In S-4 square wave voltage converted in to sine wave by resonant network (RN), S-5 step up the voltage from one level to other by high voltage high frequency transformer (HVHF), this high frequency sine wave is converted into DC by high frequency output rectifier (HFOR) in S-6 and finally DC voltage applied to load section (LS) where energy storage capacitor is connected (i.e. S-7).

### 5.3.1 Development features

Rating of the charging power supply has been given the following Table.5.5.

Input voltage	500V
Output voltage	±50 kV
J/s rating	45 kJ/s
Load capacitor	0.9μF for +ve and 0.9μF for -ve
Repetition rate	10 Hz

Table.5.5: Rating of 45 kJ/s CCPS

Charging voltage =  $V_{\text{load}} = 100\text{kV}$  (+ve + -ve)

Two  $0.9\mu\text{F}$  capacitors are connected as shown in Figure.2. The equivalent load capacitance becomes  $0.45\mu\text{F}$ . Where repetition rate =  $10\text{Hz}$  (i.e. 10 cycles).

The average energy stored in the load capacitor ( $0.45\mu\text{F}$ ) per cycle =  $0.5C_L V^2 = 2250\text{J}$

Average energy stored in the capacitor ( $0.45\mu\text{F}$ ) per 10cycles =  $2250*10 = 22500\text{J} = 22.5\text{kJ}$

The peak power delivered to the load capacitor in one sec is nothing but the average energy stored divided by charging time and it is given by

Peak power delivered to the load capacitor is the ratio of average energy per cycle to charging

$$\text{time} = \frac{2250}{50e^{-3}} = 45\text{kJ/s}$$

$$I_{Lr1\text{rms}} = \frac{V_{\text{rms}}}{\omega_0 L_{r1}} \text{ (where } V_{\text{rms}} = 450\text{V)}$$

$$I_{L\text{avg}} = C_L \frac{dv}{dt}, t_c = \text{charging time} = 50\text{ms}, I_{L\text{avg}} = 0.45*10^{-6}(100*10^3 / 50*10^{-3}) = 0.9\text{A}$$

The input current flowing through resonant inductor ( $L_{r1}$ ) is sinusoidal current. So, the rms current is given by

$$I_{L1\text{rms}} = 1.11 I_{L\text{avg}}$$

Turn ratio,  $n = 200$ ,

$$I_{L1\text{rms}} = 200*0.9\text{A} = 180\text{A} = I_{Lr1},$$

$$I_{L1\text{rms}} = 1.11*180 = 199.8\text{A} = 200\text{A}$$

The peak current through resonant inductor

$$I_{Lr1\text{peak}} = 1.414 I_{L1\text{rms}} = 1.414*200 = 283\text{A}$$

$$I_{Lr1\text{rms}} = \frac{V_{\text{rms}}}{\omega_0 L_{r1}} = 200 = \frac{450}{125e^3 L_{r1}}$$

$$L_{r1} = 18\mu\text{F}, L_{r2} = 2L_{r1} = 36\mu\text{H}.$$

$$\text{Then } \omega_0^2 = \frac{1}{L_{r1}C_{r1}} \text{ and } C_{r1} = 3.54\mu\text{F}, C_{r1} = C_{r2} = 3.54\mu\text{F}$$

Components used to development of this power supply are listed in Table.5.6.

Components	No's	Components	No's
IGBTs	4	Input rectifier module	1
DC link capacitor ( $C_{DC} = 14\text{mF}$ )	10	Current transformer (Ferrite core based)	1
Output rectifier diodes	432	SMPS (24V,15V and 5V)	1
Gate drivers	4	Load capacitors (0.9 $\mu\text{F}$ )	2
Discharge resistors	5	Resonant inductors (18 $\mu\text{H}$ and 24 $\mu\text{H}$ )	1
Current limiting resistor	1	Resonant capacitors (3.92 $\mu\text{F}$ )	2
DC filter inductor	1	Control card	1
3- $\emptyset$ Line filter inductors	3	Contactors	2
Diodes for soft start	6	Charging resistors for soft start	9
GUI	1	HVHF Transformer ( $\pm 50\text{kV}$ )	1

Table.5.6: Components list of 45 kJ/s CCPS

### 5.3.2 Experimental setup

Constant current charging source along with 10 Hz repetitive 1kJ Marx based system and dynamic load experimental set up has been shown in Figure.5.15. Power supply has been showed in Figure.5.16 covers four views to show how call components are managed to accommodate. DC link capacitor (14mF) used and filter inductor (5mH) connected in the circuit filter out ripples in the rectified output of 3-phase diode rectifier.

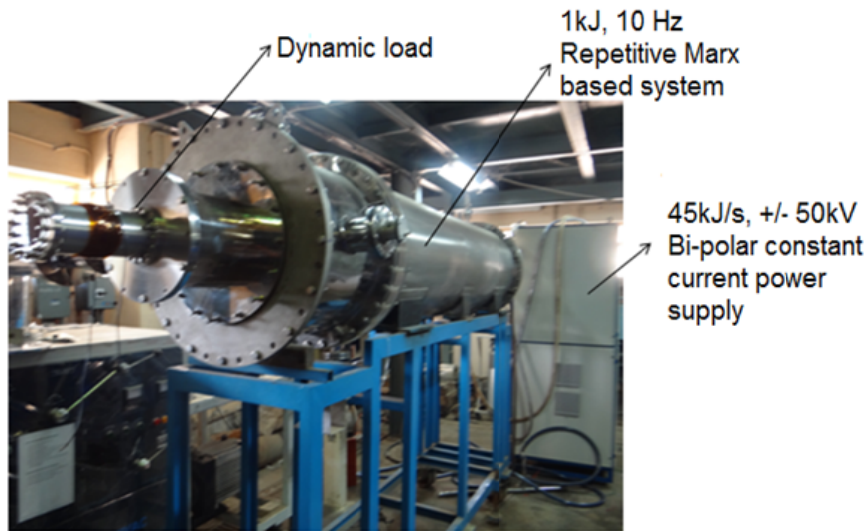


Figure.5.15: Experimental setup of 45 kJ/s CCPS along with 1kJ/s Marx based system

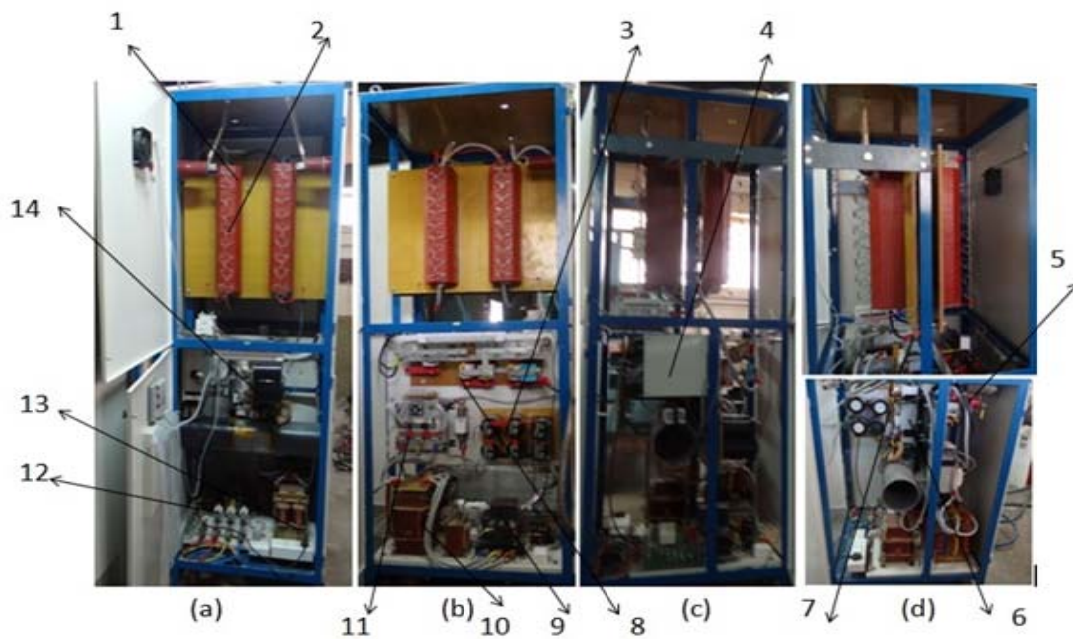


Figure.5.16: Experimental setup of 45 kJ/s (a) Front view (b) Back view (c) Left hand side view (d) Right hand side view

Where

1. HVHF transformer. 2. HF diode rectifier. 3. Bleeder resistor of DC link capacitor. 4. Control and low power electronics box. 5. Resonant capacitor. 6. Heat sink. 7. IGBTs. 8.

Resonant inductor. 10. Soft start. 10. 3-Phase line filters. 11. 3-Phase diode rectifier. 12. Input fuses. 13. DC Filter inductor. 14. DC link capacitors

A semikron make diode mono blocks are used to design 3-Phase input diode rectifier whose RMS line current is 80A. Infenion make 1200V, 800A IGBTs are used and connected in H-fashion to form a full bridge high frequency inverter. A HVHF transformer with a switching frequency of 20 kHz has been developed in the laboratory to provide  $\pm 50\text{kV}$  voltage at the output. The core details are OD = 100mm, ID = 55mm, height = 20mm and effective core area =  $436\text{mm}^2$  with maximum flux density of 0.2wb. Fast recovery diodes used in the design are BYM26E, whose voltage and current ratings are 1kV (reverse recovery voltage) and 2A forward carrying current.

### 5.3.3 Energy density

Energy density is a physical parameter, which describes the power supply size and weight. A good designer looks into the compactness, cost, rugged and proper protection for power supply when interfaced with high dynamic loads. In the present design the average energy already been calculated in the previous section as 22.5kJ/s. A 28\*28\*72 inch rack has been used to accommodate all the power components and control circuitry etc.

$$\text{Volume of the supply in m}^3 = (70*10^{-2}) (70*10^{-2}) (180*10^{-2})$$

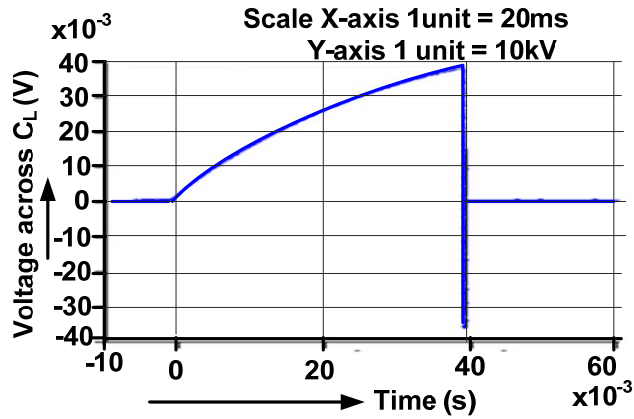
$$\text{Volume of the supply in m}^3 = 0.882\text{m}^3$$

$$\text{Energy density} = \text{Average energy/volume} = 22.5*10^3/0.882$$

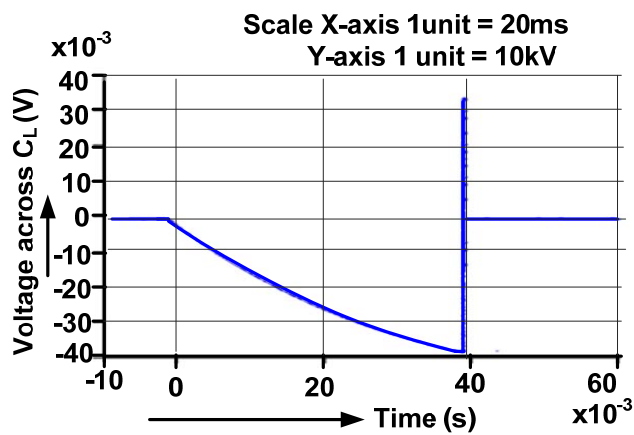
$$\text{Energy density} = 25.53\text{kJ/s per m}^3$$

### 5.3.4 Results

In this section presented the results obtained from experimental to verify various factors such as charging voltage, peak current thorough IGBT's and soft switching of IGBT switches.



(a)



(b)

Figure.5.17: Charging voltage profile across load capacitor ( $0.9\mu\text{F}$ )

(a) +ve charging (b) -ve charging

Charging profile across  $0.9\mu\text{F}$  for both (+ve and -ve) are showed separately in Figure.5.17a and 5.17b. The experimental set up has been tested with  $0.9\mu\text{F}$  both for +ve and -ve to charge 40kV in 40ms at the time of writing this paper is shown in Figure.5.17. There is reversal of same amount of reversal getting across the load capacitor, since the load connected to the pulsed power system is a highly dynamic in nature.

The power supply designed for  $\pm 50\text{ kV}$  but tested up to 40 kV due to limitation of capacitor rating. Both  $0.9\mu\text{F}$  capacitors are charge to +ve 40 kV and -ve 40 kV simultaneously. Current through resonant inductor is monitored and is shown in Figure.5.18. This current

profile is to identify how much peak current flowing through the IGBT switches in the inverter circuit. The current measurement has been done with the help of current transformer (CT).

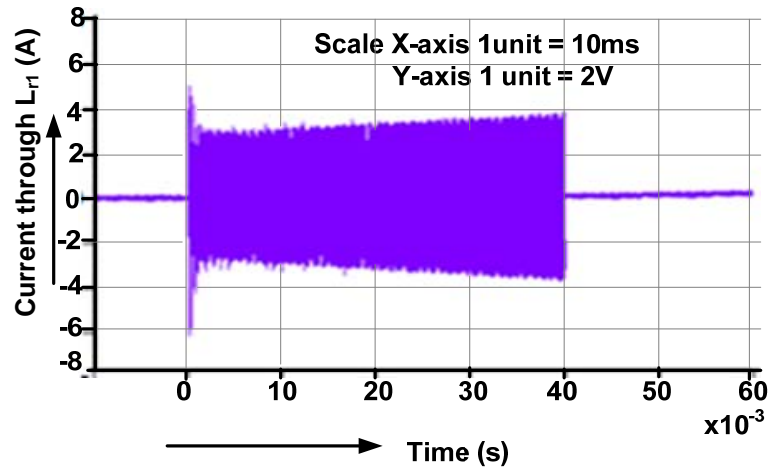


Figure.5.18: Current profile through resonant inductor ( $L_{r1}$ )

The current flowing through the resonant inductor ( $L_{r1}$ ) is nothing but the current carried by each IGBT switch in the inverter circuit. A 1:120 CT with a burden of  $2\Omega$  is used to measure the current. It is observed that 3.8V is the peak voltage getting across  $2\Omega$  resistor is shown in Figure.5.18.

It means 1.9A current flows through the load resistor. The equivalent current flowing through primary winding of CT is 70 times of 1.9A from turn's ratio.

$$\text{Current through burden} = 3.8/2$$

$$=1.9 \text{ A,}$$

Then, the current through primary of CT = Current through  $L_{r1}$

$$I_{Lr1} = 1.9 * 120$$

$$I_{Lr1} = 228 \text{ A}$$

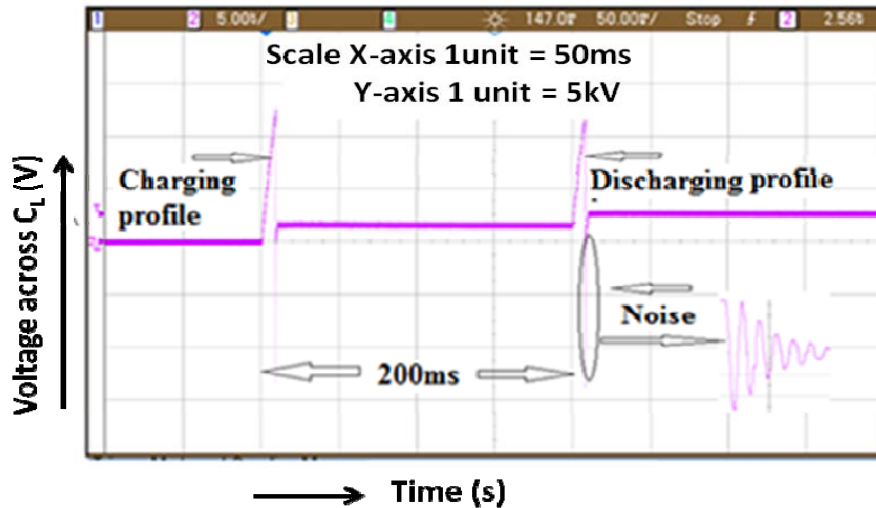


Figure.5.19: Voltage profile across  $0.9\mu\text{F}$  capacitor (+ve) with 5Hz repetition rate. So, the maximum peak current flowing through IGBT is 228A. Charging and discharging profile across load capacitor ( $0.9\mu\text{F}$  for +ve) with a repetition rate 5Hz has been in Figure.5.19. The difference between two pulses is 200ms, which means 5Hz repetition rate. The charging voltage is 13kV and the voltage reflection is also about 11 to 13kV when energy storage capacitor discharges across BWO.

### 5.3.5 Soft switching

In practical the resonant frequency is not equal to the switching frequency, because practical resonant inductor value won't match with calculated value.

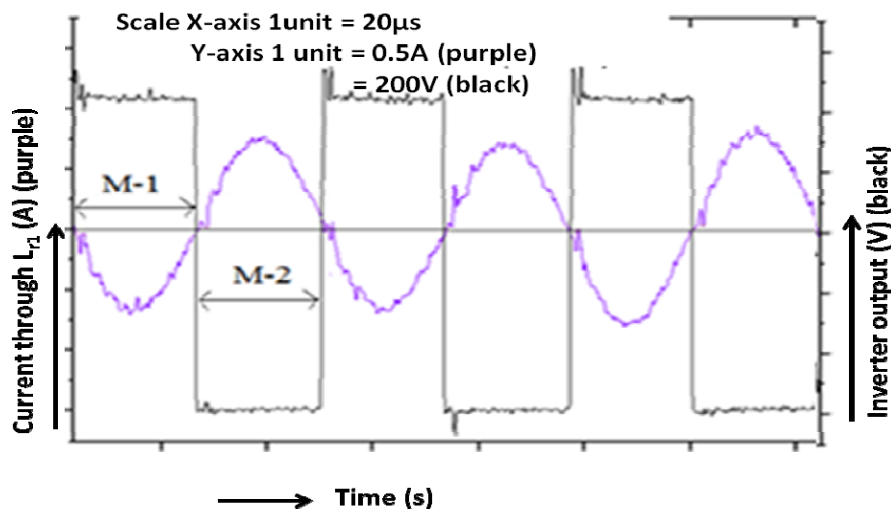


Figure.5.20: Current through  $L_{r1}$  vs inverter output voltage to verify ZCS

One should need to adjust the switching frequency such that it nearly equal to the resonant frequency. The time period of 20 kHz switching frequency ( $f_s$ ) is equal to  $50\mu s$ , but the switching period of resonant frequency obtained experimentally as  $46\mu s$ , it means the resonant frequency ( $f_r$ ) becomes  $\approx 21.5kHz$ . At this frequency achieved the ZCS, is shown in Figure.5.20 where M-1 and M-2 are the operating modes. In M-1 IGBT switches 1 and 3 get turned on, then current flows from source to load via IGBT 1 and 3. When current becomes zero the other two switches will get turned on, then current flows from source to load via switches 2 and 4. This operation repeated in next cycles unless the load capacitor reaches its specified value.

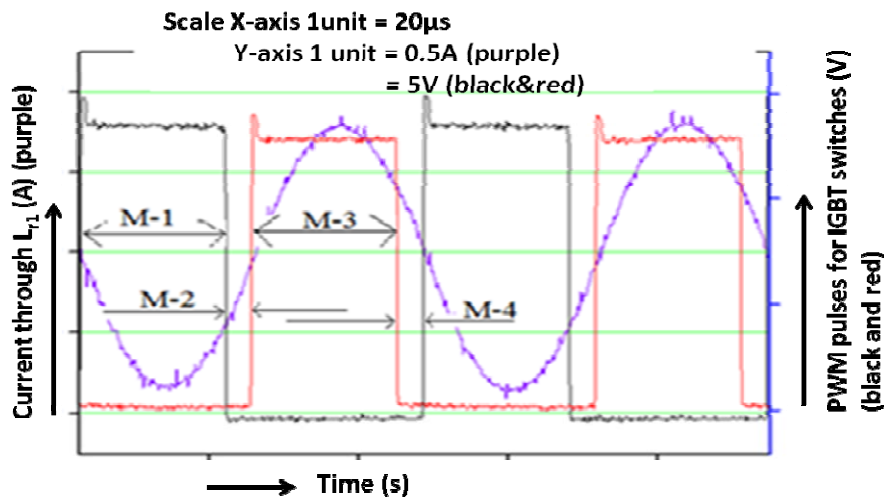


Figure.5.21: Current through  $L_{r1}$  vs PWM controlling signals for IGBTs in the inverter circuit to verify ZVS

Zero voltage switching (achieved by adjusting the dead time dead time between two PWM signals which are used to turn on two IGBT switches of same leg. There are 4 common mode modes are possible in ZVS operation which is shown in Figure.5.21. In Mode-1 (M-1) IGBT switches ( $S_1$  and  $S_3$ ) are in conduction whereas their respective diodes ( $D_1$  and  $D_3$ ) are in off state. When control signals for switches ( $S_1$  and  $S_3$ ) are removed the switches get turn off but the current won't become zero instantly, the current still in same direction but the path is different.

In this is Mode (i.e. M-2) diodes ( $D_2$  and  $D_4$ ) are forward biased and get turned on. At this instant switches ( $S_2$  and  $S_4$ ) are turned on and the voltage across these devices is zero because their respective diodes in conduction. In Mode-3 (M-3) IGBT switches ( $S_2$  and  $S_4$ ) are in conduction whereas their respective diodes ( $D_2$  and  $D_4$ ) are in get turned off.

When control signals for switches ( $S_2$  and  $S_4$ ) are removed the switches get turn off but the current won't become zero instantly, the current still in the same direction but it flows in different path. In M-4 diodes ( $D_1$  and  $D_3$ ) are get forward biased. At this instant of time the voltage across switches ( $S_1$  and  $S_3$ ) is zero and they get turned on, this cycle repeats for further (M-1 to M-4). In this types of power supply ZVS is more preferable compared to ZCS, because the switches get sufficient time get turn on and turn off. It avoids leg dead short circuit in the inverter stage.

#### **5.4 Comparative analysis of 2<sup>nd</sup>, 3<sup>rd</sup> and 4<sup>th</sup> order resonant converters**

In this section an attempt has been made to simulate 2<sup>nd</sup>, 3<sup>rd</sup> and 4<sup>th</sup> order resonant converter based capacitor charging source for 1kJ Marx based repetitive pulsed power system to verify various parameters. Observed the peak current flowing through the resonant inductor ( $L_r$  or  $L_{r1}$ ) in case of series LC, parallel LC, LCL-T and LCLC resonant based CCPS. The design input parameters have been taken from Table.5.5. Equations showed in chapter 3 have been used to find out the values of resonant components (inductor and capacitor).

Simulation has been done in ORCAD simulation tool and the circuit is shown in Figure.5.22. Capacitor charging power supply with series LC, parallel LC, LCL-T and LCLC resonant converters are connected and simulated separately. Important parameters are listed in Table.5.7 to make comparison between series LC, parallel LC, LCL-T and LCLC resonant converter based CCPS. This table confirms why fourth order resonant converter based CCPS is superior to all other resonant (second order and third order) converter based CCPS.

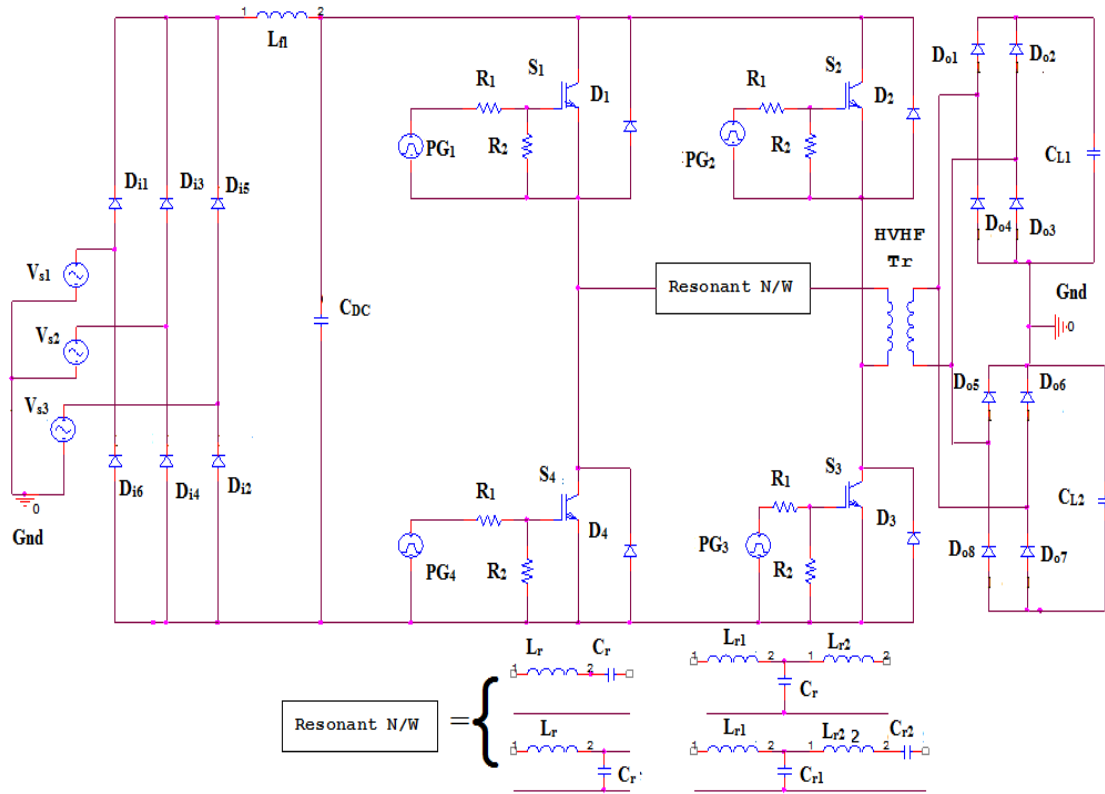


Figure.5.22: Simulation circuit of CCPS for comparative analysis

S. No.	Parameters	Series LC	Parallel LC	LCL-T	LCLC
1	Number of components	2	2	3	4
2	Peak currents through the IGBT switches	705A (approx)	$(2/3)^{\text{rd}}$ of series LC	$(3/7)^{\text{th}}$ of series LC	$(3/7)^{\text{th}}$ of series LC
3	DC Blocking	Present	Absent	Absent	Present
4	Complexity	Less	Less	Little complex	More complex
5	Resonant Inductor	$5\mu\text{H}$	$15.5\mu\text{H}$	$18\mu\text{H}$	$18\mu\text{H}$ $36\mu\text{H}$
6	Resonant Capacitor	$2\mu\text{F}$	$4.32\mu\text{F}$	$3.52\mu\text{H}$	$3.52\mu\text{F}$
8	ZCS	$f_r \geq 2f_s$	$f_r = f_s$	$f_r = f_s$	$f_r = f_s$

Table.5.7: Comparison table

Peak current flowing through the switch is very high in case of series LC, so handling of this current needs parallel operation of switches. In addition thermal management to remove heat caused due to high conduction in switches of inverter stage is so difficult, in addition overall size of power supply increases. Peak currents are less in case of parallel LC and LCL-T networks but they suffer from part load efficiency and lack of DC blocking. Part load efficiency is, at particular load ranges the current tries to flow from the switches and it will not be contributing to the load. So, the energy is wasted and efficiency is decreases.

In parallel resonant converter based CCPS, whenever the load is below certain value the efficiency of power supply is very low due to circulating currents. These circulating currents increases losses in the controlled switches of H-bridge inverter I.e. conduction losses are high due to circulating currents). To control the resonant converter, it needs to be small signal analysed. Once we get the small signal the dynamic ratio from output current to duty cycle will be achieved and then PID controller will be used to control and stabilize the loop. The extended describing functions are the method to derive the small signal analysis.

## **Summary**

A 1kV and 500J/s constant current power supply developed to study spark gap recovery times based on proposed CLCL resonant topology to study the recovery characteristics of spark gap in various gases. Peak current of 8A obtained through IGBT switches in the inverter stage, are verified in simulation as well as in experimental, which are in comparable with that of mathematical result (i.e. 7.85A).

A 4kV, 9 kHz repetitive constant current charging power supply for solid state switch based pulser application. Voltage profile across load capacitor (47nF) with a repetition rate of 9 kHz has been monitored in both simulation and through experimental. A high charging rate capacitor charging power supply has been developed based on fourth topology shown in

Figure.3.2 for repetitive Marx based system. Capacitor charging power supply with a peak charging rate of 45kJ/s,  $\pm 50$  kV has been developed for repetitive Marx based system. The power supply successfully interfaced and tested with 5Hz repetition rate with 10Hz repetitive Marx based system.

Summarized various parameters like number of resonant components, complexity, characteristic impedance, condition for zero current switching and DC blocking in case of series LC, parallel LC, LCL-T and LCLC resonant converter based CCPS. Concluded that the series LC resonant based CCPS is not a suitable CCPS for pulsed power applications in terms of size, thermal management, cost and efficiency. Parallel LC and LCL-T resonant based CCPS are not been attractive due to lack of DC blocking and part load efficiency. On other hand 4<sup>th</sup> order resonant based CCPS is more suitable for higher rating in all means like cost, size, efficiency and DC blocking.

# Chapter-6

## Protection and control features

---

Designing a reliable and compatible power supply for pulsed power applications is always a difficult job when charging rate in multiples of 10kJ/s. one should aware of its protection against various problems when interfaced with pulsed power system and operating with a highly dynamic loads. Most of the power supplies suffer from protection when they are interfaced with highly dynamic loads.

### 6.1 Protection

Protection for charging power supply is needed both in charging as well in discharging when power supply inter faced with highly dynamic loads. Protection facilitated in charging period formally known as primary protection, where as in discharging period is called as secondary protection. Further these two are classified into the following

#### 1. Primary protection

- Short circuit protection
- Over voltage protection
- Arc protection
- Thermal protection
- Protection for false triggering
- Short circuit protection of switch in the inverter stage
- dv/dt protection

## 2. Secondary protection

- Radiated noise
- Conducted noise

### **6.1.1 Primary protection**

This protection is a basic protection for any power supply, in which the protection has been provided to components of power supply when load capacitor in charging condition.

#### **6.1.1.1 Short circuit protection**

Short circuit protection can be achieved by choosing proper resonant topology; with this topology one can achieve constant current at a particular operating condition. It means the load capacitor does not draw short circuit current from the mains, wherein the current drawn from the source purely depends on the impedance offered by the resonant network.

#### **6.1.1.2 Over voltage protection**

Over voltage is controlled during charging itself, it means the feedback network continuously monitor the voltage across the load capacitor. Control signals have been generated for switches in the inverter stage based error signal generated by comparator.

#### **6.1.1.3 Arc protection**

Arc protection at the load end can be achieved by proper connection of load terminals at the output (i.e. high voltage and ground terminals are isolated properly).

#### **6.1.1.4 Thermal protection**

Thermal protection can be achieved by choosing proper heat sink which can dissipate heat loss uniformly. Forced air cooling with blower makes the system at comfortable condition without over heating of switches of inverter stage. Since, most of the losses in the power supply take place in the inverter stage itself. So, a proper heat sink has to be chosen to

dissipate heat. Cooling for other components can be achieved by heat extraction method like using exhaust fans and are arranged in various places to remove heat.

#### **6.1.1.5 Protection against false triggering**

This protection is one of the important protections in the power supply, because false triggering of switches in the inverter stage leads to unwanted charging of load capacitor or else it may leads to failure of switches in the inverter stage. False triggering can be overcome only with the gate drivers which are used to provide control signals for switches. Suitable gate driver should have the capability to protect against these kinds of problems. If a pulsed whose pulsed duration is less than a particular value (mentioned in the datasheet) cannot turn on the switch, rather it generates an error signal. Gate driver (SKHI 10/17R) is such kind of driver is suitable for these kinds of applications.

#### **6.1.1.6 Short circuit protection of switch in the inverter stage**

Short circuit protection protects the controlled switches in the inverter stage of CCPS. It means that if due to any reason the collector-emitter (CE) terminals of IGBT switch is shorted the IGBT should not get turn on. The chosen gate driver (SKHI 10/17R) continuously monitors the collector-emitter (CE) of switch in the inverter stage. If due to any reason the CE terminals are shorted then gate driver generates an error signal and it won't provide the control signals at the GE terminals of IGBT switch in the inverter stage. A gate driver selection plays an important role in protecting power supply from various problems.

#### **6.1.1.7 dv/dt protection**

This protection is necessary for each device in the inverter stage. More popularly RCD snubbers are used to protect the device. A sudden rise in the voltage across switch in the inverter stage may leads to the failure of switch. The sudden change in voltage occurs due to the energy storage elements like lead inductances. The whole energy of lead inductance

appears across switch for very short duration of time with high rise time. At this instant of time the snubber capacitor comes into picture and stores the energy through diode, intern the device protected from  $dv/dt$ . The device when it is in conduction mode the stored energy in the snubber capacitor dissipates across snubber resistor.

### **6.1.2 Secondary protection**

Secondary protection plays important role in the power supply design, most of the times many power supplies are lacks in providing protection against noise generated in the system due to highly dynamic loads. Pulsed power systems with highly dynamic loads like klystron, backward oscillator (BWO) and magnetron generates highly dynamic noise in the power supply. This dynamic noise leads to frequent failure of IGBT switches in the inverter stage of power supply. Electromagnetic interference (EMI) is a combination of conducted noise and radiated noise [88,89]. As per international standards conducted noise frequency range is  $\leq 30$  MHz where as radiated frequency range is  $> 30$ MHz. In the present scenario the differential mode EMI is not much problematic compared to common mode EMI. Because the chosen resonant topology playing important role in attenuating differential mode EMI. That means the fourth order resonant converter act as low pass filter for differential mode EMI.

On the other side the common mode EMI which is existing between live conductor and ground is not much attenuated. It is depending on the copper shielding which we are providing between primary and secondary of high voltage and high frequency transformer. So, there is limitation in keeping these sheets between primary and secondary. So, up to some extent the amplitude of common mode EMI can be reduced and it should be within the rating of IGBT switch in the inverter stage of H-bridge.

#### **6.1.2.1 Radiated noise**

Radiated noise can be arrested by keeping low power electronic circuits in a closed metal box provided that the metal box properly grounded. The noise propagated to the inverter stage

from load via output diode rectifier, high voltage, high frequency transformer and resonant network. Due to this noise the voltage across IGBT switch in the inverter stage increases above its rated value and leads to the failure controlled device.

Semi conductor switches (IGBTs) which are available in the market are of 3300 A, 1700V when operated at 25° C ambient temperature and 60 kHz switching frequency. But these devices have less  $t_{rr}$  (reverse recovery time). Instead the power electronic designers using low current high  $t_{rr}$  IGBT devices to handle high power (series and parallel combination IGBTs) and to achieve targeted rating.

#### **6.1.2.2 Conducted noise**

Conducted noise is a sub class of EMI and it is again sub-categorized into two so called differential mode (DM) noise, as measured between the power feed and its return path. Common mode (CM) noise is measured between each power line and to the ground. Contributors to these two modes are inherent to the basic operation of a switching mode power supply. Out of these two noises conducted noise is more vulnerable for the power supply compared to radiated noise. Highly dynamic loads are main victims for the generation of noise. The above two mentioned noise are basically subclass of electromagnetic interference (EMI), some of the mitigating techniques are discussed in the further section.

#### **6.1.3 EMI mitigation techniques**

Power supply when operated at high frequency (Typically > 20 kHz) may undergo different electromagnetic interferences (EMI). Some of the EMI mitigation techniques are listed below

- ✓ EMI Filter
- ✓ Soft switching
- ✓ Compensation

- ✓ Snubbers
- ✓ EMC solutions

### 6.1.3.1 EMI Filter

Adopting EMI filter in a power circuit is a common technique to meet the international standards in power supplies [90] and it is a higher in cost. There are several active and passive filtering solutions have been introduced previously for EMI solutions [92]. This active and passive filter will collectively used to reduce the effects due to common mode and differential mode noise.

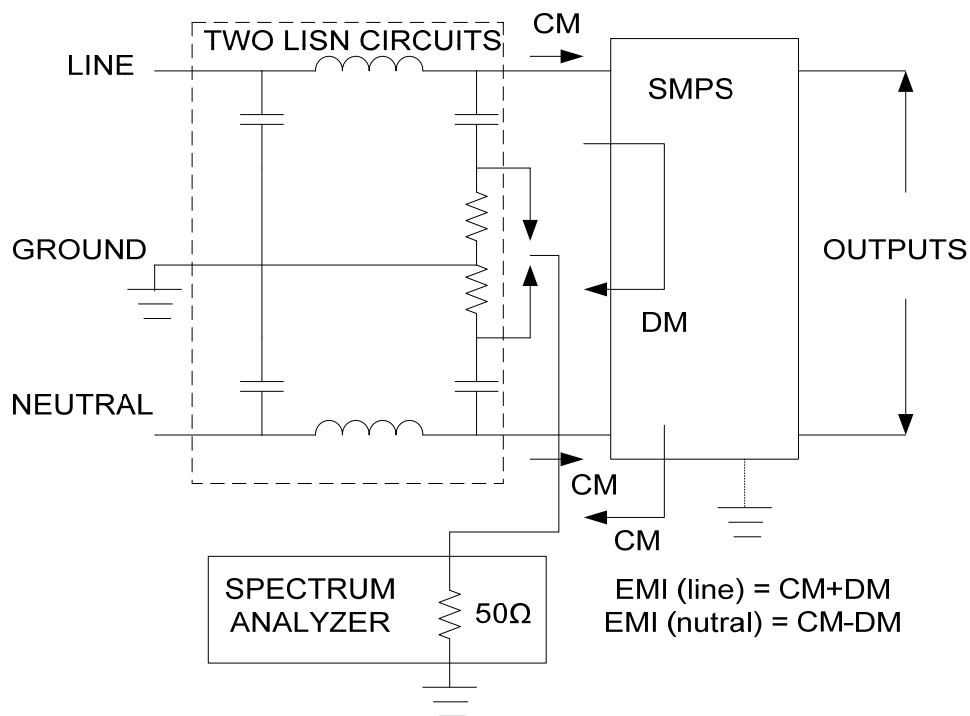


Figure.6.1: Typical EMI filter network

The main objective of these kinds of filtering circuits to sense the current and given to a compensation network to minimise the higher order frequencies through RC branch connected to power supply. A commonly used EMI filter is shown in Figure.6.1. In the figure one can see that the filter inductor and capacitor forms a low pass filter to attenuate high frequency components. Two line impedance stabilization network (LISN) has been used to

handle CM. CM noise will be getting between lines to ground and neutral to ground, so it needs two LISN networks. The abbreviation of LISN is line impedance stabilization network. It is used to provide precise impedance at the supply of any equipment which is going to test. Another important function of an LISN is to prevent the high-frequency noise of the power source from coupling in the system. It acts as a low pass filter, which provides high impedance to the outside Radio frequency (RF) noise while allowing the low-frequency power to flow through to the equipment which is going to test. DM is appearing across lines (i.e. line to neutral), one set of inductor and capacitor combination can handle DM effectively. The signal is brought out with Bayonet Neil-Concelman (BNC) cable and connected to spectrum analyzer to verify the signal frequencies. The noise present in the line wire is the addition of CM and Dm, where as noise present in the neutral is the difference of CM and DM.

#### **6.1.3.2 Soft switching**

Soft switching technique is another way to overcome EMI generated due to hard switching. Soft switching of semi conductor devices reduces  $dv/dt$  and  $di/dt$  to a very low level to effects related to EMI due to hard switching has been studied in [93-95]. Comparison soft and hard switching has been done previously come out with how EMI got reduced with soft switching [96-98]. Soft switching circuits are more capable of reducing EMI, but some of the topologies may not reach the EMC standards. In addition by employing extra elements leads to generation of EMI.

#### **6.1.3.3 Compensation**

The main objective of this method is to reduce the effect due to common mode noise, in this technique the leakage current flowing through the earth wire or common mode voltage got minimized [99 - 100]. An auxiliary circuit has been added in the power section for compensation of noise that may be achieved with either active or passive. Active

compensation is costlier than passive, so designers prefer passive compensation compared to active compensation. Proper selection of component values leads to a reduction in leakage current. This method can cancel the oscillatory ground current, even though a small amount of ground current still remains [101]. The CM passive cancellation technique [102] replaces the boost converter inductor with an anti-phase transformer. This technique influence the CM EMI whose frequency spectrum in the range of 20MHz. A DSP based digital active cancellation technique applied to the converter input with closed loop control to reduce the effect of CM EMI of 10 MHz frequency spectrum [103].

#### **6.1.3.4 Snubber and clamp**

EMI mitigation has been achieved with an auxiliary circuit connected in the power circuit to minimize the effect of  $dv/dt$  and  $di/dt$ . Traditionally, Snubbers are divided into passive and active circuits. Snubber's decreases noise, on the other simultaneously increases the power dissipation and yield efficiency reduction. Different active and passive snubbers have been employed previously in various circuits in EMI mitigation [104-106]. All these kinds of circuits are complex and cost effective methods. A loss less snubber has some advantages such as providing zero voltage switching (ZVS) for the main switch by transferring the recovered energy to the source and load by controlling  $dv/dt$  of the switch. The energy transferred to the snubber capacitor ( $C_s$ ) during the off-time, intern eliminates the ringing. More popular resistor-capacitor-diode (RCD) snubber circuits can be used to transfer energy from main switching element to the snubber capacitor.

#### **6.1.3.5 PCB layout and placement optimization**

Printed circuit boards (PCB) consists of various electronic components laid side by side. The layout of PCB and placement of components significantly influences on both conducted and radiated EMI. Layers, tracks and components must be optimized to reach EMC standards [107-108]. In recent years so many computer aided design CAD tools are available in the

market for to design effective PCBs [109-111]. Software CAD tools for simulating signal integrity (Hyperlynx from Mentor Graphics) and PCB parasitic extraction (Maxwell Q3D from Ansoft) have been developed which can help power electronic system designers to deal with EMC in the PCB design stage. In some cases ferrite beads also used in the circuits for EMI mitigation in some cases in power boards [112-113]. Proper shielding (like enclosing all PCB in a metal box and grounding) grounding are also a good practice in arresting the noise and it passes to the ground.

Pins of electronic components on PCB will acts as antennas, which can catch the high frequency radiated noise signals very easily. Some more ways one can handle EMI effective using parasitic cancellation, balance approach and interleaving. These techniques are not much effective in handling EMI and at the same time they are more complex and may not be used in most of the cases, more on these techniques literature is present in [114-120].

The above mentioned EMI mitigation techniques come in cost of complex, extra elements, extra circuits and they are costlier. So, the deeper analysis has been carried out to draw more advantages from the proposed 4th order resonant converter structure which has already been discussed in the previous chapters.

The 4th order resonant network which is already discussed in chapter 3 provides load independent constant current and soft switching in the forward direction. Simultaneously it will act as a low pass filter for differential mode noise in the opposite direction. In another way this differential mode noise can be overcome by adding auxiliary circuits in the power supply. Common mode noise can be overcome by incorporating faraday shielding between primary and secondary of HVHF transformer. Mathematical analysis has been carried out in the further sections to see prove proposed 4th order resonant network overcomes the effect of DM noise and how faraday shielding can overcome CM noise in experimentally.

## **6.1.4 Conducted noise analysis and protection of 45 kJ/s and $\pm 50$ kV LCLC resonant based CCPS**

### **6.1.4.1 Analysis of conducted EMI in CCPS**

Development features of chosen 45 kJ/s, 10 Hz and  $\pm 50$  kV repetitive LCLC resonant based CCPS have already been discussed in chapter 5. When pulsed power system discharges all its energy to the highly dynamic loads like klystron, vircator, backward oscillator (BWO) and magnetron for very short duration of time, generates noise. This noise is the combination of both radiated and conducted.

Radiated noise does not create much problem to the charging system and it can be handled by keeping all low power electronic circuits in a grounded closed metal box. On the other hand, handling of conducted noise (common mode and differential mode) is much difficult in power supply. Conducted noise generated at the load end induces common mode current ( $I_{CM}$ ) and differential mode voltage ( $V_{DM}$ ) in to power supply is shown in Figure.6.2.

The generated conducted noise has been carried to the inverter stage from load via output diode rectifier, high voltage high frequency (HVHF) transformer and resonant network. Voltages across insulated gate bi-polar transistor (IGBT) switch increases to above its rated value due to noise which leads to failure of IGBT. IGBT switches which are available in the market are of 3300 A, 1700V when operated at 25° C ambient temperature and 60 kHz switching frequency. But these devices are having less  $t_{tr}$ , instead one can use series-parallel combination to meet the requirements.

In the circuit,  $C_C$  is the coupling capacitance between primary and secondary,  $C_{CG}$  is the capacitance between cores to chassis,  $V_{N1}$  and  $V_{N2}$  are noise voltages,  $I_{CM}$  is the current due to common mode current and  $V_{DM}$  is the differential mode voltage. Due to  $V_{N2}$  common

mode current ( $I_{CM}$ ) has been generated and  $V_{N1}$  differential mode voltage ( $V_{DM}$ ) has been generated in the circuit.

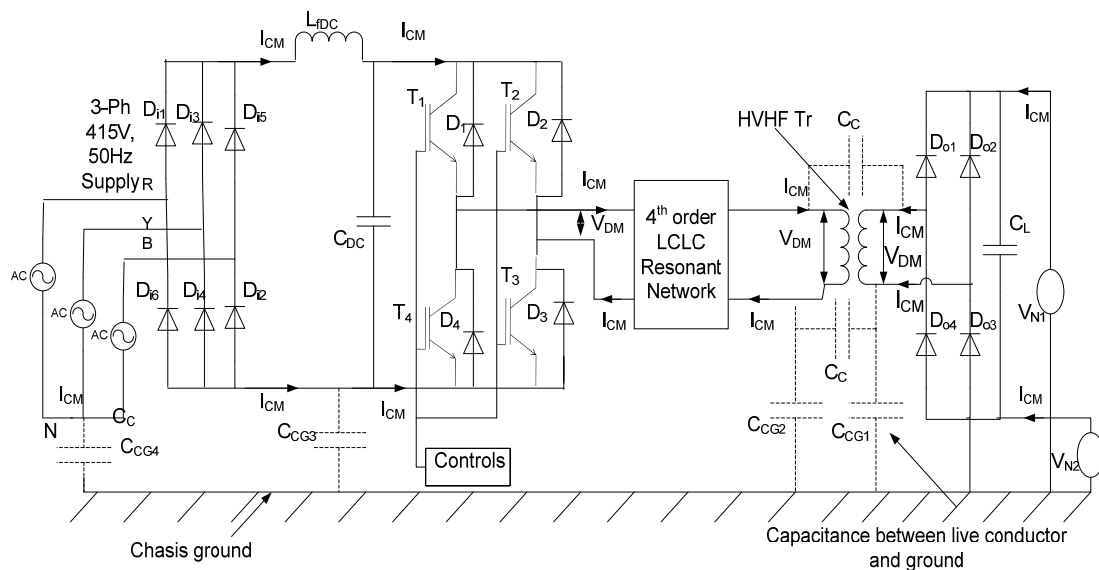


Figure.6.2: Circuit diagram of power supply with parasitic capacitance without faraday shielding

In the present paper concentrated to minimize the effect of common mode and differential mode noise by incorporating faraday shielding between primary and secondary of HVHF transformer and with LCLC low pass filter. Noise is generated in the system when load capacitor discharges all its energy to the dynamic load for very short duration of time. Due to this noise the voltage across CE terminals of IGBT ( $V_{CE}$ ) switch in the inverter stage increases beyond its specified rated value (i.e. 1700 V typically as per manufacturer's data). It may lead to the failure of IGBT. This conducted noise is carried to CE terminals of IGBT via coupling capacitance of HVHF transformer. More about EMI generation, effect and optimization has already been discussed in [13].

#### 6.1.4.2 Effect of common mode noise on IGBT

To understand the effect of common mode noise on the IGBT switch in the inverter stage used Kirchoff,s voltage law (KVL). The effective voltage across collector emitter terminals

of IGBT switch found from loop 2 is shown in Figure.6.3b. The common mode current ( $I_{CM}$ ) flows through two loops, first loop  $C_{CG1} - C_C - C_{CG2}$  and the second loop is  $C_{CG2} - C_{CG3} - C_{CE}$ . Where  $C_{CG}$  is the capacitance between live conductor and ground,  $C_C$  is the coupling capacitance between primary and secondary of HVHF transformer and  $C_{CE}$  is the collector-emitter capacitance. As an when noise generated  $I_{CM}$  flows in loop 1 is shown in Figure.6.3a and charges capacitor  $C_{CG2}$  through  $C_C$ . The same  $I_{CM}$  flows through loop 2 shown in Figure.6.3b charges  $C_{CE}$  through  $C_{CG3}$ .

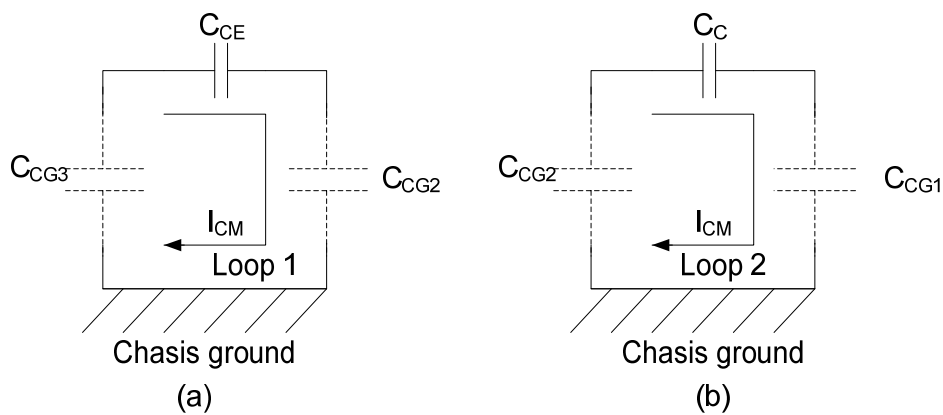


Figure.6.3: Common mode current ( $I_{CM}$ ) to find the effective voltage across CE terminals of IGBT

The amount of voltage developed across  $C_{CG2}$  depends on  $C_C$ , whereas the amount of voltage developed across  $C_{CE}$  depends on  $C_{CG3}$ . In general  $C_{CG}$  values are very less (Typically in pF range), so the maximum amount of voltage drops takes across them. But if  $C_{CG3}$  value is in the range of  $C_{CE}$  value, nearly equal amount of voltage appears across both  $C_{CG3}$  and  $C_{CE}$ . This increment in voltage across  $C_{CE}$  leads to damage of IGBT due to over voltage. Typical value is 1700V voltage, if the voltage exceeds this values IGBT will leads to failure.

One can overcome this issue by providing shielding between primary and secondary of HVHF transformer, which is shown in Figure.6.4, this leads to reduction in the value of  $C_C$ . This means, by reducing  $C_C$  value, the voltage drop across  $C_C$  such that the voltage appearing across  $C_{CG2}$  is minimum. The reduction in the voltage across  $C_{CG2}$  leads to reduction in the

voltage across  $C_{CE}$ . The overall concept of introducing shielding primary and secondary of HVHF transformer is to reduce the ratio between  $C_C$  and  $C_{CE}$  as lower as compared to the previous value (i.e. ratio before inserting shielding).

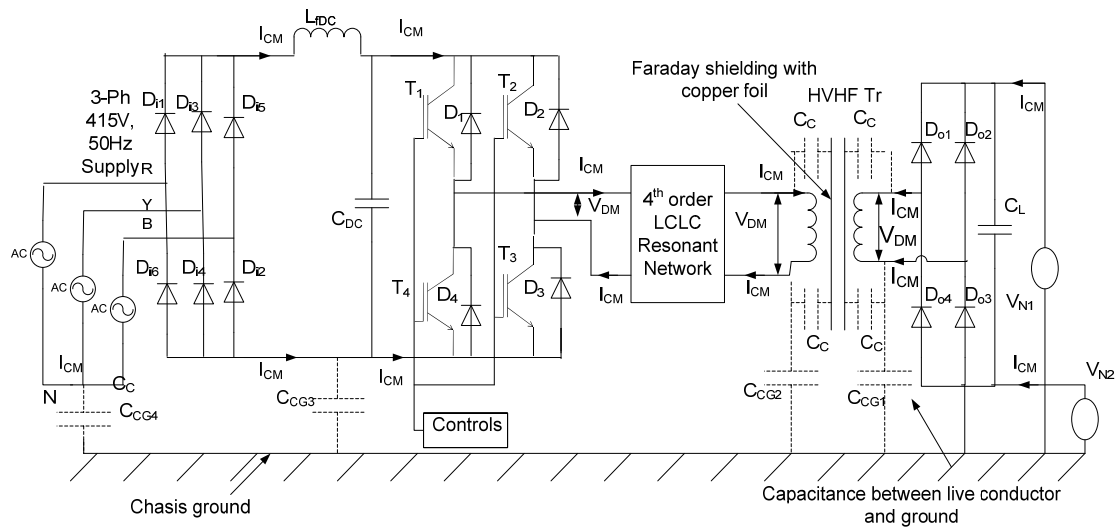


Figure.6.4: Circuit diagram of power supply with parasitic capacitance with faraday shielding

Reduction in the value of  $C_C$  blocks more voltage, so the maximum voltage drop appears across  $C_C$  and a negligible (or minimum) amount of voltage drop appears across CE terminals of IGBT ( $V_{CE}$ ). The equivalent circuit diagram with faraday shielding is shown in Figure.6.5.

To make clear that how much amount of reduction in common mode voltage magnitude has been explained with the help of Bode diagram.

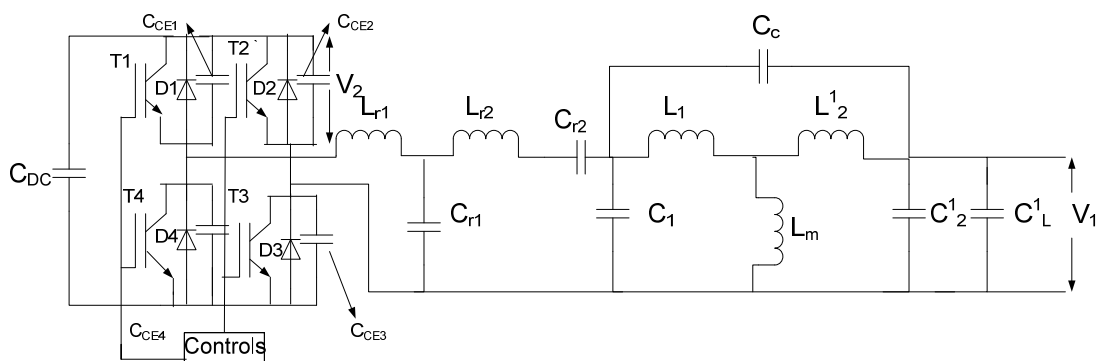


Figure.6.5: Topological structure of LCLC network with high frequency transformer parameters

$(1/sC_{ce})$  = Collector to emitter capacitance of IGBT switch,  $sL_{r1}$  = Resonant capacitor,  $(1/sC_{r1})$  = Resonant capacitor,  $sL_{r2}$  = Resonant inductor,  $(1/sC_{r2})$  = Resonant capacitor,  $(1/sC_1)$  = Winding capacitance of primary,  $sL_1$  = Leakage inductance of primary,  $sL_2^1$  = Leakage inductance of secondary referred to primary,  $sL_m$  = Magnetizing inductance,  $(1/sC_c)$  = Capacitance between primary and secondary,  $(1/sC_2^1)$  = Capacitance of secondary reflected to primary and  $(1/sC_L^1)$  = Load capacitor reflected to primary.

$C_{ce} = 3\text{nF}$  (2.7nF from data sheet for chosen IGBT),  $L_{r1} = 18\mu\text{H}$ ,  $C_{r1} = 3.54\mu\text{F}$ ,  $L_{r2} = 26\mu\text{H}$ ,  $C_{r2} = 3.54\mu\text{F}$ ,  $C_1 = 2\text{nF}$ ,  $L_1 = 12\mu\text{H}$ ,  $L_2^1 = 5.4\text{nH}$ ,  $L_m = 0.45\text{mH}$ ,  $C_c = 0.1\text{nF}-5\text{nF}$ ,  $C_2^1 = 2.6\mu\text{F}$  and  $C_L^1 = 18\text{mF}$ .

To draw bode diagram the total circuit is solved for gain (nothing but the ratio between voltages due to noise to the voltage across CE terminal of IGBT, in which the circuit is realized with all parameters including HVHF transformer parameters (experimentally measured quantities). Topological structure of the circuit is shown in the Figure.6.5.

Where  $V_1$  = Reversal voltage and  $V_{eq}$  = Voltage across equivalent reactance offered by the combination  $1/sC_{ce}$ ,  $sL_{r1}$ ,  $1/sC_{r1}$ ,  $sL_{r2}$ ,  $1/sC_{r2}$  and  $1/sC_1$ . The voltage gain of the circuit shown is given by

$$\frac{V_{eq}}{V_1} = \frac{s^5 L_{r1}^2 C_{r1} C_{ce} C_c + s^3 L_{r1}^2 C_{ce} + s C_{r1}}{s^7 L_{r1}^2 C_{r1}^2 C_{ce}^2 C_c + s^6 (L_{r1}^2 C_{r1}^2 C_{ce}^2 + L_{r1}^2 C_{r1}^2 C_{ce} C_c) + s^5 L_{r1}^2 C_{r1} C_{ce}^2 + 2s^4 (L_{r1}^2 C_{ce}^2 + L_{r1}^2 C_{cr1} C_{ce}) + s^3 L_{r1} C_{r1} C_c + s^2 (2L_{r1} C_{ce} + L_{r1} C_{r1}) + s C_{r1}} \quad \dots (6.1)$$

As per industrial standards, up to 30 MHz range frequency are considered as conducted noise and above 30 MHz are called as radiated noise. So, the point of interest is in the frequency varying from 10 MHz to 30 MHz. Magnitude and phase plots are drawn for Equation.6.1 for various coupling capacitor values is shown in Figure.6.6.

Results reveal that, there is no reduction in magnitude (i.e. 0dB shown in Figure.6.6a.) for  $C_c$  value of 5nF. But, if  $C_c$  value in between 5nF to 10pF observed a considerable reduction in the magnitude has been observed in Figure.6.6.

Figure.6.6: Magnitude and phase plot for equation 6.1

Noise voltage magnitude can be reduced further if the ratio between  $C_C$  to  $C_{CE}$  is smaller as possible. It means, lower the value of  $C_C$ , better the attenuation can be achieved. In the present design, the  $C_C$  value got reduced from 5nF to nearly 10pF after providing shielding. The maximum reduction in gain is achieved with 10pF coupling capacitor (i.e. -10dB gain obtained 10pF coupling capacitor is shown in Figure.6.6d)

The gain in dB is given by  $20\log_{10}(V_{eq}/V_1) = -10\text{dB}$  at 10MHz frequency.

If  $V_1=2\text{kV}$  (Peak) then  $V_{eq}$  becomes 500V with 10pF.

### 6.1.4.3 Effect of differential mode noise on IGBT

Differential mode noise is generated between any two live wires in the system. The differential noise increases the voltage across IGBT ( $V_{CE}$ ) beyond its rated value, which intern leads to the failure of IGBT. Proper protection can overcome failure of IGBT against differential noise. More frequently series LC resonant based capacitor charging power supply suffers with this kind of noise. The proposed CCPS has overcome differential noise with the proposed forth order LCLC resonant converter.

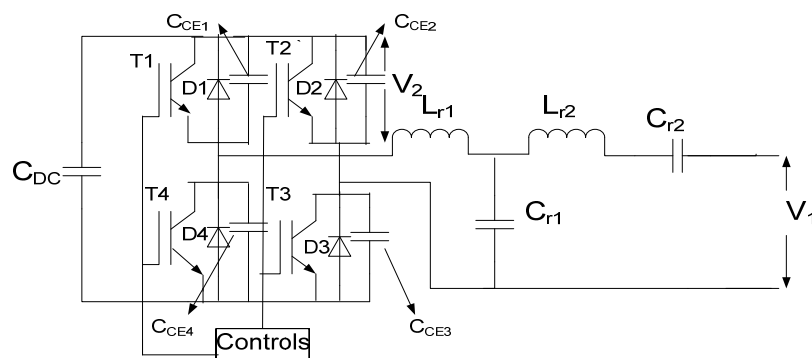


Figure.6.7: Topological structure of LCLC network with CE capacitance of IGBT with resonant network

$(1/sC_{ce})$  = Collector to emitter capacitance of IGBT switch,  $sL_{r1}$  = Resonant capacitor,  $(1/sC_{r1})$  = Resonant capacitor,  $sL_{r2}$  = Resonant inductor,  $(1/sC_{r2})$  = Resonant capacitor. The proposed LCLC resonant converter act as constant current and soft switching in the forward direction and the same LCLC resonant converter acts as low pass filter in the reverse direction against high frequency differential noise. The proposed LCLC filter handle this noise effectively and reduces the voltage magnitude across IGBT ( $V_{CE}$ ) to a safe value (i.e. less than  $1700V = V_{CE}$  as per manufacturers data). Topological structure for the analysis is shown in Figure.6.7.

$$\frac{V_{ce}}{V_1} = \frac{s^3 L_{r1} C_{r1} C_{ce} + s C_{r1}}{s^6 L_{r1}^3 C_{r1} C_{ce}^2 + s^5 L_{r1}^2 C_{r1} C_{ce}^2 + 2s^4 (L_{r1}^2 C_{ce}^2 + L_{r1}^2 C_{r1} C_{ce}) + s^3 L_{r1} C_{r1} C_{ce} + s^2 (2L_{r1} C_{ce} + L_{r1} C_{r1}) + s C_{r1}} \dots (6.2)$$

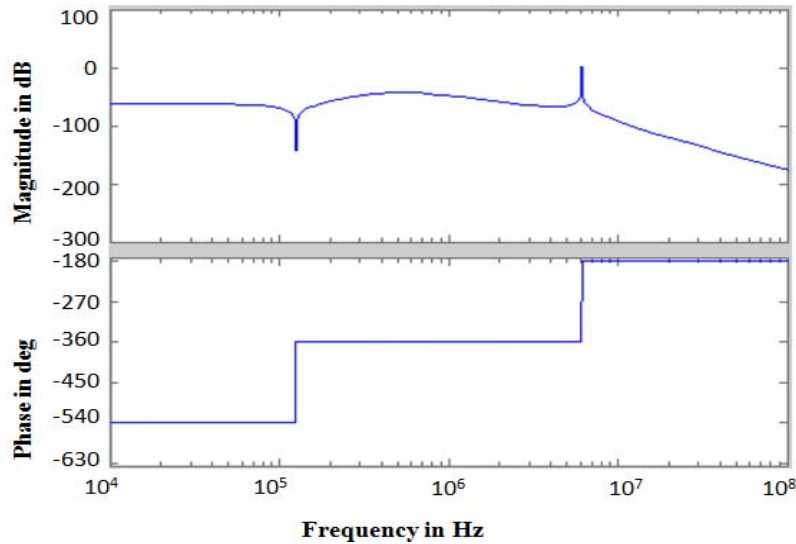


Figure.6.8: Magnitude and phase plot for the equation 6.2

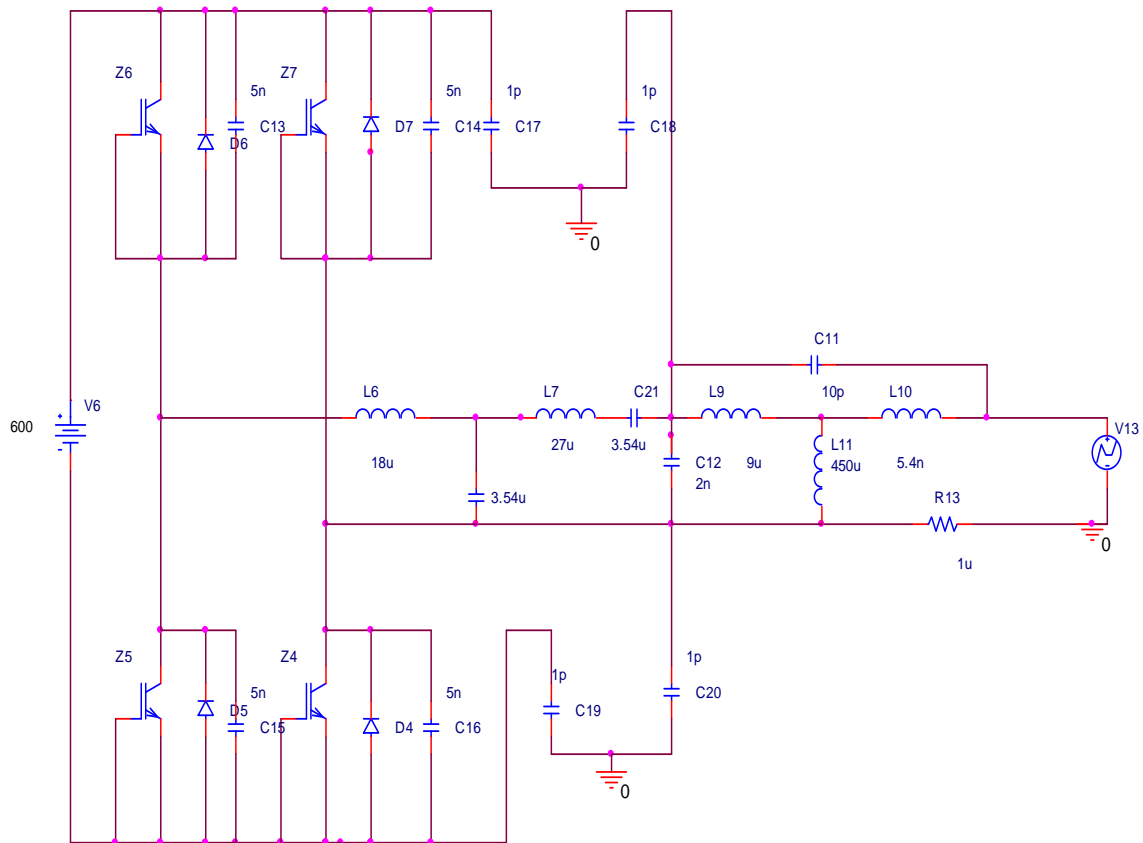
Effect of differential noise on the CE terminals of IGBT of inverter circuit is explained with the help of magnitude plot as shown in Figure.6.8. This plot is drawn for the equation 5 to verify the noise signal strength on CE terminal of IGBT switch. The voltage appearing across primary terminals of HVHF transformer due to differential noise is the input voltage to the network shown in Figure.6.7. This voltage got attenuated about -120dB at 100 MHz , as shown in Figure.6.8.

$V_1=2\text{kV}$  (Peak), the gain in dB is given by  $20\log_{10} (V_{ce}/V_1) = -75\text{dB}$  at 100MHz frequency.

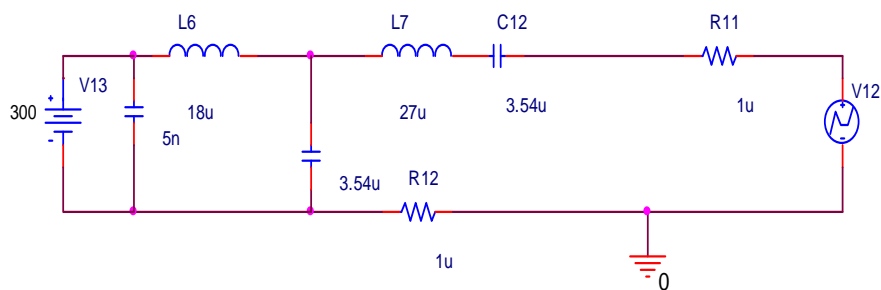
$V_{ce}= 0.4\text{V}$ , so this voltage does not lead to failure of IGBT in the inverter stage of power supply which is already been discussed in section I. It means, the combination of  $L_{r2}$ ,  $C_{r2}$  and  $C_{r1}$  forms a typical low pass filter for these kinds of noises. The effect of differential noise has been explained with help of bode diagram in the further section.

#### 6.1.4.4 Simulation results

Simulation has been done in orcad simulation tool and the circuit shown in Figure.6.9a is to see the effect of common mode noise and differential mode noise on CE terminals of IGBT.



(a)

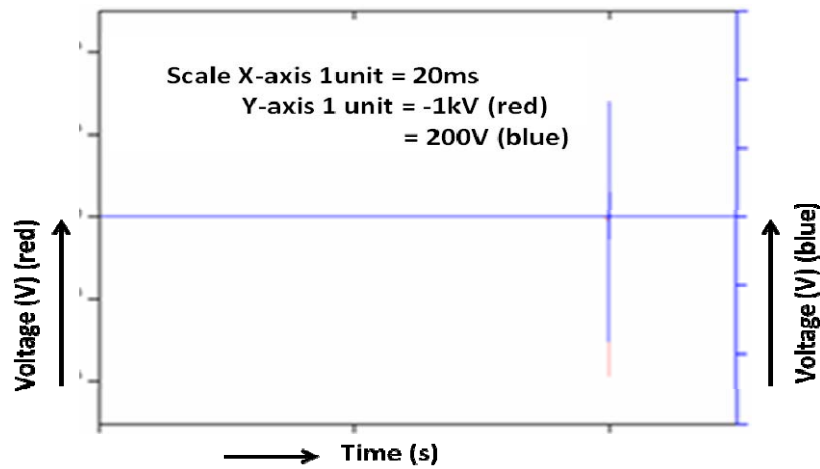


(b)

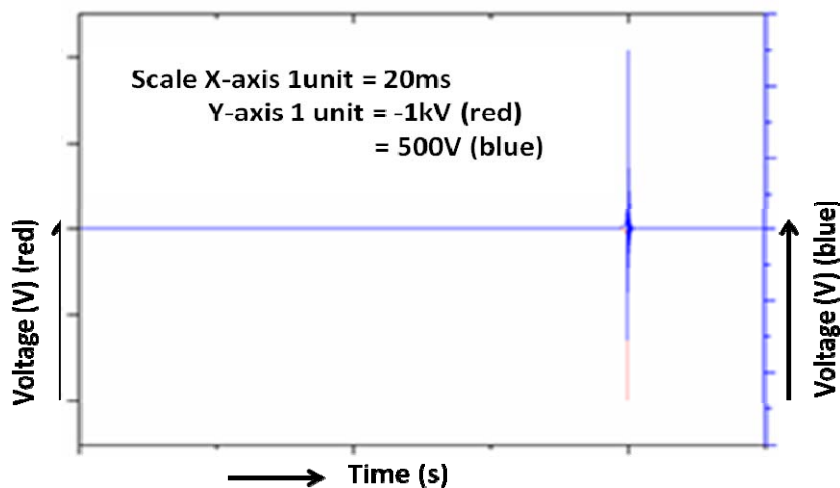
Figure.6.9: Simulation circuit to see the effect of conducted noise (a) For common mode noise (b) For differential noise

In this circuit, the capacitance between one of the primary terminal of HVHF transformer to the ground has been taken as 1pF. In general, it is difficult to measure capacitance between live conductor and ground because at different points get different capacitance values. The capacitance between collector-emitter terminals of IGBT switch has been taken as 5nF (from

datasheet) and the noise voltage provided with a voltage pulsed generator whose pulsed width is 100ns (equal to 10 MHz) and 2 kV peak.



(a)



(b)

Figure.6.10: Conducted noise voltage (Red) and voltage across the capacitor (Blue) [Between one of the terminal of HVHF transformer to the ground] (a) For 10pF  $C_c$  (b) For 5nF  $C_c$

Measured the voltage across capacitor (1pF) connected between 1<sup>st</sup> terminal of primary of HVHF transformer to the ground with 5nF and 10pF for coupling capacitance ( $C_c$ ). The voltage magnitude reduced from 1200V (peak) to 400V (peak) when  $C_c$  value varied from 5nF to 10pF, is shown in Figure.6.10. The other important observation is, if the capacitance between live conductor and ground comes in comparable with 5nF capacitor (across CE

terminals of IGBT), then the noise voltage across collector-emitter terminals increases further, which leads to failure of IGBT due to over voltage.

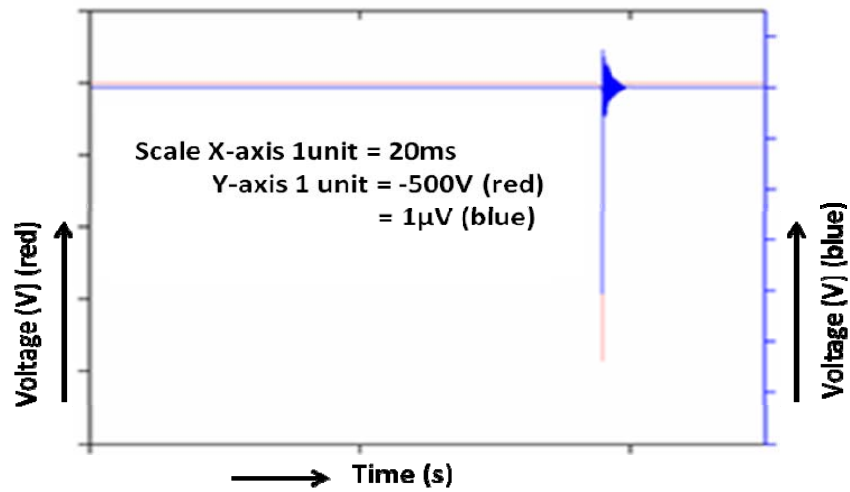
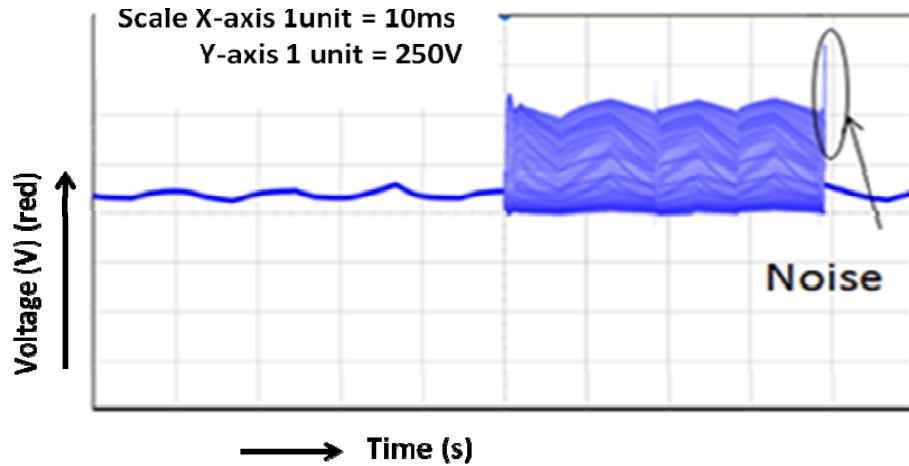


Figure.6.11: Differential noise voltage (Red) and voltage across CE terminal capacitance of IGBT (Blue)

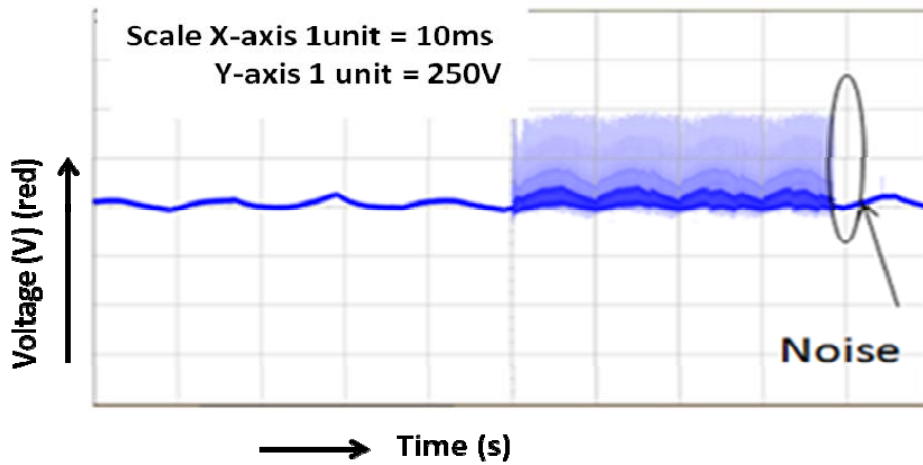
To control and to limit the noise voltage below the rated value of IGBT, one should provide shielding such that the  $C_C$  value is much lesser than 10pF. Effect of differential noise on collector-emitter terminals of IGBT has been simulated and the simulation circuit is shown in Figure.12b. The differential noise getting across primary terminals of HVHF transformer is applied to the LCLC resonant network and observed the effect on collector-emitter terminals of IGBT. The noise voltage of 2 kV with 100ns pulsed width applied across LCLC resonant network at the output terminals. The magnitude of noise voltage (2 kV) got reduced to 0V which is shown in Figure.6.11.

#### 6.1.4.5 Experimental results

Noise generated at the load end leads to the failure of IGBT switch in the inverter circuit, which is already been discussed in the previous sections.



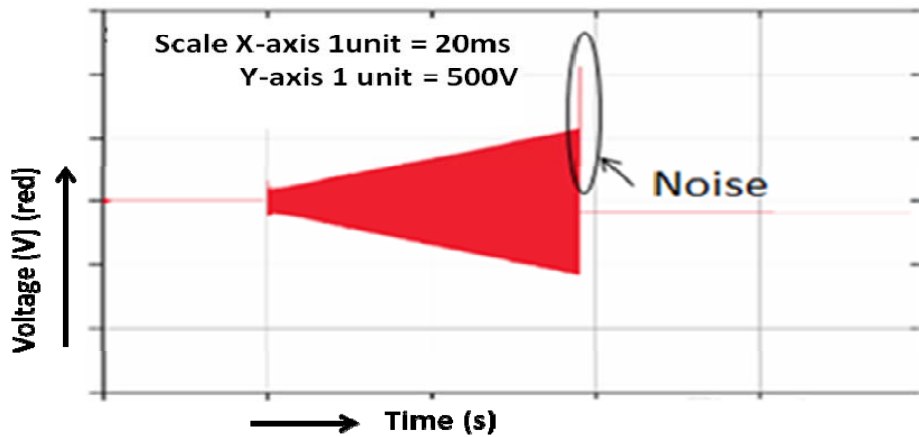
(a)



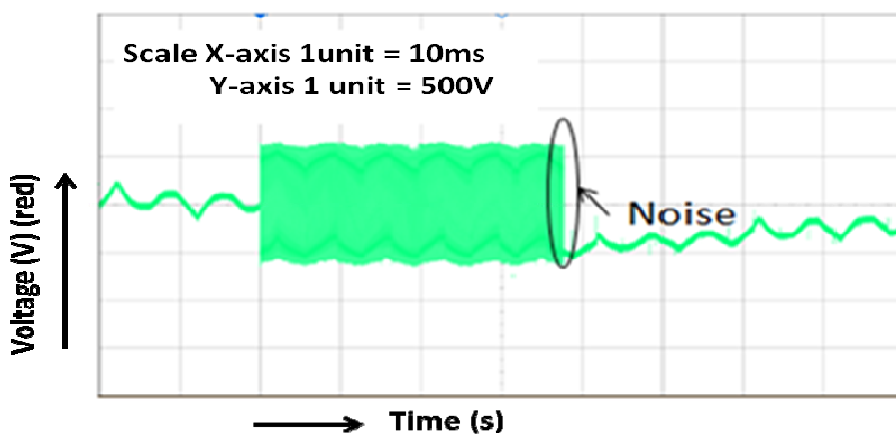
(b)

Figure.6.12: Common mode noise (a) Voltage between 1<sup>st</sup> terminal of primary of HVHF transformer to ground (b) Voltage between 2<sup>nd</sup> terminal of primary of HVHF transformer to the ground

The voltage due to common mode noise has been measured between first terminals of HVHF transformer and ground, is presented in Figure.6.12. In Figure.6.12a, it is observed that there is a sudden peak in voltage at 38ms. This peak is due to noise generated at load. The value of peak varies short to short, since due to dynamic nature of load, the noise voltage peak and its frequency vary. After inserting shielding the peak in voltage got reduced and comes in with in the limit and it is shown in Figure.6.12b.



(a)



(b)

Figure.6.13: Differential mode noise (a) Voltage across primary terminals of HVHF transformer (b) Voltage across inverter output

It means voltage by inserting the value of coupling capacitance between primary and secondary got reduced and more voltage drop took place across  $C_C$  instead 1<sup>st</sup> terminals of HVHF transformer and ground. The amplitude of differential noise voltage had been reduced with the proposed LCLC resonant topology. Differential noise voltage measured across the output terminals of inverter stage and across primary of HVHF transformer are shown in Figure.6.13.

Noise voltage (circled portion in Figure.6.13a) has become zero with the proposed LCLC resonant converter. It means the LCLC resonant converter acts as low pass filter and bypasses high frequency (12 MHz) noise signal through resonant inductor ( $L_{r2}$ ) and resonant capacitors

( $C_{r1}$  and  $C_{r2}$ ). The noise voltage becomes negligible at the inverter output terminals, which is shown in Figure.6.13b. Noise measurement confirms that the proposed LCLC resonant converter and shielding successfully attenuates the noise signal.

## 6.2 Controlling Techniques

Controlling techniques plays an important role in the power supply design, wherein the voltage across load capacitor is controlled. Recently pulsed power systems are using controlled spark gaps, so called trigetrons. In this case spark gap electrodes are charged to a specified voltage with charging source and then supplied a controlled low voltage to break down spark gap. So, a controlling mechanism is required to charge the load capacitor to a specified voltage level. Otherwise spark gap continuously breaks down due to over voltage across load capacitor. Feedback controlling techniques are adopted in CCPS to charge load capacitor to various voltage levels. Pulsed power facility with feedback is shown in Figure.6.14.

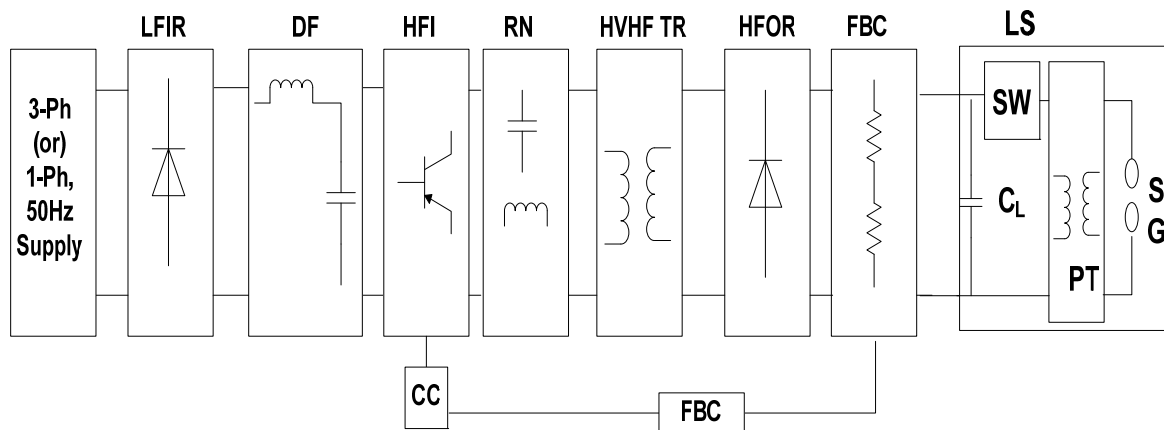


Figure.6.14: Block diagram of pulsed power facility with feedback control circuit

The most common feedback technique is voltage feedback, and it is implemented by resistive divider connected across the load capacitor. The voltage across load is divided across the resistive divider and the feedback voltage is obtained from the lower arm resistor of resistive divider. This feedback voltage then applied to either isolation transformer (AD202 or AD210

or AD215) or optocouplers to provide isolation. All these provides up to 5kV (maximum). The isolation in optocouplers is depends on the pitch between the pins of optocouplers IC. In addition there is a limitation on the output voltage provided across output terminals. The proposed analog voltage feedback controlling technique can overcome above two difficulties. The proposed feedback control technique is implemented with the use of photo diode and LED, whose circuit is shown in Figure.6.15.

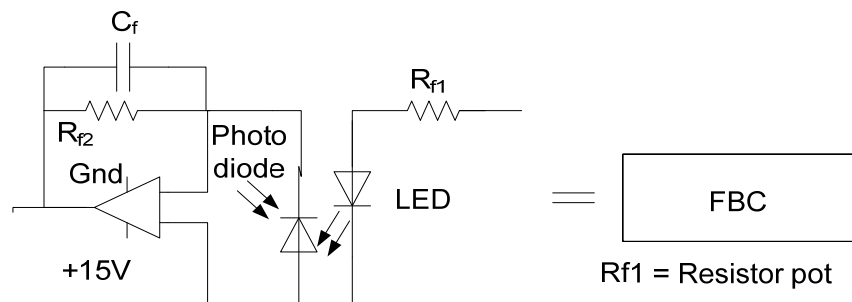


Figure.6.15: Internal circuit of feedback box is shown in Figure.6.10.

The design features of resistive divider is depends on the current flowing through photo diode. The minimum current that required for the conduction of photo diode in the feedback circuit is not less than 4mA from its datasheet. The average load current of the design is 1A. The input parameters taken from chapter 5 and they are charging voltage 1kV, charging time 100ms, load capacitor is 100 $\mu$ F and load current is 1A. Required current to flow through the feedback should be  $> 4$ mA. The maximum voltage across the feedback = Voltage across 100 $\mu$ F capacitor =1kV (max). The current flowing through the resistive divider = 9mA (approx). The value of the resistive divider is

$$R_{total} = 1000 / (9 \times 10^{-3})$$

$$R_{total} = 110k\Omega$$

The chosen resistor values are  $R_1 = 100k\Omega$  and  $R_2 = 10k\Omega$  current is 9mA threw these resistive divider. To operate photo diode in ohmic region adjusted the resistor pot value lesser than the

lower arm resistor of resistive divider, in this case the maximum amount of current will flow through the resistor pot ( $R_{f1} = 5k\Omega$  is shown in Figure.6.15). The value of feedback capacitor ( $C_{f1}$ ) and feedback resistor ( $R_{f2}$ ) are chosen such that it should by pass the high frequency signal to ground when load capacitor discharges whole energy across the dynamic load.

### 6.2.1 Operation

Initially the resistor pot is adjusted such that its value should be less than the value of lower arm resistance of resistive divider to make sure the maximum amount of current should flow through the  $R_{f1}$ . The current flowing through the photo diode via  $R_{f1}$  is more than 4mA, this current makes conducting of photo diode. The conduction of diode makes the LED to glow, at this point of time a small amount of voltage generated appears across resistor ( $R_{f2}$ ).

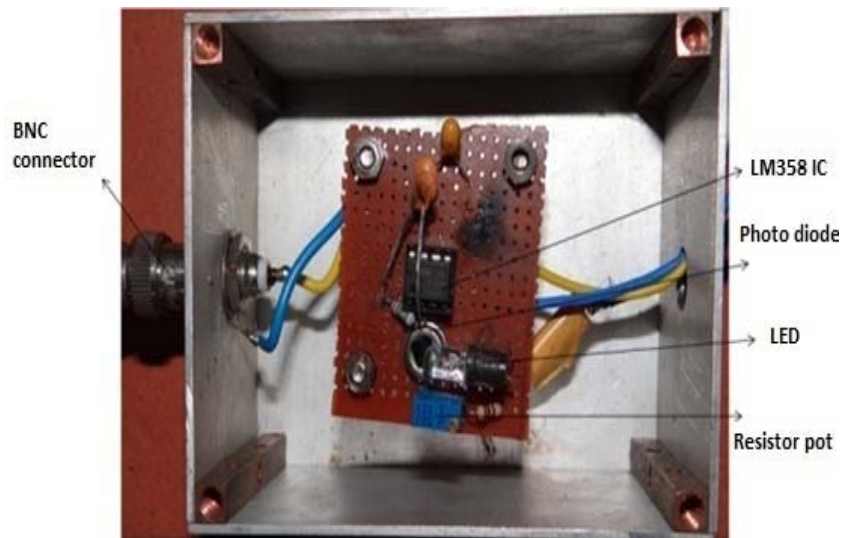


Figure.6.16: Experimental setup of feedback (top view)

The magnitude of generated voltage is depends on the distance between the head position of LED with photodiode. This voltage is compared with the reference voltage in the comparator and generates the controlled error signal. The referecne voltage is continuously compared with the ramp signal from the feed back circuit unless until the error of

comparator becomes zero. The experimental set up of the proposed feedback control is shown in Figure.6.16. The maximum voltage variation is obtained across the output terminals of feedback circuit is the first advantage of this feedback control. The maximum output voltage range enables to control the load voltage effectively for smaller charging voltages. The second advantage is that the proposed feedback control provides a sufficient and isolation between power circuits to control circuit compared to isolation amplifier and optocouplers.

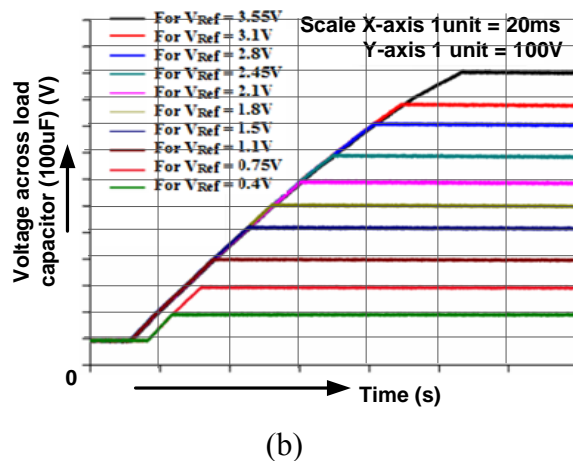
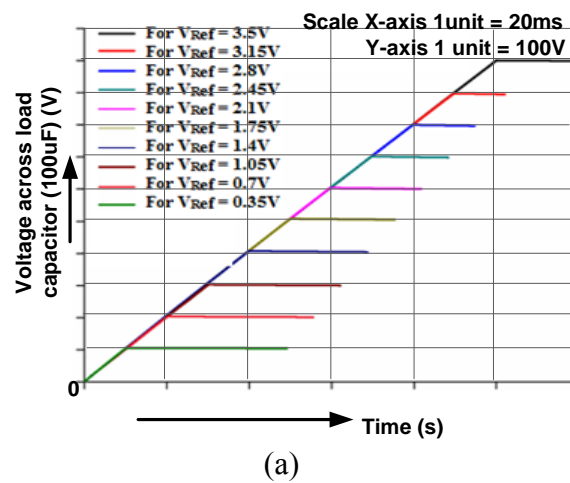


Figure.6.17: Voltage profile across load capacitor (100µF) (a) Simulation (b) Experimental

The load capacitor (100µF) have been charged to 1kV in step by step from 100V is shown in Figure.6.17. Both simulation and experimental are shown in Figure.6.17a and 6.17b, there is a difference in reference signal in case of simulation with that of experimental. This difference because of practical considerations. In simulation the reference signal can be

generated as we wish. But, when it comes to experimental this reference signal is generated on the tip position of light emitting diode (LED) with photo diode. If the distance the vary intensity of light changes at the same time the reference voltage is also changes.

The reference voltage has been setted in the comparator by controller for each voltage (from 100V to 1kV). As soon as target voltage raches to its setted value controller acknowledges the PWM controller, then PWM controller stops providing PWM signals to IGBT switches in the inverter stage.

#### **6.4.2 Observations**

- ✓ Analog voltage feedback control circuit is implemented and tested by charging an energy storage capacitor (100 $\mu$ F) to various voltages from 100V to 1kV.
- ✓ The proposed feedback circuit simulated and tested experimentally with the 4<sup>th</sup> order LCLC resonant based CCPS.
- ✓ The proposed feedback will provide greater isolation between high voltage section to low voltage controlling section as compared to isolation amplifierr and optocouplers based feedback circuits.
- ✓ The range of output voltage provided by this feedback circuit is high, which enable to control the lower voltages also.

#### **Summary**

Protection and controlling features of CCPS are discussed in this chapter, which are key factors in power supply when they are interfaced with pulsed power systems operated with highly dynamic loads like BWO, magnetron and klystrons. In addition discussed the various EMI mitigation techniques like EMI filter, soft switching, snubbers and compensation networks have been studied. Failure of IGBT switch in the inverter stage of CCPS due to conducted (common and differential mode) noise has been reported. Protections schemes to

overcome of failure of IGBT switches due to common mode noise and differential noise has been demonstrated with insertion of shielding and with that of proposed 4<sup>th</sup> order LCLC resonant converter. Shielding between primary and secondary of HVHF transformer will enable us to keep coupling capacitor ( $C_C$ ) value as low as possible ( $\leq 10\text{pF}$ ). The proposed 4<sup>th</sup> order LCLC resonant topology acts as low pass filter for differential mode noise. Shielding and LCLC low pass filter scale down the noise voltage magnitude at a rate of -10dB and -75dB gain. Experimental and simulation results of conducted noise (Common mode and differential mode) results are presented. Low pass LCLC filter makes the differential noise voltage magnitude negligible, where as common mode noise voltage gain is about -10dB for 10pF coupling capacitor at 10MHz noise frequency.

A photodiode and LED based control scheme has been demonstrated and tested with 1kV and 500 J/s CCPS by charging load capacitor (100 $\mu\text{F}$ ) to various voltages from 100V to 1kV. Simulation and experimental results are presented to verify. The proposed control feedback provides greater isolation than isolation amplifier and optocouplers. In addition the voltage range provided by this feedback circuit is high, which enable us to control voltage across load capacitor precisely from its lower voltage to its rated voltage.

# Chapter-7

## Conclusion and future scope

---

### 7.1 Conclusion

Noticed some of the pulsed power systems like Marx based system, linear induction accelerator, inductive energy storage system, pulser and power modulator named few pulsed generators. Pulsed power systems are usually represented with an energy storage element, so called an energy storage capacitor. A suitable charging source is required to charge this capacitor. Switched mode power supplies become popular for DC power applications over conventional DC power supplies due to higher efficiencies, lesser in weight and compact. Resonant converter based DC-DC converters using now a days for their superior advantages like constant voltage, constant current and soft switching. Capacitor charging power supply is also a kind of switched mode power supply utilizes resonant converters to derive advantage like constant current, soft switching and inherent short circuit proof. Second order series LC and parallel LC and third order LCLC-T and CLL resonant converters have been adopted for the design of CCPS for pulsed power applications. But all these (2<sup>nd</sup> order and 3<sup>rd</sup> order) CCPS are suffers with various disadvantages like enormously high peak currents, lack of DC blocking, poor part load efficiency and not in condition to handle noise generated by highly dynamic loads. In view of all these proposed a 4<sup>th</sup> order LCLC resonant converter based CCPS for pulsed power applications. The proposed converter had overcome the aforementioned disadvantages of 2<sup>nd</sup> and 3<sup>rd</sup> order resonant based CCPS in addition protect the power supply from noise generated by highly dynamic loads effectively. Identified four 4<sup>th</sup> order resonant converters which are suitable and meets the pulsed power demands are

presented and discussed in detail in the chapters. Conditions for load independent constant current, ZCS, current gain, voltage gain and relationship between resonant components for the chosen 4<sup>th</sup> order resonant converters are summarized and presented in a table. A prototype with a rating 20 J/s capacitor charging power supply has been developed based on 4<sup>th</sup> order resonant converter and tested with 100  $\mu$ F capacitor to see the basic requirements like load independent constant current and soft switching. Remaining three 4<sup>th</sup> order resonant converters has been used in the development of CCPS for three different pulsed power applications. A comparative study has been carried out to show the importance of proposed 4<sup>th</sup> order resonant converter as compared to 2<sup>nd</sup> and 3<sup>rd</sup> order resonant converter based CCPS.

A detailed mathematical and experimental analysis has been done in minimizing conducted noise. Faraday shielding and proposed 4<sup>th</sup> order resonant converter had overcome the conducted noise effectively. Bode plot has been drawn and explained how much reduction can be achieved with faraday shielding. Shielding between primary and secondary of HVHF transformer will enable us to keep coupling capacitor ( $C_C$ ) value as low as possible ( $\leq 10$ pF). The proposed 4<sup>th</sup> order LCLC resonant topology acts as low pass filter for differential mode noise. Shielding and LCLC low pass filter scale down the noise voltage magnitude at a rate of -10dB and -75dB gain. Experimental and simulation results of conducted noise (Common mode and differential mode) are presented. Low pass LCLC filter makes the differential noise voltage magnitude negligible, where as common mode noise voltage gain is about -10dB for 10pF coupling capacitor at 10MHz noise frequency.

The overall motive of this research work is to design a reliable, efficient and compatible resonant converter based fast CCPS for pulsed power application. Complications with the usage of higher order resonant converter in the power stage have been overcome effectively. The present research work enables the researchers work in higher order resonant converters to make charging power supplies more reliable and efficient.

The major contribution of this research work is in the design of fast CCPS for pulsed power applications are

1. A 4<sup>th</sup> order resonant converter based CCPS has been designed and simulated for high pulsed power and dynamic load applications. The proposed converter provides load independent constant current and soft switching when operated at switching frequency equal to resonant frequency.
2. To validate the simulation and mathematical model, a prototype CCPS rated at 200 V, 20 J/s has been developed and load independent constant current is demonstrated with soft switching operation.
3. A high repetition rate CCPS of 4kV, 3.7kJ/s and 9 kHz is designed. High voltage high frequency transformer's leakage inductance is used as one of the resonant inductor.
4. Developed a high charging rate (45 kJ/s) and repetitive (10 Hz) CCPS for 1kJ Marx based system based on 4<sup>th</sup> order LCLC resonant converter and successfully interfaced.
5. The failure of controlled switches (IGBTs) in the inverter stage of CCPS due to conducted noise are prevented by effective shielding and proposed LCLC resonant network.
6. With the proposed topology the cost and size of CCPS has reduced due to minimal number of controlled switches, low peak currents and minimum conduction losses in the inverter stage.
7. A photo diode-LED based voltage control circuit has been developed and tested successfully. This control circuit provides more isolation as compared to other electronic components like isolation amplifier and opto-couplers.

The academic contribution of the thesis is in bringing out a better understanding of high voltage fast CCPS design aspects and noise mitigation with proposed 4<sup>th</sup> order LCLC resonant converter and shielding. The data on application of 4<sup>th</sup> order LCLC resonant converter as constant current source in the design and development of CCPS for pulsed

power application, as well as the protection of fast (>40 kJ/s) CCPS against conducted noise with repetitive pulsed power system operating with highly dynamic load has been published.

## **7.2 Future research**

- Research still open for higher order resonant converters for CCPS applications
- Converter cum inverter based CCPS with four switching elements is still a barrier for researchers.
- Battery based CCPS with 4<sup>th</sup> order even higher order resonant based CCPS are better option for isolated charging source to overcome noise.
- Compact CCPS are possible by utilizing transformer parameters (leakage inductance and distributed capacitance) are as resonant components.

Present work has contributed to a better understanding of noise related issues and their handling with proposed 4<sup>th</sup> order LCLC resonant converter and shielding. The study carried out in this thesis is useful in the development of a reliable, compatible and efficient fast capacitor charging power supply for pulsed power application.

## References

---

1. Hidenori Akiyama, Takashi Sakugawa, Takao Namihira, "Industrial Applications of Pulsedd Power Technology", IEEE Transactions on Dielectrics and Electrical Insulation Vol. 14, No. 5, Oct 2007, pp. 1051-1064.
2. E. L. Neau, "Environmental and Industrial Applications of Pulsedd Power Systems", IEEE Transactions on Plasma science, Vol. 22, No. 1, Feb 1994, pp. 2-10.
3. Rui Xie, Jiande Wu, Wuhua Li and Xiangning He, "A High Voltage Pulsedd Power Supply with Magnetic Switch for ESP", IEEE Power electronics and applications 2007 European conference, 2-5th Sep, 2007, pp. 1-7.
4. J.L. Liu, Y. Yin, T.W. Zhan, J.H Feng and H.H Zhong, "Application of A Self-Breakdown Hydrogen Spark Gap Switch on High Power Pulsed Modulator", 16th International Pulsed power conference, 2007, 17-22nd Jun, 2007, pp. 455-458.
5. A. Welleman and R. Leutwyler, "Solutions with Solid State Switches for Pulsed Modulators", IEEE International Power modulator and high voltage conference, 2008, 27-31st May, 2008, pp. 29-32.
6. Sokal N.O, "Flyback Charging with Current Mode Controlled Flyback Converter", US patent 5,485,361, 16 Jan 1996.
7. Michael A.V. Ward, "DC to DC Converter Current Pump", U.S. Patent number 4, 868, 730,
8. K. Liu, R. Oruganti and F.C. Lee, "Quasi-Resonant Converters – Topologies and Characteristics", IEEE Transaction on Power Electronics, Vol. 2, No. 1, Jan 1987, pp. 62-71.
9. G. Hua, E. Yang, Y. Jiang and F. C. Lee, "Novel Zero-Current-Transition PWM Converters", IEEE Transaction on Power Electronics, Vol. 9, No. 6, Nov 1994, pp. 601-606.

- 
10. P. K. Jain, W. Kang, H. Soin and Y. Xi, "Analysis and Design Considerations of A Load and Line Independent Zero Voltage Switching Full Bridge DC/DC Converter Topology", IEEE Transaction on Power Electronics, Vol. 17, No. 5, Sep. 2002, pp. 649-657.
  11. J. G. Cho, J. A. Sabate, G. Hua and F. C. Lee, "Zero-Voltage and Zero-Current Switching Full Bridge PWM Converter for High Power Applications", IEEE Transaction on Power Electronics, Vol. 11, No. 4, Jul 1996, pp. 622-627.
  12. M. Jovanovic, "Merits and Limitations of Resonant and Soft-Switched Converters", Proceedings of 14th IEEE International Telecommunications Energy Conference, 4-8th Oct 1992, pp. 51-58.
  13. M. Jovanovic, "Resonant, quasi-resonant, multi-resonant and soft-switching techniques - merits and limitations," International Journal of Electronics, Vol. 77, No. 5, 1994, pp. 537-554.
  14. S. Gonzalez, M Valla and C. Muravchik, "Analysis and Design of Clamped Mode Resonant Converters with Variable Load", IEEE Transactions on Industrial Electronics, Vol. 48, No. 2, Aug 2001, pp. 812-819.
  15. M.H. Rashid, Power electronics: Circuits, Devices and Applications [Book], Prentice hall, Inc, 1988.
  16. V. Caliskan, J. Gegner and C. Lee, "Current-Driven Zero-Voltage Switched Resonant Converter with Capacitive Output Filter", Proceedings of IEEE Applied Power Electronics Conference, 23-27th Feb 1992, pp. 211-218.
  17. M. Matsuo, T. Suetsugu, S. Mori and I. Sasase, "Class DE Current-Source Parallel Resonant Inverter", IEEE Transactions on Industrial Electronics, Vol. 46, No. 2, Apr 1999, pp. 242-249.

- 
18. A. Shenkman, B. Axelrod and V. Chudnovsky, "A New Simplified Model of Dynamics of the Current-Fed Parallel Resonant Inverter", IEEE Transactions on Industrial Electronics, Vol. 47, No. 2, Apr 2000, pp. 282-286.
  19. M. Elbuluk and M. Chavez, "A Complete Normalized Analysis of the Current Fed Series Resonant DC/DC Converter", IEEE Industrial Electronics Conference, 6-10th Nov 1989, pp. 27-32.
  20. S. Sooksatra and C. Lee, "Current Driven Series Resonant Converter", Proceedings of IEEE Applied Power Electronics Conference, 11-16th Mar 1990, pp. 128-136.
  21. L. Hobson and D. Tebb, "Transistorized Power Supplies for Induction Heating", International Journal of Electronics, Vol. 59, No. 5, 1985, pp. 543-552.
  22. F. Forest, E. Laboure and J. Yves, "Principle of A Multi-Load/Single Converter System for Low Power Induction Heating", IEEE Transactions on Power Electronics, Vol. 15, No. 2, Mar 2000, pp. 223-230.
  23. E. Dede, V. Esteve, J. Garcia, A. Navarro, E. Maset and E. Sanchis, "Analysis of Losses and Thermal Design of High Power High Frequency Resonant Current Fed Inverters for Induction Heating", IEEE Industrial Electronics Conference, 1993, pp. 1046-1051.
  24. P. Jain, "Parallel Tuned Resonant DC/DC Converter Topologies", Proceedings of IEEE International Telecommunication Conference, 04-08th Oct 1992, pp. 74-80.
  25. A.K.S. Bhat and S. B. Dewan, "Analysis and Design of A High Frequency Resonant Converter Using LCC-Type Commutation", IEEE Transactions on Power Electronics, Vol. 2, No. 4, Apr 1987, pp. 291-301.
  26. A.K.S. Bhat, "Analysis and Design of A Series-Parallel Resonant Converter", IEEE Transactions on Power Electronics, Vol. 8, No. 1, Jan 1993, pp. 1-11.

- 
27. M. Foster, H. Sewell, C. Bingham, D. Stone and D. Howe, "Methodologies for the Design of LCC Voltage-Output Resonant Converters," IEE Proceedings on Electric Power Applications, Vol. 153, No. 4, Sep 2006, pp. 559- 567.
  28. Y. Ang, C. Bingham, M. Foster, D. Stone and D. Howe, "Design Oriented Analysis of Fourth-Order LCLC Converters with Capacitive Output Filter", IEE Proceedings on Electric Power Applications, Vol. 152, No. 2, Mar 2005, pp. 310- 322.
  29. P. Jain, H. Soin and M. Cardella, "Constant Frequency Resonant DC-DC Converters with Zero Switching Loss", IEEE Transactions on Aerospace and Electronic Systems, Vol. 30, No. 2, Apr 1994, pp. 534-543.
  30. Mangesh B. Borge, "Resonant Converter Topologies for Constant-Current Power Supplies and Their Applications", Ph. D Thesis, HBNI 2011.
  31. M. Cosby and R. Nelms, "Designing A Parallel-Loaded Resonant Inverter for An Electronic Ballast Using The Fundamental Approximation", IEEE Applied Power Electronics Conference Proceedings, 7-11th Mar 1993, pp. 418-423.
  32. M. Gulko and S. Ben-Yaakov, "Current-Sourcing Push-Pull Parallel Resonance Inverter (CS-PPRI): Theory and Application As Discharge Lamp Driver", IEEE Transactions on Industrial Electronics, Vol. 41, No. 3, Jun 1994, pp. 285-291.
  33. M. Schutten, R. L. Steigerwald and M. Kheraluwala, "Characteristics of Load Resonant Converter Operated in High-Power Factor Mode", IEEE Transactions on Power Electronics, Vol. 7, No. 2, Apr 1992, pp. 304-314.
  34. W. Sulistyono and P. Enjeti, "A Series Resonant Ac-Dc Rectifier with High Frequency Isolation", IEEE Applied Power Electronics Conference Proceedings, Vol. 1, 13-17th Feb 1994, pp. 397-403.

- 
35. H. W. Koertzen, J. D. Van Wyk and J. A. Ferreira, "Comparison of Swept Frequency and Phase Shift Control for Forced Commutated Series Resonant Induction Heating Converters", IEEE Industry Applications Society Annual Meeting, Vol 3, 8-12th Oct 1995, pp. 1964-1969.
36. S. Dieckerhoff, M. Ryan and R. Doncker, "Design of An IGBT-Based LCL-Resonant Inverter for High Frequency Induction Heating", IEEE Industry Applications Society Annual Meeting, Vol. 4 3-7th Oct 1999, pp. 2039-2045.
37. H. Pollock and J. O. Flower, "New Method of Power Control for Series-Parallel Load Resonant Converters Maintaining Zero Current Switching and Unity Power Factor Operation", IEEE Transactions on Power Electronics, Vol. 12, No. 1, Jan 1997, pp. 103-115.
38. W. Zhou and H. Ma, "Design Considerations of Compensation Topologies in ICPT System", IEEE Applied Power Electronics Conference Proceedings, 25th Feb–1st Mar 2007, pp. 985-990.
39. P. Jain and H. Soin, "A Constant Frequency Parallel Tuned Resonant DC/DC Converter for High Voltage Applications", IEEE Power Electronics Specialist Conference Proceedings, Vol. 1, 29th Jun-3rd Jul 1992, pp. 71-77.
40. Y. Liu and X. He, "PDM and PFM Hybrid Control of A Series-Resonant Inverter for Corona Surface Treatment", IEE Proceedings on Electric Power Applications, Vol. 152, No. 6, Nov 2005, pp. 1445- 1450.
- 41 J.R. Davis, "Welding Brazing and Soldering, American Society of Metals", Metals Handbook, Vol-6, 9th edition, 1983.
42. D. Novotny, D. Breckinridge and K. Hartke, "Power Supplies Adapted for Diode Pumped Laser Systems", Laser Focus World, Apr 2002, pp. 97-99.
43. C. Coleman and R. Sherwood, "Inductive Storage Yields Efficient Power Alternative", Laser Focus World, Apr 2003, pp. 94-97.

- 
44. F. Bordry and A. Dupaquier, "High Current Low Voltage Power Converters for LHC: Present Development Directions", Proceeding of European Particle Accelerator Conference, Proceedings EPAC1996, Sitges, 1996.
  45. M. Day, "LED Driver Considerations", Electronics design news – Asia, Jan. 2004, pp. 62-65.
  46. "Switch Mode, Linear and Pulsed Charging Techniques For Li+ Batteries in Mobile Phones And Pdas", Application note, Maxim Semiconductors, AN 913, Dec. 2001.
  47. A. C. Lippincott and R. M. Nelms, "A Capacitor-Charging Power Supply Using A Series-Resonant Topology, Constant On-Time/Variable Frequency Control", IEEE Transactions on Industrial Electronics, Vol. 38, No. 6, Dec 1991, pp. 438-447.
  48. B. Pollard and R. Nelms, "Using The Series-Parallel Resonant Converter in Capacitor Charging Applications", IEEE Applied Power Electronics Conference Proceedings, 23-27th Feb 1992, pp. 245-252.
  49. H. Pollock, "High Efficiency, High Frequency for Capacitor and Battery Charging", IEE Colloquium on Power Electronics for Demanding Applications, 1999, pp. 9/1-9/10.
  50. P. Pollak, "DC Power Supplies", publication no. 103, Dyna power Corporation.
  - 51 H. Eckoldt, F. Faubladiere and N. Heidbrook, "Constant-Power Supplies for The Tesla Modulators", Proceedings EPAC2000, pp.2199-2201.
  52. A.C. Lippincott, R.M. Nelms, M.Garbi and E.Strickland, "A Series Resonant Converter with Constant On-Time Control for Capacitor Charging Applications", Proceedings of the fifth annual IEEE applied power electronics conference, March 1990, pp. 147-154.
  53. B.E. Strickland, M. Garbi, F. Cathell, and S. Eckhouse, "2 kJ/s, 25 kV High Frequency Capacitor Charging Power Supply Using MOSFET Switches", Proceedings of nineteenth power modulator symposium, June 1990, pp. 531-534.

- 
54. Francis C. Schwarz, "A Method of Resonant Current Pulsed Modulation for Power Converters", IEEE Transactions on Industrial Electronics and Control Instrumentation, Vol. 17, No. 3, May 1970, pp. 209-221.
55. Francis C. Schwarz, "An Improved Method of Resonant Current Pulsed Modulation for Power Converters", IEEE Transactions on Industrial Electronics and Control Instrumentation, Vol. 23, No. 2, May 1976, pp. 133-141.
56. Nathan O. Sokal and Richard Redl, "Control Algorithms and Circuits Designs for Optimally Flyback- Charging an Energy-Storage Capacitor ( E.G for a Falsh Lamp)", Proceedings of the Fifth Annual IEEE Applied power Electronics Conference, March 1990, pp. 295-302.
57. N. Tilgenkamp, S. De Hann and H. Huisman, "A Novel Series Resonant Converter Topology", IEEE Transactions on Industrial Electronics, Vol. 34, No. 2, May 1987, pp. 240-246.
58. P. Jain and S. Dewan, "A Performance Comparison of Full and Half-Bridge Series Resonant Inverters in High Frequency High Power Applications", IEEE Transactions on Industrial Applications, Vol. 26, No. 2, March/April 1990, pp. 317-323.
59. J. Vieira and I. Barbi, "Constant Frequency PWM Capacitor Voltage-Clamped Series Resonant Power Supply", IEEE Transactions on Power Electronecs, Vol. 8, No. 2, April 1993, pp. 120-126.
60. Rim, G.H., Ryoo, H.J. and Kim, J.S. "A Constant Current High Voltage Capacitor Charging Power Supply for Pulsed Power Applications," IEEE Pulsed Power Plasma Science Conference, Vol.2, 17-22nd Jun 2001, pp. 1284-1286.
61. Ryoo, H.J., Jang S.R., Kim, J.S. and Kim, Y.B. "Design and Testing of the High Voltage Capacitor Charger for 150kJ Pulsed Power Application," IEEE Pulsed Power Conference, 28th Jun-2nd Jul 2009, pp. 1376-1379.

- 
62. Mangesh Borage, "Parallel Resonant Converter as A Current Source", J. Indian Inst. Sci., Sept.–Dec. 2003, 83, pp. 117–125.
63. C. Chakraborty and M. Ishida, "Performance Design and Control of A Series-Parallel (CL2-Type) Resonant DC-DC Converter", IEE Proceedings on Electric power applications, Vol. 149, No. 2, September 2002, pp. 360-368.
64. I. Batarseh, "State-Plane Approach for Analysis of Half-Bridge Parallel Resonant Converters", IEE Proceeding on Circuits Devices Systems, Vol. 142, No. 3, Jun 1995, pp. 200-204.
65. I. Batarseh and K. Siri, "LLC-Type Series Resonant Converter With PWM Control", IEE Proceeding on Circuits Devices Systems, Vol. 141, No. 2, Apr 1994, pp. 73-81.
66. A. K. S. Bhat, "Analysis and Design Of LCL-Type Series Resonant Converter", IEEE Transactions on Industrial Electronics, Vol. 41, No. 1, Feb 1994, pp. 118-124.
67. A. K. S. Bhat, "Analysis and Design of A Fixed-Frequency LCL Type Series Resonant Converter with Capacitive Output Filter", IEE Proceeding on Circuits Devices Systems, Vol. 144, No. 2, 1997, pp. 97-103.
68. H. Pollock and J. O. Flower, "Series-Parallel Load-Resonant Converter for Controlled-Current Arc Welding Power Supply," IEE Proceedings on Electric Power Applications, Vol. 143, No. 3, May 1996, pp. 211-218.
69. J. Hayes and M. Egan, "A Comparative Study of Phase-Shift, Frequency and Hybrid Control of Series Resonant Converter Supplying The Electric Vehicle Inductive Charging Interface", IEEE Applied Power Electronics Conference Proceedings, 14-18th Mar 1999, pp. 450-457.
70. Patel A, Nagesh KV, Kolge T, Chakravathy DP, "Design and Development of Repetitive Capacitor Charging Power Supply Based on Series-Parallel Resonant Converter Topology" Review of Scientific Instruments, Vol 82(4), No. 045111, Aug 2011, pp. 1-10,.

- 
71. Pollock, H, "Constant Frequency, Constant Current Load Resonant Capacitor Charging Power Supply", IEE proceedings on Electric Power Applications, 1999, Vol 146, No. 2, pp. 187-192.
72. Mangesh Borage, Sunil Tiwari and Swarna Kotaiah, "LCL-T Resonant Converter with Clamp Diodes A Novel Constant –current power supplies for capacitor charging", IEEE Transactions on Industrial Electronics, Vol. 54, No. 2, April, 2007, pp. 741-746.
73. P. Jain, "Performance Comparison Of Pulsed Width Modulated Resonant Mode DC/DC Converters for Space Applications," IEEE Industry Applications Society Annual Meeting, 1-5th Oct 1989, pp. 1106-1114.
74. M. Kazimierczuk and M. Jutty, "Fixed-Frequency Phase Controlled Full Bridge Resonant Converter with A Series Load", IEEE Transactions on Power Electronics, Vol. 10, No. 1, Jan 1995, pp. 9-18.
75. M. Kazimierczuk, "Synthesis of Phase Modulated Resonant DC/AC Inverter and DC/DC Converters," IEE Proceedings on Electric Power Applications, Vol. 139, No. 4, Jul 1992, pp. 387-393.
- 76 H. Kifune, Y. Hatanaka and M. Nakaoka, "Cost Effective Phase Shifted Pulsed Modulation Soft Switching High Frequency Inverter for Induction Heating Applications," IEE Proceedings on Electric Power Applications, Vol. 151, No. 1, Jan 2004, pp. 19- 25.
77. P. Jain, A. Martin and G. Edwards, "Asymmetrical Pulsed Width Modulated Resonant DC-DC Converter Topologies," IEEE Transactions on Power Electronics, Vol. 11, No. 3, May 1996, pp. 413-422.
78. J. M. Burdío, L. A. Barragán, F. Monterde, D. Navarro and J. Acero, "Asymmetrical Voltage-Cancellation Control for Full-Bridge Series Resonant Inverters," IEEE Transactions on Power Electronics, Vol. 19, No. 2, Mar 2004, pp. 461-469.

- 
79. G. Joung, C. Rim and G. Cho, "Integral Cycle Mode Control of Series Resonant Converter", IEEE Transactions on Power Electronics, Vol. 4, No. 1, Jan 1989, pp. 83-91.
80. M. Z. Youssef and P. K. Jain, "Series-Parallel Resonant Converter in Self-Sustained Oscillation Mode with The High-Frequency Transformer-Leakage-Inductance Effect: Analysis, Modeling and Design," IEEE Transactions on Industrial Electronics, Vol. 54, No. 3, Jun 2007, pp. 1329-1341.
81. Mohammad Rouhollah, Yazdani, Hosein Farzanehfard and Jawad Faiz, "Classification and Comparison of EMI Mitigation Techniques in Switching Power Converters A Review", Journal of Power Electronics, Vol. 11, No. 5, Sep 2011, pp. 767-777.
82. D. Cochrane, D. Chen, and D. Boroyevic, "Passive cancellation of common-mode noise in power electronic circuits", IEEE Transactions on Power Electronics, Vol. 18, No. 3, May 2003, pp. 756-763
83. A. Abramovitz, T. Cheng, and K. Smedley, "Analysis and Design of Forward Converter with Energy Regenerative Snubber", IEEE Transactions on Power Electronics, Vol. 25, No. 3, Mar. 2010, pp. 667-676.
84. H. Akagi, H. Hasegawa, and T. Doumoto, "Design, Performance of A Passive EMI Filter for Use with Voltage Source PWM Inverter Having Sinusoidal Output Voltage, Zero Common-Mode Voltage", IEEE Transactions on Power Electronics, Vol. 19, No. 4, Jul 2004, pp. 1069-1076.
85. Bushnell A.H, "Interfacing Pulsed Power System to Switching Power Supplies," A 25th Power modulator symposium and high voltage workshop, 30th Jun-3rd July, 2002, pp. 290-292.
86. Bhadani P.K., Capacitor charging power supply for laser pulsedrs using boost circuit, Review of Scientific Instruments, Vol. 60(4), Apr 1989, pp. 605-607.

- 
87. Marcle P.J.Gaudreau, Jeffrey A.Casey, Solid-state pulsed power systems for the next linear collider, Diversified Technologies Inc., 35 Wiggins Ave. Bedford, MA, USA.
88. Bob Mammano and Bruce Carsten, "Understanding and Optimizing Electromagnetic Compatibility in Switchmode Power Supplies", Copyright 2003, Texas Instruments, pp. 1-18.
89. P. Caldeira, R. Liu, D. Dalal, and W.J. Gu, "Comparison of EMI Performance of PWM and Resonant Power Converters", Proceeding of IEEE Power Electronics Specialist Conference, 20-24th Jun1993, pp. 134-140.
90. D. Qu, "EMI Characterization and Improvement of Bi-Directional DC/DC Converters", Master Thesis, Virginia Polytechnic Institute and State University, Virginia, 1999.
91. W. Chen, X. Yang, and Z. Wang, "An Active EMI Filtering Technique for Improving Passive Filter Low-Frequency Performance", IEEE Transactions on Electromagnetic Compatibility, Vol. 48, No. 1, Feb. 2006, pp. 172-177.
92. Y. C. Son and S. K. Sul, "A New Active Common-Mode EMI Filter for PWM Inverter", IEEE Transactions on Power Electronics, Vol. 18, No. 6, Nov. 2003, pp. 1309- 1314.
93. Q. Zhaoming, W. Xin, L. Zhengyu, and M. H. Pong, "Status of Electromagnetic Compatibility Research in Power Electronics", in Proceeding of IEEE PIEMC' 2000, pp. 46-56.
94. H. Chung, S. Y. R. Hui, and K. K. Tse, "Reduction of Power Converter EMI Emission Using Soft-Switching Techniques", IEEE Transactions on Electromagnetic Compatibility, Vol. 40, No. 3, Aug. 1998, pp. 282-287.
95. M. Yoshida, E. Hiraki, and M. Nakaoka, "Actual Efficiency and Electromagnetic Noises Evaluations of A Single Inductor Resonant AC Link Snubber-Assisted Three-Phase Soft-Switching Inverter", Proceeding of IEEE International Telecommunications Energy Conference, 18-22nd Oct, 2003, pp. 721-726.

- 
96. L. A. Barragan, D. Navarro, J. Acero, I. Urriza, and J. M. Burdio, "FPGA Implementation of A Switching Frequency Modulation Circuit for EMI Reduction in Resonant Inverters for Induction Heating Appliances", IEEE Trans. Ind. Electron., Vol. 55, No. 1, Jan. 2008, pp. 11-20.
97. S. Johnson and R. Zane, "Custom Spectral Shaping for EMI Reduction in High Frequency Inverters and Ballasts", IEEE Transactions on Power Electronics, Vol. 20, No.6, Nov. 2005, pp. 1499-1505.
98. D. Zhang, D. Y. Chen, and F. C. Lee, "An Experimental Comparison of Conducted EMI Emissions Between Zero-Voltage Transition Circuit and A Hard Switching Circuit", Proceeding of IEEE Power Electronics Specialist Conference, 23-27th Jun 1996, pp.1992-1997.
99. S. Ogasawara and H. Akagi, "Modeling and Damping of High-Frequency Leakage Currents in PWM Inverter-Fed AC Motor Drive Systems", IEEE Transactions on Industrial Applications, Vol. 32, No. 5, Sep./Oct. 1996, pp. 1105-1114.
100. A. L. Julian, T. A. Lipo, and G. Oriti, "Elimination of Common Mode Voltage in Three Phase Sinusoidal Power Converters", Proceeding of IEEE Power Electronics Specialist Conference 23-27th Jun 19 96, pp. 1968-1972.
101. S. Ogasawara, H. Ayano, and H. Akagi, "An Active Circuit for Cancellation of Common Mode Voltage Generated by A PWM Inverter", IEEE Transactions on Power Electronics, Vol. 13, No. 5, Sep 1998, pp. 835-841.
102. W. Xin, N.K. Poon, C. M. Lee, M. H. Pong, and Z. Qian, "A Study of Common Mode Noise in Switching Power Supply from A Current Balancing Viewpoint", Proceeding of IEEE Power Electronics and Drive Systems, Vol. 227-29th Jul 1999, pp. 621-625.

- 
103. Y. Zhang, K. Zhang, J. Zhou, Y. Kang, and Y. Gao, "Digital Active Common Mode EMI Suppression Technique for Switching Converters", Proceeding of IEEE International Electronics Conference, 5-8th Nov 2007, pp. 2073-2078.
104. K. Fujiwara and H. Nomura, "A Novel Lossless Passive Snubber for Soft Switching Boost-Type Converters", IEEE Transactions on Power Electronics, Vol. 14, No. 6, Nov. 1999, pp. 1065-1069.
105. S. S. Lee, S. W. Choi, and G. W. Moon, "High Efficiency Active Clamp Forward Converter with Synchronous Switch Controlled ZVS Operation", Journal of Power Electronics, Vol. 6, No. 2, Apr. 2006, pp. 131-138.
106. H. Mao, S. Deng, J. Abu-Qahouq, and I. Batarseh, "Active-Clamp Snubbers for Isolated Half-Bridge DC-DC Converters", IEEE Transactions on Power Electronics., Vol. 20, No. 6, Nov. 2005, pp. 1294-1302.
107. K. Kam, D. Pommerenke, F. Centola, C. Lam, and R. Steinfeld, "EMC Guideline for Synchronous Buck Converter Design", Proceeding of IEEE ISEMC'09, pp. 47-52.
108. M. H. Pong, C. M. Lee, and X. Wu, "EMI Due to Electric Field Coupling on PCB", in Proceeding of IEEE Power Electronics Specialist Conference, 22-24th May 1998, pp.1125-1130.
109. M. I. Montrose, "EMC and The Printed Circuit Board: Design, Theory and Layout Made Simple", Wiley-IEEE Press, 1998.
110. L. B. Gravelle and P. F. Wilson, "EMI/EMC in Printed Circuit Boards - A Literature Review", IEEE Transactions on Electromagnetic Compatibility, Vol.34, No. 2, May 1992, pp. 109-116.
111. L. Rossetto, S. Buso, and G. Spiazzi, "Conducted EMI Issues in A 600- W Single-Phase Boost PFC Design", IEEE Transactions on Industrial Applications, Vol. 36, No. 2, Mar./Apr. 2000, pp. 578-585.

- 
112. A. Mediano, "EMI/EMC Troubleshooting Techniques in Switching Mode Power Supplies", Proceeding of IEEE European Conference on Power Electronics, 8-10th Sep 2009, pp. 1-5.
113. S. Basu and T. M. Undeland, "Diode Recovery Characteristics Considerations for Optimizing EMI Performance of Continuous Mode PFC Converters", in Proceeding of IEEE European Conference on Power Electronics, 11-14th Sep 2005, pp. 1-9.
114. S. Wang, R. Chen, J. D. Van Wyk, F. C. Lee, and W. G. Odendaal, "Developing Parasitic Cancellation Technologies to Improve EMI Filter Performance for Switching Mode Power Supplies", IEEE Transactions on Electromagnetic Compatibility, Vol. 47, No. 4, Nov. 2005, pp. 921-929.
115. B. J. Pierquet, T. C. Neugebauer, and D. J. Perreault, "Inductance Compensation of Multiple Capacitors with Application to Common, Differential Mode Filters", IEEE Transactions on Power Electronics, Vol. 21, No. 6, Nov. 2006, pp. 1815- 1824.
116. M. Shoyama, M. Ohba, and T. Ninomiya, "Balanced Buck-Boost Switching Converter to Reduce Common-Mode Conducted Noise", Journal of Power Electronics, Vol. 2, No. 2, Apr.2002, pp. 139-145.
117. P. Kong, S. Wang, and F. C. Lee, "Common Mode EMI Noise Suppression for Bridgeless PFC Converters", IEEE Transactions on Power Electronics Vol. 23, No.1, Jan. 2008, pp. 291-297.
118. P. Zumel, O. Garcia, J. A. Oliver, and J. A. Cobos, "Differential-Mode EMI Reduction in A Multiphase DCM Flyback Converter", IEEE Transactions on Power Electronics, Vol. 24, No. 8, Aug. 2009, pp. 2013-2020.
119. P. Barbosa, "Three-Phase Power Factor Correction Circuits for Low-Cost Distributed Power Systems", Ph.D. Thesis, Virginia Tech, 2002.

---

120. Y. Jang and M. M. Jovanovic, "Interleaved Boost Converter With Intrinsic Voltage-Doubler Characteristic for Universal-Line PFC Front End", IEEE Transactions on Power Electronics Vol. 22, No. 4, Jul. 2007, pp. 1394-1401.

---

# Appendix

## A.1 Series LC resonant network analysis

The total impedance  $Z_{TOT} = Z_L + j \left\{ \omega L_r - \left( \frac{1}{\omega C_r} \right) \right\}$  . . . . .

(A.1)

Where

$Z_{TOT}$  = Total impedance of circuit seen by source

$Z_L$  = Equivalent impedance referred to primary side of high voltage high frequency transformer

$$Z_L = \frac{8R_L}{n^2\pi^2}$$

Where  $V_{DC}$  is DC input voltage,  $R_L$  is the load resistance,  $n$  is the turns ratio,  $Z_L$  is the AC equivalent resistance at the primary side of high frequency transformer and.

The circuit has a resonant frequency when the imaginary part of  $Z_{TOT}$  equal to zero and it is given by

$$\omega_o = \frac{1}{\sqrt{L_r C_r}} \quad . . . . .$$

(A.2)

The resonant frequency is independent of  $Z_L$  and the current at this time of instant is given by

$$I_L = \frac{V_{in}}{Z_L} \quad . . . . .$$

(A.3)

Where

---

$V_{in}$  – The RMS voltage of output of inverter

$I_L$ - Current through  $Z_L$

The characteristic impedance of the circuit is represented with  $Z_n$  and is given by

$$Z_n = \sqrt{\frac{L_r}{C_r}} \quad . . . . .$$

(A.4)

Quality factor of the circuit is represented with  $Q$  and is given by

$$Q = \frac{\omega_o L_r}{R_L} = \frac{1}{\omega_o C_r R_L} = \frac{Z_n}{Z_L} \quad . . . . .$$

(A.5)

The magnitude of characteristic impedance ( $Z_n$ ) of the circuit is a function of frequency with  $Q$  as parameter, keeping  $Z_L$  constant.  $Z_n$  is pure resistance when  $\omega_s = \omega_o$ , but inductance impedance dominates when operated below resonant frequency ( $\omega_o$ ) whereas capacitive impedance dominates when operated above resonant frequency ( $\omega_o$ ).

## A.2 Parallel resonant network analysis

$$\text{RMS value of square wave voltage of inverter} = V_{rms} = \frac{2\sqrt{2}V_{DC}}{\pi} \quad . . . . .$$

(A.6)

Where  $V_{rms}$  is the RMS voltage of square wave voltage at the input.

$$\omega_o = 0 \quad . . . . .$$

(A.7)

$$\omega_1 = \sqrt{\frac{C_r Z_L^2 - L_r}{L_r C_r^2 Z_L^2}} \quad . . . . .$$

(A.8)

---

Where

$\omega_0$  = First resonant frequency of parallel circuit

$\omega_1$  = Resonant frequency at which zero current switching occurs

### A.3 Third (3<sup>rd</sup>) LCL-T resonant network analysis

$$Z_{TOT} = \frac{Z_L + j(\omega^5 L_{R1} C_r^2 L_{R2}^2 - 2\omega^4 L_{R1} C_r L_{R1} + \omega^4 L_{R1} C_r^2 Z_L^2 + \omega^4 C_r L_{R2}^2 + \omega^2 L_{R1} + \omega^2 L_{R2} + \omega^2 C_r^2 Z_L^2)}{\omega^4 C_r^2 L_{R2}^2 - 2\omega^2 C_r L_{R2} + \omega^2 C_r^2 Z_L^2 + 1}$$

(A.9)

On making imaginary part of  $Z_{TOT}$  equal to zero, one can obtain number of resonant frequency as well as soft switching. In this particular resonant converter there are three resonant frequencies and they are

$$\omega_0 = 0$$

$$\omega_1 =$$

$$\sqrt{\frac{(2L_{R1}C_rL_{R1} - L_{R1}C_r^2Z_L^2 + C_rL_{R2}^2) + \sqrt{[(-2L_{R1}C_rL_{R1} + L_{R1}C_r^2Z_L^2 - C_rL_{R2}^2)^2 - 4L_{R1}C_r^2L_{R2}^2(L_{R1} + L_{R2} - C_r^2Z_L^2)]}}{2L_{R1}C_r^2L_{R2}^2}}$$

(A.10)

$$\omega_2 =$$

$$\sqrt{\frac{(2L_{R1}C_rL_{R1} - L_{R1}C_r^2Z_L^2 + C_rL_{R2}^2) - \sqrt{[(-2L_{R1}C_rL_{R1} + L_{R1}C_r^2Z_L^2 - C_rL_{R2}^2)^2 - 4L_{R1}C_r^2L_{R2}^2(L_{R1} + L_{R2} - C_r^2Z_L^2)]}}{2L_{R1}C_r^2L_{R2}^2}}$$

(A.11)

Where

$\omega_0$  = First resonant frequency of LCL-T resonant circuit

---

$\omega_1$  = Resonant frequency at which zero current switching occurs

$\omega_2$  = The resonant frequency at which zero current switching does not occur occurs

#### A.4 Fourth (4<sup>th</sup>) order LCLC resonant network analysis

On applying voltage divider rule, then the voltage across  $X_2$  is given by

$$V_{X_2} = \frac{X_2(Z_L + X_3)V_{in}}{X_1X_2 + X_1X_3 + X_2X_3 + Z_L(X_1 + X_2)} \quad \dots \dots$$

(A.12)

Then the current through load is expressed by

$$I_{Load} = \frac{V_{X_2}}{Z_L + X_3} \quad \dots \dots$$

(A.13)

$$I_{Load} = \frac{X_2 V}{X_1X_2 + X_1X_3 + X_2X_3 + Z_L(X_1 + X_2)} \quad \dots \dots$$

(A.14)

Where

$$X_1 = \frac{1 - \omega^2 L_{r1} C_{r1}}{j\omega C_{r1}}, \quad X_2 = \omega L_{r2}, \quad X_3 = \frac{1}{j\omega C_{r2}} \quad \text{and} \quad Z_L = \frac{8R_L}{n^2 \pi^2}$$

Solving the above equation after substituting the values  $X_1$ ,  $X_2$ , and  $X_3$  make the coefficient of  $Z_L$  equal to zero, then the load current  $I_L$  becomes independent of  $Z_L$  at  $\omega_0 = \frac{1}{\sqrt{(1+x)L_{r1}C_{r1}}}$  at

$$y = \frac{1+x}{x} \quad \dots \dots$$

(A.15)

By equating imaginary part of  $Z_{TOT}$  is zero at  $\omega_0$

---

$$1+x = xy \quad \dots$$

(A.16)

Where

$$x = \frac{L_{r2}}{L_{r1}}$$

$$y = \frac{C_{r2}}{C_{r1}}$$

$$\text{Normalized frequency } \omega_n = \frac{\omega_s}{\omega_0} \quad \dots$$

(A.17)

Where

$\omega_s$  = Switching frequency

$\omega_0$  = Resonant frequency

$$\text{Current gain} = H = \frac{nI_0}{V_d/Z_n}, \text{ voltage gain} = M = \frac{V_o/n}{V_d}$$

Where

$V_d$  = DC voltage applied to inverter